NEURONAL CORRELATES OF PERCEPTUAL SALIENCE IN LOCAL FIELD POTENTIALS IN THE PRIMARY VISUAL CORTEX

YASAMIN MOKRI

NATIONAL UNIVERSITY OF SINGAPORE

2012

NEURONAL CORRELATES OF PERCEPTUAL SALIENCE IN LOCAL FIELD POTENTIALS IN THE PRIMARY VISUAL CORTEX

YASAMIN MOKRI

(MSc, Sharif University of Technology)

A THESIS SUBMITTED FOR THE DEGREE OF DOCTOR OF PHILOSOPHY OF ENGINEERING

DEPARTMENT OF ELECTRICAL & COMPUTER ENGINEERING

NATIONAL UNIVERSITY OF SINGAPORE

2012

Acknowledgements

I am deeply grateful to my advisor, Dr. Shih-Cheng Yen. He inspired and encouraged me throughout my Ph.D. by setting high expectations, and supported me by his insightful guidance and immense knowledge.

My appreciation goes to my colleagues and good friends Omer, Roger, Jit Hon, Esther, Seetha, and Ido for being such pleasant and caring companies. I am especially thankful to Dr. Roger Herikstad and Dr. Bong Jit Hon for their help and for the stimulating discussions.

Lastly, I would like to say many thanks to my dear parents, Darioush and Pirasteh, and my brothers and best friends Sourena and Soroush for their advice, support, love, and patience.

The work present in this thesis was supported by grants from the National Eye Institute and the Singapore Ministry of Education Academic Research Fund, and is the result of collaboration between Dr. Shih-Cheng Yen and Yasamin Mokri from the National University of Singapore, and Professor Charles M. Gray and Dr. Rodrigo F. Salazar form the Center for Computational Biology, Montana State University.

Contents

Summary

In this study, neural correlates of figure-ground segregation, and in particular, the correlation between neuronal synchrony and visual grouping were investigated. To perform this, electrophysiological recordings were conducted in the primary visual cortex of macaque monkeys, while they were engaged in a contour detection task. It has been shown that changing the saliency of figure can affect perception, and, as a result, the performance of the subjects in figure-ground segregation. So, the visual saliency of the contour was changed throughout the experiment, and the aim of the study was to discover if the neuronal responses were modulated as a function of visual saliency. Frequency domain analysis techniques were applied to the local field potentials either recorded on single electrodes or simultaneously on pairs of electrodes. Oscillation in gamma band of local field potentials is thought to be due to the synchronous oscillatory activity of a large population of neurons, so we assessed the power responses in gamma band of local field potentials on single channels. We found when the receptive field of a neuron was part of the contour (figure condition) the power responses were significantly different compared to when the receptive field was part of the background (background condition) for 29.69% of the recording sites (106 out of 357). For the sites with significant differences between the responses in the figure and background conditions, we examined the changes in the responses as a result of changes in visual saliency. We found 52 (49.05%) sites out of the 106 significant sites exhibited significant modulations as a function of visual saliency. We then directly examined the synchrony of the gamma band responses on pairs of simultaneously recorded electrodes. The synchrony of the simultaneously recorded

responses elicited significant differences between the figure and background conditions for 48.74% (97 out of 199) of the pairs. This is while 68.04% (66 out of 97) of these pairs also exhibited significant modulations as a function of visual saliency.

We were also interested in the time course of these observed modulations. Although the time resolutions of both single channel and multi-channel analyses were very low, we observed modulations in both early and late components of the responses. We speculated that, potentially, the earlier modulations represented the contribution of V1 in figure-ground segregation in the feedforward sweep, while the later modulations represented the effect of feedback from extra-striate cortex to V1.

Overall, these results may add to the evidence supporting binding-by-synchrony hypothesis as the mechanism underlying visual grouping in the primary visual cortex. Also, these findings indicate that primary visual cortex may contribute to figure-ground segregation very early in vision.

List of Tables

List of Figures

Chapter 1

Introduction

One of the early processing steps that seems to precede pattern recognition in the visual system is scene segmentation. Scene segmentation, also called figure-ground segregation, is the process through which individual components of the objects in a scene are grouped together and form distinct objects, segregated from both the background and each other. While the neuronal correlates of scene segmentation in the brain have been widely studied, our knowledge of how and where in the brain this process occurs is still very limited. However, as scene segmentation is performed very rapidly (Zipser et al., 1996; Fabre-Thorpe et al., 2001; Maldonado et al., 2008; Uhlhaas et al., 2009), early cortical areas, such as primary visual cortex, could be the potential regions of the brain associated with this process.

In this study, we investigated a potential mechanism for binding and scene segmentation proposed by Milner (1974) and von der Malsburg (1981; 1985), i.e. binding-by-synchrony. This hypothesis, which has been supported by experimental evidence (for reviews, please see Singer, 1995; Gray, 1999), suggests that the neurons that represent different features of an object in a scene fire synchronously to convey the coherent percept of the object. The role of neuronal synchrony extends beyond binding neuronal responses in one region, and has been shown to be involved in binding responses in different regions and even different modalities in a large body of studies. It is also believed to be the mechanism underlying several cognitive processes

(Uhlhaas et al., 2009). However, the role of synchrony in binding visual features in the primary visual cortex is still poorly understood. This necessitates further investigation into synchrony and its association with binding visual features in this area.

To perform this, we conducted a contour detection experiment in macaque monkeys. It has been shown that the performance of subjects in a scene segmentation task can be correlated with the saliency of the individual objects composing the scene (Supèr et al., 2001; Lee et al., 2002), which suggests that investigating the representation of visual saliency could shed light on the physiological substrates of scene segmentation process. Thus, in our experiment, we manipulated the saliency of visual stimuli. Then, we examined the modulation of synchrony as a function of visual saliency using local field potentials (LFP). LFPs, instead of spikes or at least in conjunction with spikes, have been shown to be more suitable for investigating synchrony (Frien et al., 1994; Bedenbaugh and Gerstein, 1997; Brosch et al., 1997).

In the next chapter, we elaborate on the binding-by-synchrony hypothesis, and the evidence found in the primary visual cortex related to perceptual grouping. Next, in Chapter 3 and Chapter 4, we describe how we assessed the correlation between changes in gamma band power and synchrony, respectively, with changes in visual saliency. Finally, in Chapter 5, we conclude with the potential contributions of the results found in this study to the understanding of the neuronal basis of scene segmentation.

Chapter 2

Literature Review

The binding problem relates to the question of how the brain integrates the different components and features of an object together into a unified whole. For example, how the color and shape of a red square defines and distinguishes a red square from a blue circle. This integration, referred to as perceptual binding or perceptual grouping, may be encountered in different forms: from binding the visual features of an object in a scene, to binding sensory and motor information, and binding cross-modal features (Roskies, 1999). Binding and scene segmentation are key steps in the sensory pathway that are believed to be precursors of pattern recognition in the brain. The Gestalt psychologists in the 1920s proposed that we perceive individual components in a scene as unified objects, and segregate them from other objects, based on some common characteristics: proximity, similarity, continuity, closure, and common fate (Köhler, 1930; Wertheimer, 1955; Koffka, 1935, 1969; Kanizsa, 1979) Other studies added some other characteristics to the list, such as size (Bergen and Adelson, 1988), texture (Julesz, 1975), binocular disparity (Nakayama and Silverman, 1986), and coincidence in time, which means that in a dynamic scene, the elements that change together tend to be bound together (Alais et al., 1998; Usher and Donnelly, 1998; Kandil and Fahle, 2001; Lee and Blake, 1999, 2001; Sekuler and Bennett, 2001; Suzuki and Grabowecky, 2002; Guttman et al.,

2005). Mostly, it is believed that grouping based on Gestalt cues is performed preattentively (Treisman and Gelade, 1980; Gray, 1999), and provides subsequent processes that require attention with the most salient objects to process. However, there are some studies that have proposed that attention may be required for this type of grouping in certain tasks (Joseph et al., 1997), or may improve performance Theeuwes et al., 1999).

This chapter elaborates on one of the potential mechanisms underlying grouping, explains why the primary visual cortex should be considered in studying scene segmentation, and concludes with a detailed review of the literature on local field potentials and its contribution to studying visual grouping.

2.1. Synchrony - a putative mechanism underlying grouping

Based on the hierarchical or convergent model, neurons in the lower levels of the visual hierarchy tend to respond to the primary features of individual components of each object, like orientation, color, and contrast. As one ascends the hierarchy, neurons tend to respond to more complex features that are the combinations of the features extracted in earlier areas. Finally, the highest ranked regions are responsible for recognizing combinations of features as integrated objects. For example, based on this model, a closed contour can be identified only in extra-striate areas, as the receptive fields of the neurons in striate cortex are small, and are not able to respond to the whole contour. Although it is true that the receptive fields of the neurons become larger, and cells respond to more complex features from lower to higher

regions in the visual hierarchy, this model demands a very large number of neurons selective for all possible combinations of features, and potentially a large number of synaptic connections between the cells contributing to the representation of these feature combinations (Singer, 1995). In addition to these reasons, an interesting study recently showed that even if the middle level regions in visual cortex (V2 and V4) are impaired, everyday visual tasks could still be performed with no difficulty, thus raising doubts on the validity of the convergent model (Gilaie-Dotan et al., 2009). As a result, although some groups of neurons are specialized in responding to feature combinations that are very frequent, including some as complex and as specific as individual faces (Page 2000; Gross, 2002; Kiani et al., 2007; Quiroga et al., 2008), a more efficient model seems to be required to explain the general mechanism underlying grouping and scene segmentation in the brain.

An alternative hypothesis for binding is based on population coding. According to this model, in contrast to the convergent model mentioned above, the neurons responding to individual elements of an object are grouped together to distinguish that object from other objects. This model demands less resources compared to convergent model, because each cell can be part of different combinations. As a result, population coding seems more promising in coding the objects of a scene, but in return, a mechanism needs to be proposed for binding the cells of the population representing an integrated perceptual entity. One of the models proposed to fulfill this purpose is the binding-by-synchrony or temporal correlation hypothesis (Singer, 1995). According to this model, the discharges of the neurons that respond to an object can be distinguished from the non-relevant responses, because their discharges are synchronous with each other and asynchronous with non-relevant discharges. The theoretical model of binding-by-synchrony was first proposed by

Milner (1974) and von der Malsburg (1981, 1985), and it is shown that this concept can easily be extended from synchrony in one region to synchrony between regions, and even modalities, providing a communication mechanism that seems essential for answering broader questions such as cognition and awareness (Uhlhaas et al., 2009). Interestingly, these studies (Milner, 1974; von der Malsburg, 1981; 1985) proposed physiological substrates for their model, although there was little or no evidence for some of these proposed mechanisms at the time. The physiological evidence for some of these proposed mechanisms were only discovered later. For instance, von der Malsburg (1981) proposed that as the components of an object are not confined to the classical receptive field of the neurons, some connections should exist to connect the cells sensitive to similar features. These connections, called horizontal connections, were discovered later in cortex (Ts'o et al., 1986; Gilbert and Wiesel, 1983, 1989; Gilbert, 1992; Malach et al., 1993; Bosking et al., 1997).

Wolf Singer's lab was the first lab to find experimental evidence that supported this model (Gray and Singer, 1987 Soc. Neurosci., abstract; Gray and Singer, 1989; Gray et al., 1989). Similar studies in the visual cortex of cats (Eckhorn et al., 1988; Gray and Singer, 1989; Gray et al., 1989, 1990; Engel et al., 1991a,b), as well as monkeys (Eckhorn et al., 1993; Frien et al., 1994; Kreiter and Singer, 1992, 1996), later provided more evidence supporting this hypothesis.

Despite these findings, some objections were raised about the binding-by-synchrony hypothesis, based on biological limitations (Shadlen et al., 1999). Shadlen et al. (1999) mainly argued that as a cell receives a large number of excitatory inputs from nearby neurons, which are activated simultaneously in response to a stimulus, i.e. the high input regime, it is probably impossible for the cell to distinguish between synchronous and asynchronous inputs, and it is very likely that synchronous inputs

happen merely by accident due to this large number of spikes received by each cell without any functional relevance. In other words, they believed that cells act as integrators and cannot be sensitive to the timing of the inputs they receive. An abundant number of studies have shown that this is not true, and neurons are influenced by the timing of their inputs (König et al., 1996; Alonso et al., 1996; Usrey et al., 1998; Azouz and Gray 2003; Bruno and Sakmann, 2006; also see Gray 1999). At the same time some studies initially failed to even observe oscillations in brain areas that could potentially be involved in feature binding, e.g. the primary visual cortex of monkeys (Tovee and Rolls, 1992; Young et al., 1992). However, this could potentially be due to the high heterogeneity of the neurons in V1 (Gray, 1999), or could be because the activity of single units or multi units recorded in these studies were dissociated from the activity of the population (Young et al., 1992; Gray, 1999). Considering the large number of studies that reported oscillations and synchrony in several areas, and in the context of various tasks (Bragin et al., 1995; Fries et al., 2001b; Brosch et al., 2002; Pesaran et al., 2002; Lakatos et al., 2005; Schoffelen et al., 2005; Buzsáki, 2006; Hoogenboom et al., 2006; Buschman and Miller, 2007), it seems that the consensus is that these oscillations exist in the brain, and the focus of attention has shifted from spotting these oscillations to the functional relevance of neuronal oscillations and synchrony to perception. Synchrony in the gamma frequency band (20-80 Hz) has been the most prominent synchrony reported, so in this study we focused on this frequency band, but the evidence for perceptual correlates of other frequency bands is also abundant (Buzsáki 2002; Jensen et al., 2002; Pogosyan et al., 2009).

Synchrony between cell discharges is thought to increase the effectiveness of spikes in the receiving regions and also to influence plasticity (Alonso et al., 1996;

König et al., 1996; Usrey et al., 1998; Azouz and Gray 2003; Perez-Orive et al., 2004; Bruno and Sakmann, 2006), and has been suggested to be the result of the interactions of a network of inhibitory interneurons (Csicsvari et al., 2003; Hasenstaub et al., 2005; Vida et al., 2006; Buzsáki, 2006; Bartos et al., 2007; Morita et al., 2008). Nonetheless, some other studies have found cells with intrinsic gamma oscillatory membrane potentials, and proposed that these neurons may serve as pacemakers (Llinás et al., 1991; Gray and McCormick 1996; Steriade et al., 1998).

As the main focus of this study is the functional role of synchrony in visual cortex, we will take a closer look at studies in the visual cortex, and in particular studies on scene segmentation and visual binding in the next section.

2.2. Visual binding and binding-by-synchrony

Although the binding-by-synchrony hypothesis was proposed initially as the mechanism underlying visual grouping and scene segmentation, the number of studies that directly assessed the potential of this hypothesis in explaining the experimental results pertaining to scene segmentation is relatively small.

Most pioneering studies used simple bar stimuli to assess neuronal oscillations and synchrony, shedding light on some aspects of the putative role of synchrony in grouping. Gray and Singer (1989) showed that when cells were stimulated by a light bar with their preferred orientation, they oscillated at a frequency close to 40 Hz. Gray et al. (1989) stimulated cells with non-overlapping receptive fields in area 17 and 18 of anesthetized cats using a single bar that stimulated both receptive fields simultaneously, and two bars that moved in opposite directions stimulating the

receptive fields independently. They showed that in the former case, the synchrony between the multi-unit recordings from the two sites was higher compared to the second case, or even compared to an intermediate case in which the receptive fields were stimulated by two separate bars with the same direction of movement. Engel et al. (1990) confirmed these results by further investigating the same phenomena using spikes and local field potentials. The synchronous cells were recorded on electrodes with up to 7 mm separation and with both overlapping and non-overlapping receptive fields. In accordance with Gray et al. (1989) they reported that even cells with non-overlapping receptive fields fired synchronously, if the stimuli inside their receptive fields had the same orientation. They also reported that phase locking between the cells was correlated with stimulus properties. These results later were replicated by Freiwald et al. (1995). After these initial findings were found in anesthetized cats, Gray and Viana Di Prisco (1997) were able to show similar oscillatory responses to bar stimuli in alert cats engaged in a fixation task, and as a result, showed that the observed effect was not due to anesthesia. This was a significant finding, as it has been shown that anesthesia can affect the neuronal responses in several ways (Bour et al., 1984; Lamme et al., 1998; van der Togt et al., 1998; Fiser et al., 2004). These findings contradicted those reported in Ghose and Freeman (1992), who reported that the oscillations in cat striate cortex were not stimulus dependent, and were even stronger during periods of spontaneous activity. Gray and Viana Di Prisco (1997) replicated the method used in Ghose and Freeman (1992), and discovered that the method could introduce spurious high oscillations, potentially contributing to the results found in this study. Later, to extend Gray et al. (1989) study, Brosch et al. (1997) recorded multi-unit activity and local field potentials in areas 17 and 18 of cats using the same paradigm as Gray et al. (1989), but added one more condition in which

some part of the stimulus was occluded, and showed that the synchrony in this case was also higher compared to the condition in which two separate bars stimulated the receptive fields. This was consistent with the hypothesis that synchrony emerged because the stimuli inside the receptive fields were grouped together as one object. However, this result may need to be reevaluated, as Palanca et al. (2005) showed later that, in a similar experiment, the cells showed high synchrony even in the absence of the components of the illusory contours, and solely because some sections of the mask were located inside their receptive fields.

In addition to these intra-area effects, Engel et al. (1991a) were able to show that multi-unit recordings as distant as those from two different hemispheres exhibited the same synchrony effect when the stimulus extended to both hemifields. The significant finding in this study was that when the corpus callosum was severed, the synchrony vanished. This ruled out the possibility that the observed synchrony was due to common subcortical inputs, and showed that the synchrony was likely elicited through cortico-cortical connections. This, once more, was at odds with Ghose and Freeman's (1992) claim that the observed oscillations in striate cortex were the result of oscillations in LGN, and also demonstrated that zero phase lag synchrony was possible even with large conduction delays, 4 to 6 ms, as could be the case when cells are located in different hemispheres. While these findings were all reported in cat striate cortex, Livingstone (1996) reported similar results in the primary visual cortex of anesthetized monkey, while Kreiter and Singer (1992, 1996) observed the same effects in area MT of awake macaques, showing that the role of synchrony in binding was not specific to cats. Nonetheless, Kreiter and Singer (1992, 1996) found some differences, such as the synchrony was more transient and also more variable in terms of the frequency of oscillation for monkeys compared to cats. Eckhorn et al. (1993)

and Frien et al. (1994), also reported the presence of gamma oscillatory signals in V1 and phase-locking between gamma band responses in V1 and V2, and again supported the binding-by-synchrony hypothesis in awake monkeys. Later, Maldonado et al. (2000) characterized the correlation between synchrony and the properties of the stimuli and receptive fields, and showed that synchrony can be modulated by stimulus properties.

The experiments mentioned above were mostly performed using simple bar stimuli. One of the first studies that used a more complex stimulus to directly investigate correlation between scene segmentation and synchrony was Lamme and Spekreijse (1998), and they failed to find such correlations in their multi-unit recordings. In this experiment, the figure was a patch of texture that could be differentiated from the background by the difference in orientation or motion direction with respect to the background. However, Gail et al. (2000) performed a similar experiment in V1 of awake monkeys, performing a fixation task, and succeeded in showing that gamma band coherence between the LFPs recorded from the cells inside and outside the figure was very low. The coherence was the highest when both receptive fields were inside one segment (both object or both background), followed by when both receptive fields were on the border, and then when one receptive field was on the border and the other receptive field on the figure or background. So, in other words, while the components of the same object were coupled, the components of different objects were decoupled (Eckhorn et al., 2001). This discrepancy could be due to the differences in the recordings, as Gail et al. (2000) used LFPs to assess synchrony, and LFPs are thought to be more sensitive measures of synchrony compared to the action potentials (Frien et al., 1994; Brosch et al., 1997).

Later, Castelo-Branco et al. (2000) used plaid stimuli to stimulate neurons in area 18 and posteromedial lateral suprasylvian area (PMLS) of anesthetized cats. This type of stimulus, which has also used in Thiele and Stoner (2003) and Lima et al. (2010), potentially provides a mechanism to generate stimuli with varying degrees of perceived motion coherence by changing the transparency of the bars and the color of the intersections. Consistent with the binding-by-synchrony hypothesis, they succeeded in demonstrating that the synchrony between neuronal responses was higher in response to a single perceptual surface, i.e. coherent plaid, compared to two individual surfaces, i.e. two non-coherent gratings. However, they later failed to find similar results in V1 of alert monkeys (Lima et al., 2010). Thiele and Stoner (2003) also reported that they could not replicate the results in area MT of alert monkeys. The main difference between the first study and the subsequent studies could be that in the first experiment, the cats were under anesthesia, while in the other two experiments, the monkeys were awake. However, considering that other groups have observed synchrony associated with binding in both anesthetized (Gray et al., 1989; Freiwald et al., 1995) and awake cats (Gray and Viana Di Prisco, 1997), as well as anesthetized (Livingstone, 1996) and awake monkeys (Eckhorn et al., 1993; Frien et al., 1994; Kreiter and Singer 1992, 1996; Maldonado et al., 2000), this seems unlikely. This reasoning would also be at odds with other findings that mostly found enhancement in figure-ground segregation effects in alert compared to anesthetized animals (Lamme et al., 1998; van der Togt et al., 1998; Li et al., 2008). In this study, only the late component of the response was considered, i.e. either 200 ms or 100 ms after stimulus onset, so most likely the responses were due to feedback from other areas. Consequently, the discrepancy could possibly be due to the different roles of recurrent connections in cats and monkeys. What should also be noted about the Lima

et al. (2010) study is that they observed significant high LFP-LFP coherence for both single grating and coherent plaid stimuli, but they failed to detect high coherence between LFP and multiunit activity. In our view, these results do not necessarily oppose binding-by-synchrony hypothesis, although they do not support the putative functionality for synchrony proposed by Womelsdorf et al. (2007). According to this model, for synchrony to be effective, the output of the region (i.e. multi-unit activity (MUA)) should be synchronized with the gamma oscillations (LFP). At the same time, it has been shown that coherence may miss short episodes of synchrony between two signals in the presence of non-stationarity (Lachaux et al., 2002), and this needs to be taken into account when one is concerned with the synchrony between MUA and other signals, as this type of synchrony probably is very transient. This may need to be emphasized considering that Kreiter and Singer (1992, 1996) found that synchrony was more transient in monkeys compared to cats. As a result, it is possible that using techniques used in other studies (Le Van Quyen et al., 2010; Denker et al., 2011) to assess the synchrony between spikes and LFPs could result in revealing synchrony between MUA and LFPs.

Most of these studies suffered from the common drawback that the stimuli inside the receptive fields varied across conditions, which made the comparison of the synchrony between conditions slightly problematic. Palanca et al. (2005) addressed this issue and designed their stimuli in a manner that stimuli inside the receptive fields were fixed. In the literature, this paper has mostly been referred to as an experiment that found evidence against binding-by-synchrony, while in fact, they found, using Fourier coherence, higher coherence in the gamma band of LFPs of pairs of cells when they were parts of one figure compared to when they were parts of individual figures. This difference was small, but significant. They also observed significantly

higher synchrony in response to two bars when they were parts of a closed contour compared to when they were independent from one another. They also found effects consistent with Kreiter and Singer's (1996) study, but the difference between the synchrony of the two conditions was smaller than those reported in Kreiter and Singer (1996). It seems that the authors were concerned that the differences, although significant, were small for all the experiments, and the effect often was not observed in lower frequency bands (0-30 Hz). While these results seemed consistent with binding-by-synchrony, after pooling all coherence values from different sites together, and performing an ROC analysis for one object versus two objects conditions, it was observed that due to the high variability of the coherence measures across sites, it was not possible to distinguish between the two conditions using the ROC analysis. So it was concluded that sysnchrony may not be robust enough to subserve grouping. However, in our view, these results could be expected due to the heterogeneity of the neuronal populations. Moreover, the Fourier coherence measure is affected by correlation between the envelopes, and does not solely represent phase locking or synchrony between two signals (Lachaux et al., 2002). The high variability in the coherence measure could be due to the variation in the correlation between the envelopes of the LFP signals across sites, and not due to variation in the level of phase-locking. So, using other methods that are less sensitive to amplitude covariation (Lachaux et al., 1999), not only could, to some extent, address this issue, but also could be a better option in investigating the modulation of synchrony across conditions. In support of this conjecture, we refer to Gysels et al. (2005), which showed that phase-locking value could be superior to Fourier coherence in discriminating between two conditions in their experiment.

In spite of these studies, which failed to find evidence in favor of binding-by-

synchrony hypothesis, recently, some studies again reported results in the primary visual cortex that seem to support correlation between synchrony and visual grouping. Samonds et al. (2006) showed an increase in the synchrony between cells with cocircular receptive fields, in addition to the cells with similar orientation preference, when they were stimulated by gratings. This was especially interesting, as according to Samonds et al. (2006), cells with cocircular receptive fields were proposed to play a critical role in contour integration (Field et al., 1993). Zhou et al. (2008), in an attempt to separate the effect of temporal and spatial integrity on synchrony, found that when the neurons with overlapping receptive fields in the primary visual cortex of cats under anesthesia were stimulated by a drifting sinusoidal grating, their responses (spikes) were coherent in gamma band and this coherency decreased when the spatial integrity of the grating was diminished by superimposing noise on the grating. This study was similar to Engel et al. (1998), which used a moving-random dot pattern as stimulus. They showed that although the synchrony between neuronal responses was weaker compared to continuous contours, they still existed, and decreased when motion coherence was impaired by adding noise to the pattern.

Recently, Meirovithz et al. (2010) found another piece of evidence supporting a correlation between increase in neuronal synchrony and colinearity. Performing voltage-sensitive dye imaging (VSDI) in the primary visual cortex of awake fixating monkeys, they found an increase in synchrony between the responses of neurons that responded to a low contrast Gabor patch (target) and its two flanking Gabor patches when the flankers were located colinear with the target patch compared to when they were located orthogonal. They reported better discrimination between the two conditions using onset synchrony compared to amplitude.

Finally, another study that indirectly supported binding-by-synchrony (Fries et

al., 1997) showed that in the presence of competition in a binocular rivalry experiment, the perceived stimulus was the one with higher synchrony in its respective neuronal population responses. This is while the spike rates of both populations responding to the two stimuli were nearly the same. They proposed that because this is similar to perceptual grouping, in which the neuronal population that is "functionally more relevant" should be selected, the same mechanism could probably subserve grouping as well (but see Gail et al. (2004)).

Here, another slightly different study (Roelfsema et al., 2004) needs to be mentioned that provided evidence against binding-by-synchrony. The main difference between this study and the ones mentioned earlier is that in their experiment, the monkeys had to trace a curve to accomplish the task, which demands shifting of spatial attention in a relatively long time interval. This type of grouping is fundamentally different from the pre-attentive binding, and is out of the scope of this study. However, accepting that attention merely is reflected in the enhancement of the firing rates and does not affect synchrony, these results certainly cast some doubt on generality of binding-by-synchrony hypothesis. Nevertheless, it should be mentioned that in contrast to their study that did not find increases in synchrony as a result of attention, other studies have reported significant enhancement in synchrony with increases in attention level in several different cortical areas (Fries et al., 2001b; Womelsdorf et al., 2006; Buschman and Miller, 2007; Fries et al., 2008; Siegel et al., 2008).

It is worth noting that in addition to studies using depth electrode recordings, other studies have also assessed the relationship between synchrony, visual grouping, and object recognition using recording methods like Electroencephalography (EEG) and Magnetoencephalography (MEG). Müller (1996, 1997) used the same stimuli as

Gray and Singer (1989) while recording EEG signals from human and monkeys, and observed higher gamma power for the single bar condition. Tallon-Baudry et al. (1996) found higher gamma band activity in human EEG recordings when the subjects responded to real triangles or Kanizsa triangles compared to no triangles on C1 and C4 electrodes. Interestingly, Csibra et al. (2000) found patterns in the gamma band activity similar to those reported by Tallon-Baudry et al. (1996) in the frontal cortex of 8-months old infants, while the pattern was different for younger subjects (6-months old infants). Siegel et al. (2007) observed increases in gamma power with increases in motion coherence in the MEG signals in area MT. Also other studies assessed the responses when subjects recognized an object in the scene compared to when they failed to recognize the object. These studies mostly investigated the modulation of gamma band activity in large-scale cognitive integration tasks. Rodriguez et al. (1999) found higher synchrony in gamma power for upright compared to upside-down Mooney faces in human EEG. Grice (2001) replicated the results, but in addition, found that the gamma-oscillation pattern was different in normal subjects and subjects that suffered from autism and Williams syndrome. In both groups of patients, object recognition ability is usually impaired. For the autistic patients, the gamma-burst was not different across conditions, while for the patients with Williams syndrome, it was entirely absent. Keil et al. (1999) found higher gamma power in human EEG on occipital electrodes for upright, bistable figures compared to upside-down figures. Schadow et al. (2009) observed that a contour stimulus, composed of circularly aligned Gabor patches, elicited significantly higher synchrony in gamma band compared to randomly oriented Gabor patches in a visual stimulus when they performed EEG recordings in healthy subjects. In contrast, in EEG recording performed in patients with homonymous hemianopia, synchrony in

the gamma band was impaired in the intact hemisphere of the patients. These patients suffer from deficits in vision in one hemifield, but it has been shown that they have difficulties in contour integration in their intact hemifield as well Schadow et al. (2009).

These findings support the correlation between gamma band activity and figure-ground segregation, but in most of these studies it is difficult to separate the neural correlates of bottom-up scene segmentation from the neural correlates of matching the target with the stored representation of the target in memory. As a result, the observed increase in gamma band activity or synchrony in some of these studies may be due to this matching and not visual binding, as speculated by Tallon-Baudry et al. (1996). Increase in gamma band activity due to this matching was suggested by Herrmann (2004) in their "match-and-utilization" model. Also, the relatively low time resolution of MEG and low spatial resolution of EEG introduce some uncertainties in terms of the exact location and time course of the effects reported. So, in these studies it was difficult to identify the exact area that the activity originated from or when the effect emerged. Also, the studies often found enhancements in the gamma band activity, which they assumed showed that a large ensemble of neurons synchronized their activity in the gamma band, but a direct measure of synchrony was rare. Moreover, a recent study Yuval-Greenberg et al. (2008) linked the enhancement in gamma band activity in EEG recordings and the muscular artifacts resulted from microsaccades, and warned that the observed enhancement in gamma band needs to be reevaluated in the experiments done earlier. However, as the result of this study was correlational and not causal, it does not necessarily invalidates the results obtained relevant to gamma band activity, as it is possible that both microsaccades and induced gamma were correlates of the same cognitive process, and as a result,

they just happened to appear simultaneously (see Martinovic and Busch (2011) for further discussion).

In summary, the debate between the advocates and the critics of binding-by-synchrony is still in progress. Some discrepancies could be due to the techniques that were used. For example, some of the analyses were performed using conventional correlation techniques, which have been found to exhibit sensitivity to rate covariations and variability. It has also been shown that the synchrony associated with grouping may be very difficult to detect, as it is probably very transient and may last only for few tens of milliseconds (Oram and Perrett, 1992; Thorpe et al., 1996). So, new techniques like the Unitary Event Analysis (Grün et al., 2002a,b) or Neuroxidence (Pipa et al., 2008) can be applied instead to make the results more reliable. Also, other methods like phase-locking statistics (PLS) (Lachaux et al., 1999) could be more reliable in examining phase-locking between LFP responses, as well as some new methods used in Le Van Quyen et al. (2010) and Denker et al. (2011) in examining phase-locking between action potentials and LFPs, compared to the traditional Fourier coherence. As a result, applying new techniques that were introduced to the field in recent years could resolve some of the discrepancies, or at least could increase the certainty in the interpretation of the results.

The other issue that might have affected the results was that some of these studies could have obscured the potential effects because they used population analysis by averaging or pooling across recording sites. Considering the heterogeneity of the neurons in the brain, this might have also led to some discrepancies in the results. Some issues can also be raised about the stimuli and the tasks used. As mentioned earlier, in some of the experiments, the stimuli within the receptive fields were changed across conditions. Also, in most of these experiments, the animals did

not perform any tasks, or a task that may be affected by the coherence of the percept. So, it was difficult to investigate the correlation between the level of synchrony and the perception of the animal.

In conclusion, it seems that recordings using depth electrodes need to be carried out in animals performing a task in which the perception of a coherent object can be modulated and behaviorally measured. The stimulus should be designed in a way such that the stimuli inside the receptive fields of the neurons remain constant, while modifying other elements changes the saliency of the object.

The next question would be to decide where the recordings should be performed. In the next section, we discuss why the primary visual cortex could be a good candidate.

2.3. Role of the primary visual cortex

In addition to the question of how neurons bind together, the other question is where this binding starts, or in other words, when is the earliest time that the visual system is aware of segregated objects in the scene. As it is believed that perceptual binding and scene segmentation occur very rapidly (Maldonado et al., 2008; Uhlhaas et al., 2009), the primary visual cortex seems like a good candidate for performing these tasks, as it receives direct projections from LGN and the responses to a visual stimulus can be recorded in the primary visual cortex as early as 40 ms after stimulus onset. Also, it has been shown that even though the classical receptive fields of the neurons in this region are rather small, the responses of these neurons can be affected by contextual modulation (Polat et al., 1998; Fitzpatrick, 2000; Kapadia et al., 1995,

2000). Some studies have reported modulation in the responses of primary visual cortex correlated with scene segmentation (Lamme, 1995; Lamme et al., 1999; Gail et al., 2000; Kapadia et al., 2000; McManus et al., 2011). Zipser et al. (1996) reported enhancement in the responses of the single units in V1 of behaving monkeys when the cells responded to a texture perceived as figure compared to when it was perceived as background. This enhancement was correlated with the behavior of the monkeys. Lee et al. (2002) also showed similar enhancements in the responses of single units in V1 when they responded to an element with a disparate shape (figure) compared to the other elements of the scene (background) in an oddball experiment. Moreover, Supèr et al. (2001) and Li et al. (2006) showed correlations between the firing rate and saliency of the figure in the primary visual cortex. It should be noted that, it is possible that the results reported in some of these studies, e.g. Lamme (1995), Zipser et al. (1996), were not due to pop-out or the figure segregation capability of V1 neurons, but merely due to center-surround discontinuity (Hegdé and Felleman, 2003), although the results still could be indicative of contextual modulation in the primary visual cortex (Smith et al., 2007).

The models proposed for the role of V1 in visual awareness can be mainly divided into two categories of hierarchical and interactive models (Tong, 2003). In the hierarchical model, primary visual cortex merely serves as a feature extractor and a channel for relaying extracted features to higher areas in the visual hierarchy. This model does not seem like the most appealing model, as it has been shown that V1 neurons can respond to complex stimuli like illusory contours (Grosof et al., 1993), and also are sensitive to occlusion (Sugita, 1999). The results of the studies mentioned earlier, which reported the contextual modulation of responses in primary visual cortex (Polat et al., 1998; Fitzpatrick, 2000; Kapadia et al., 1995, 2000), impose

restrictions on this model as well. In the interactive model, in addition to providing information about the visual stimulus to other visual areas in a feed-forward manner, V1 interacts with downstream visual areas by receiving feedback from those areas. Several studies have proposed different possible functionalities for these feedback connections received by the primary visual cortex (Lee et al., 1998; Rao and Ballard, 1999; Gilbert et al., 2000; Lee et al., 2002; McManus et al., 2011). This model extends the role of the primary visual cortex beyond a pure feature extractor, but does not specify when and to what extent the primary visual cortex is aware of the feature combinations that are not confined to the classical receptive fields of its neurons.

Most of the studies mentioned above (Lamme, 1995; Zipser et al., 1996; Lamme et al., 1999; Gail et al., 2000; Supèr et al., 2001; Lee et al., 2002; Li et al., 2006) observed significant differences between the responses to figure and background in the late response, which presented a potential role of feedback and recurrent connections from extra-striate cortex, as well as lateral connections in the primary visual cortex. This was supported by Lamme et al. (1998) and later by Li et al. (2008), who explicitly showed that the effect of contour integration diminished in V1 under anesthesia, and also by Supèr and Lamme (2007) who showed the effect reduced by lesions in the dorsal extra-striate cortex. In other words, these studies did not find evidence supporting the direct role of primary visual cortex in bottom-up scene segmentation. However, considering that preattentive binding occurs very rapidly, it is possible that the primary visual cortex has a more critical role in this process, and these studies failed to confirm this due to some issues in the methods used. For example, these studies often performed population analysis, which might have obscured the subtle effects that could have been detected by analyzing individual recording sites and even single trials separately, considering the presence of high

heterogeneity in neuronal populations (Shamir and Sompolinsky, 2006; Yen et al., 2007; Chelaru and Dragoi, 2008). These experiments often involved a delayed saccade task as compared to a task that demands a faster reaction to the stimulus, which may have recruited other processes after the initial binding of the scene has been completed. Moreover, these studies mainly investigated the modulation in spike rates in the primary visual cortex. As mentioned in Section 2.1, another possibility is that binding happens by synchrony, and one may observe an earlier effect by assessing the synchrony instead of spike rates. Recently, Maldonado et al. (2008) reported an increase in synchrony between the spikes only 30 ms after fixation onset, when subjects were engaged in a natural scene free viewing task. This is in contrast to an enhancement in firing rates much later than this, peaked at 90 ms after fixation onset. These results could support this conjecture along with other studies that showed modulation in synchrony independent of significant changes in the firing rate (Vaadia et al., 1995; Hatsopoulos et al., 1998; Riehle et al., 1997, 2000; Grammont and Riehle 2003; Heinzle et al., 2007). In this regard, using local field potentials, which represent the activity of a larger population of neurons, instead of single-unit or multi-unit activity may be useful in investigating the role of primary visual cortex in binding, as local field potentials could be more sensitive to synchrony (Frien et al., 1994; Brosch et al., 1997). In the next section, we review the literature on local field potentials.

2.4. Local field potential

The recorded signals in an electrophysiological recording can be divided into two parts. One part, which is found in the high frequency components of the signal, represents spikes. Spikes reflect the activity of an individual (single-unit activity,

SUA) or a group of neurons (multi-unit activity, MUA). The other part, which is found mostly in frequencies lower than 300 Hz, represents the local field potentials (LFP). The contribution of LFP signals to various processes in the brain has been widely investigated in neuroscience. Despite its popularity, the exact origin of LFP signals has remained elusive, and as a result, the interpretation of LFPs has remained controversial. While the exact origin of the LFP has not been completely understood, the current consensus is that it represents the aggregate synaptic input to a region, as well as the synaptic activity of a large population of neurons (constituting of thousands of neurons) within the region, also it correlates well with subthreshold fluctuations of membrane potentials of these neurons. This is in contrast to action potentials that mostly represent the output of pyramidal cells and the output of the region (Caesar et al., 2003; Kayser et al., 2003; Logothetis, 2003; Henrie and Shapley, 2005; Rainer, 2008; Belitski et al., 2008).

The area surrounding the electrode that is reflected in the recorded LFP has not been accurately determined yet. While some studies have reported areas of several millimeters (Mitzdorf, 1985; Logothetis et al., 2001; Kreiman et al., 2006; Nauhaus et al., 2009), some other studies have estimated the area to be hundreds of micrometres (Engel et al., 1990; Liu and Newsome, 2006; Berens et al., 2008) surrounding the electrode. Recently, Katzner et al. (2009) combined electrophysiological recordings and voltage-sensitive dye imaging (VSDI) techniques, and concluded that based on the correlation of orientation tuning between these signals, the LFP is probably an aggregated signal from an area of 250 microns with respect to the electrode, although Jia et al. (2011) suggested that this may be valid only for evoked LFP and not for induced gamma responses. At the same time, while Logothetis et al. (2007) has claimed that all the frequency components of the LFP

propagate equally well through brain tissue (resistive model), other groups have claimed that the brain tissue attenuates the higher frequencies faster than the lower frequencies according to a model based on electric polarization and ionic diffusion of the medium (Bédard et al., 2006; Bédard and Destexhe, 2009), or capacitive model (Liu and Newsome, 2006). As a result, they proposed that the lower frequency components of the recorded LFP are the result of aggregation of a larger area surrounding the electrode compared to the higher frequency components (Bédard et al., 2004). However, Liu and Newsome (2006) came up with this explanation as they observed that LFPs were more highly tuned at higher frequencies compared to lower frequencies, and as a result, concluded that lower frequencies were the result of the aggregation of neuronal responses in a larger area compared to higher frequencies. Results of Jia et al. (2011) cast doubts on this conclusion, as they showed that high selectivity does not necessarily mean spatial concentration. They observed that LFPs could be highly tuned with similar selectivity across a span of several millimeters of cortex depending on the stimulus.

Despite all these controversies, LFPs have been widely used to investigate different aspects of the sensory system. LFPs have been shown to be modulated by different features of the stimuli. For instance, Gail et al. (2004) found correlations between the LFPs and perception in binocular rivalry, Montemurro et al. (2008) reported modulation of the phase of the LFP with natural movies, Kayser et al. (2003) showed differences in the LFPs when responding to natural movies and drifting gratings, and Roux et al. (2006) found correlations between expectancy and LFP responses in a motor task. Other groups have reported selectivity of LFPs for orientation, contrast, spatial and temporal frequency in the cat and monkey primary visual cortex (Eckhorn et al., 1988; Frien et al., 2000; Kayser et al., 2004; Henrie and

Shapley, 2005), as well as speed in the macaque area MT (Liu and Newsome, 2006), and sound frequency in the rhesus monkey auditory cortex (Kayser et al., 2007).

In addition to the evidence that LFPs may be responsive to sensory stimulation, and correlated with the cognitive state of the brain, it has also been shown that, in some cases, it can be used in place of spikes (Andersen et al., 2004). Mehring et al. (2003) showed explicit increases in decoding performance when combining LFPs and single unit activities (SUA) compared to using only SUAs in the motor cortex of rhesus monkeys performing center-out arm movements. They also observed more information in the LFP response for predicting the time course of the hand speed, and also predicting the arm that was moved, showing that LFP responses carry information potentially different from that contained in spikes. Belitski et al. (2008) also showed that the low frequency components of LFPs (< 40 Hz) recorded in the primary visual cortex of anesthetized macaques showed small signal and noise correlations with spikes in response to natural movies. As a result, they concluded that these frequencies were potentially generated using a mechanism independent of spike activity, and carried information different from that contained in spikes. Henrie and Shapley (2005) observed that modulation of the LFP with visual contrast continued even when the spike rates were saturated, providing evidence for a difference in the source of these two responses. Also, Pesaran et al. (2002) found that LFPs in lateral intraparietal cortex (LIP) of awake macaques were more informative when decoding the time course of a planned movement. Finally, Wilke et al. (2006) showed that the perceptual visibility of a target in a scene (the target in some trials of their experiment vanished perceptually from the scene) was reflected in low frequencies of LFP (9-30 Hz) in V1 and V2 of monkeys, while it was absent in spiking activity. In contrast to these findings, another study has showed that LFP signals can be predicted using the

spikes from a large area around the electrode (Nauhaus et al., 2009). As a result, it is possible that the differences observed between LFPs and spikes reported in other studies were due to the dissociation of the activity of single neurons from the activity of a large population of neurons represented by LFPs (Nir et al., 2007). Moreover, the discrepancies between unit activity and LFP could be because a large portion of the LFP activity probably originates in the activity of inhibitory interneurons, which are typically missed by single-unit recordings due to their small size and small spike amplitudes (Nir et al., 2007).

Even considering these results, it appears that local field potentials may capture information that may not be present in spike trains. Therefore, using local field potentials instead of spikes, or in conjunction with spikes, may potentially be useful in investigating perception, and particularly binding-by-synchrony as a mechanism underlying pre-attentive visual binding in the primary visual cortex, because LFPs are thought to reveal synchrony between neurons better compared to the spiking activity as mentioned earlier.

2.5 Aims and significance of the study

While the mechanism underlying scene segmentation has been widely studied in the field of neuroscience, it seems:

- the controversy surrounding the binding-by-synchrony hypothesis as a mechanism underlying visual binding has not yet been resolved

- the studies conducted on scene segmentation to date mostly have failed to detect an early effect in the primary visual cortex potentially due to the techniques and experimental paradigms used

The general aim of this study was to address some of the issues that probably contributed to these. The specific objective in this research was to find evidence for the binding-by-synchrony hypothesis in primary visual cortex. To perform this, we needed to

- use a stimulus and task that meets all the criteria essential for studying pre-attentive visual binding (Gray, 1999),
- use the activity from populations of neurons, as revealed by local field potentials, instead of single- or multi-unit activity, and
- use methods suitable for investigating synchrony in very short time windows.

The results of this study may shed some light on the correlation between visual saliency and neuronal responses in the primary visual cortex. If it can be shown that the neuronal responses in the primary visual cortex of monkeys can be modulated as a function of visual saliency, this may

- contribute to a better understanding of the mechanisms underlying scene segmentation in the primary visual cortex of primates,
- provide evidence that scene segmentation is initiated in this area of the brain.

In the subsequent chapters we will describe the experimental paradigm, followed by the methods applied to assess oscillation and synchrony.

Chapter 3

Single-Channel Analysis

An increase in power in the local field potentials in a particular frequency band may imply synchronous oscillatory activity in a large population of neurons in that frequency band (Gail et al., 2004; Beshel et al., 2007). In this chapter, we assessed the oscillatory power in different frequency bands to investigate the correlation between increases or decreases in power and the different stimulus conditions.

3.1. Experimental setup

3.1.1. Subjects and Surgical Procedures

The subjects were three adult, female rhesus monkeys (*Macaca mulatta*). The animals underwent two sterile surgical procedures to prepare them for training and recording. In the first procedure, a pair of scleral search coils for monitoring eye position (Judge, et al., 1980) and a stainless steel post for head restraint (Gray & Viana Di Prisco, 1997) were implanted. Following the behavioral training described below, the animals underwent a second surgical procedure, in which a hard plastic recording chamber was mounted over the opercular surface of striate cortex and secured to the skull with orthopedic screws and dental acrylic. A craniotomy was made in the bone overlying one hemisphere. The animals were given approximately

20 days to recover from each surgical procedure before behavioral training or recording was initiated. Surgical and experimental techniques were in accordance with institutional and NIH guidelines.

3.1.2. Behavioral Training

The animals were trained to maintain their gaze within 1.0° of a fixation spot, in the presence of moving or stationary visual stimuli, for a period of up to 3s. Successful trials were rewarded with a drop of apple juice. During behavioral training and recording, the animals' access to water was restricted. On days the animals were working, they were given a minimum of 30 ml/kg/day of water or juice in the form of fixation rewards or supplemental water. In practice, the animals earned an average of 50–80ml/kg/day. On Fridays and Saturdays, the animals received 80ml/kg/day of water. The animals were given supplemental water if any of the routinely monitored physiological parameters (i.e. plasma osmolality, urine specific gravity, body weight) became unacceptable.

3.1.3. Recording Techniques

Neuronal signals were recorded with multiple (2 to 8), tungsten micro-electrodes (1–2 MΩ resistance) from Microprobe (Gaithersburg, MD). The electrodes were mounted inside a multi-channel micro-manipulator and coupled to a recording chamber with a grid of 64 (8x8) guide holes (Gray et al., 2007). Each grid position was separated by 800 μm from the next grid position in the same row or column. Electrodes were loaded into grid positions that were separated by at least 3 grid positions, resulting in minimum separations of 2.4 mm. The electrodes were advanced

under computer control to a depth at which neural activity was first encountered. To further confirm the recording depth, the electrodes were retracted and the depth at which the last neural activity was encountered was recorded.

The signals were amplified (4000x), bandpass filtered (0.6 kHz–6 kHz), digitized (30kHz/channel) and stored for off-line analysis. After a recording was completed at a given site, the electrodes were always moved at least 200 μm before another recording was obtained. This sampling procedure was continued until activity could no longer be measured at a given guide tube location, at which time the recording locations were changed. Sometimes the sampling procedure across sessions involved recording from a second layer of V1 in the head of the Calcarine sulcus. This was confirmed by changes in receptive field position.

3.1.4. Visual Stimuli

The visual stimuli consisted of a perceptually salient contour embedded in a background pattern. Both contour and background were constructed from monochromatic Gabor patches presented on a gray screen of equal mean luminance. Each patch drifted within a stationary window in a direction orthogonal to its orientation. The background pattern consisted of a two-dimensional array of randomly oriented patches, having a uniform spatial density, and random positional jitter to avoid alignment cues (Bradley and Petry, 1977). The contours were formed by aligning a subset of the patches along a closed path and assigning them a common direction of movement. This configuration resulted in a perceptually salient contour that popped out from the background (Figure 3.1) and appeared to continually contract or expand. A movie example of the stimulus is available at http://cortex.nus.edu/Research/Contour.html.

Each contour was designed on-line during an experiment to optimally stimulate the non-overlapping receptive fields of two or more neurons under study. This was done using Hermite interpolation (Farin, 1990) during the experiment after the position, preferred orientation, and the direction of motion of each receptive field was characterized using mouse-controlled orientated bars and/or sinewave gratings. Given a pair of points (the centers of the receptive fields) and their tangents (the orientations of the receptive fields), this algorithm allowed us to generate intermediate points, with corresponding tangents, so that they formed a contour segment from the first receptive field to the second that was continuous in its first derivative. By reversing the order of the pair of receptive fields and repeating the interpolation, we were able to create a second contour segment going from the second receptive field to the first, thus creating a closed contour. In order to generate a contour that exhibited inter-patch distances equivalent to the patches in the background, we performed an initial interpolation with 10 patches for each contour segment. This allowed us to add the inter-patch Euclidean distances together to obtain an estimate of the segment length. This length was then divided by the inter-patch distance in the background to obtain the appropriate number of intermediate patches. Using this information, we then performed a second interpolation to obtain the positions and orientations of the intermediate patches.

This condition served as our high-salience condition, while two additional salience conditions were generated by adding orientation jitter (e.g. ±15˚ and ±30˚) to the Gabor patches that were not stimulating the receptive fields of the recorded cells. The stimulus within the classical receptive field was the same in all conditions. In this study, these saliency conditions, in which the receptive fields of the recorded neurons were part of the figure, are referred to as high-, intermediate- and low-salience figure

conditions respectively. In the remainder of this study, when we refer to the “figure” condition, we mean the high-salience figure condition unless otherwise stated.

These contours, at all three salience conditions, also appeared with equal probability at an alternative "control" location, at which the center of gravity of the contour was equidistant from the fixation point. This prevented the animals from developing a bias to the figure location. In addition, to prevent the animals from using small differences in the density of patches to perform the task, all the patches at the figure and control locations were present in every single trial, and the orientations of the patches at the control location were randomized for the figure conditions and vice versa. The only exceptions were the patches stimulating the receptive fields, as these remained constant across all conditions. The corresponding patches at the control location were also held constant, so the animal would not be able to key in on the patches stimulating the receptive fields and become unduly biased towards the contour location. In this study, the high-salience control condition is simply referred to as the “background” condition, as in this condition the receptive field of the recorded neurons were part of the background. The intermediate- and low-salience control conditions are referred to as intermediate- and low-salience background conditions.

Figures 3.1A to 3.1D show the high-, intermediate-, low-salience figure, and background conditions used for one recording. The receptive fields of the two simultaneously recorded neurons are highlighted using black rectangles. It can be seen that the Gabor patches in the receptive fields of the neurons were fixed across all conditions.

In each recording session, we typically generated 24 unique stimuli for each figure and background saliency condition, and repeated each of them twice for a total

of 6*24*2 = 288 trials. A small portion of "catch" trials were also included, in which no contour was present, i.e. the orientation of the patches at both the figure and control locations were randomized, but we continued to monitor one of the locations as the "correct" window. The animal's performance in these catch trials allowed us to estimate the chance performance of the animal. We typically generated 24 of these stimuli, half were figure trials and the other half were background trials, and repeated them twice as well, for a grand total of 288 + 2 * 24 = 336 trials in each recording session.

In this study, we particularly analyzed the data from high-, intermediate-, low-salience figure conditions, and the high-salience background condition. For these conditions, the stimulus in the receptive field was always the same and optimal for the recorded neuron. In the remaining conditions, i.e. intermediate- and low-salience background conditions, as well as in the catch trials, we varied the orientation and direction of the Gabor patch in the receptive field in order to obtain the direction-tuning curve of the neuron. We typically measured the responses at 4 directions on either side of the preferred direction with steps of 15˚. This meant that 18 (144 trials/ 8 directions) measurements were performed at each direction within the range of ±60˚ from the preferred direction.

All stimuli were presented on a 21" monitor, at a viewing distance of 57 cm, with a resolution of 1280 x 1024, and a refresh rate of 85 Hz.

3.1.5. Experimental paradigm

After an initial fixation of 500 ms, the stimulus was presented and the animals were free to saccade to the target as soon as it was detected. The animals received a juice reward if they made a saccade within 300 ms to the correct target window and

remained there for an additional 300 ms. If the animals failed to satisfy both criteria within a total of 600 ms, the trial was considered incorrect. In some cases, the animals performed multiple saccades, first to one window and then switching to the other window. If any of the saccades were to a location outside the target window, we considered the trial incorrect.

The eye positions were tracked from stimulus onset to the start of the saccade for all the trials in the selected recordings. Instead of measuring the eye positions with respect to the location of the fixation cross, we calculated the mean eye position for each session and used the deviation from this mean value for all the trials in each session. We did this because we found that the animal often exhibited small, but systematic, gaze deviations from the fixation target location. By computing eye positions in this manner, we were able to impose much stricter limits (±0.25˚ for two monkeys and ±0.5 for one monkey) to detect fixations.

The reaction time was computed by first separating the eye movements of the animal into saccades and fixations. The onset of the first saccade after stimulus onset was used as the reaction time.

3.1.6. Behavior

The distributions of the reaction times and performance for all 4 stimulus conditions (background, high-salience, intermediate-salience, and low-salience) are shown for all subjects (Figure 3.2A and Figure 3.2B), and for individual subjects (Figures 3.2C to 3.2H). It can be seen that, as expected, the reaction time systematically increased while the performance decreased as the saliency of the figure decreased. The reaction times and performance of the high-salience figure and background conditions, which contained an equivalent high-salience figure at the

control location, did not deviate significantly from each other (2-sample Kolmogorov-Smirnov test, $p < 0.01$).

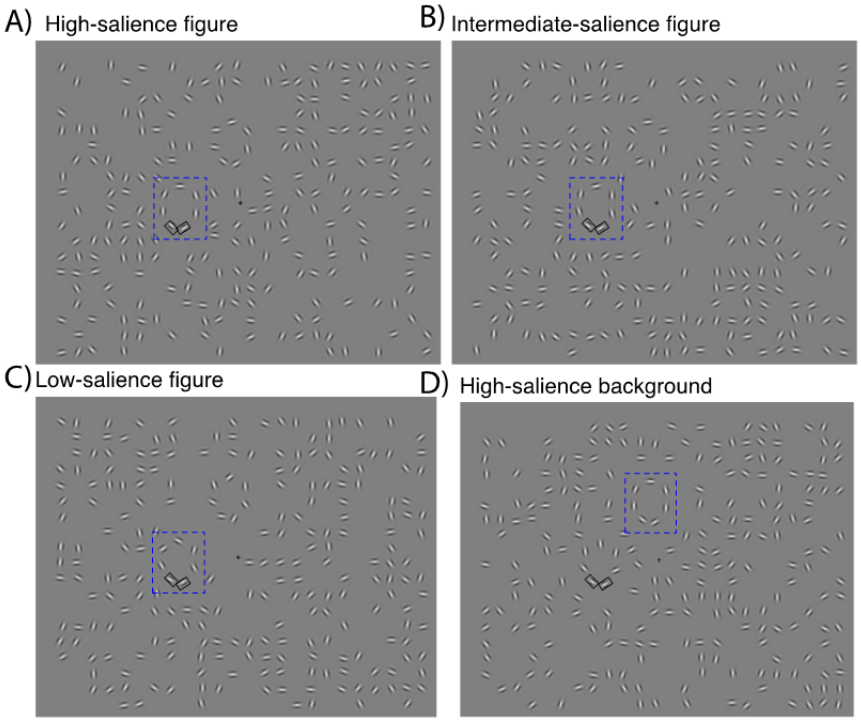

Figure 3.1. The visual stimuli consisted of an array of oriented, drifting Gabor patches, with a subset aligned to form a contour. The receptive fields of the neuronal populations under study are highlighted with two black rectangles. The location of the target contour for each condition is shown using a blue rectangle. The stimulus conditions depicted are: A) high-, B) intermediate-, C) low-salience figure conditions, and D) background condition.

3.2. Neuronal responses

3.2.1. Local field potentials

All raw waveforms were down-sampled to 5 KHz and filtered between 10 and 600 Hz using a Chebyshev Type II filter, which provided us with a steep roll-off and ripples in the stopband instead of the passband. These characteristics were useful for our analysis in Chapter 4, in which we needed to separate the signal into narrow band signals, so we decided to use the same type of filter for the initial filtering of the local field potentials as well. We used 10 Hz as the lower cut-off frequency for the filter

because this removed the DC component from the signal, and at the same time enabled us to use a filter of a smaller order compared to a filter with a lower cut off frequency of 1 Hz. This filtering was computationally less expensive, while the result of the analysis using this method was not different from using 1 Hz as the lower cut-off frequency. This was because the frequency resolution of our method was relatively low and we did not analyze frequency components lower than 10 Hz.

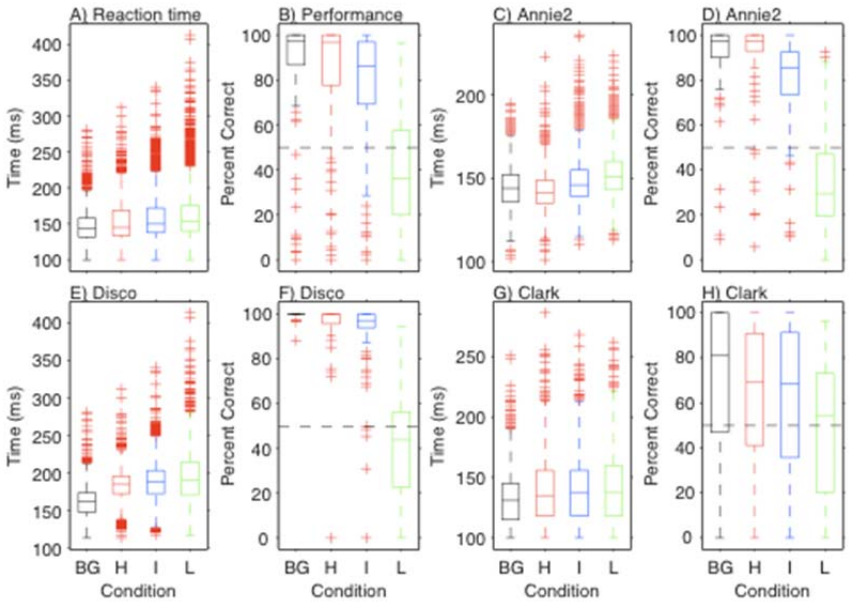

Figure 3.2. Distributions of the reaction times and performance of the subjects. A, B) All subjects. C - H) For 3 individual subjects. (BG: Background, H: High-, I: Intermediate-, and L: Low-salience figure).

To prevent the lower frequency components in the spikes from contaminating the local field potentials (Zanos et al., 2011), the spikes were removed from the raw data before filtering by applying a method similar to the method used in (Manning et al., 2009; Le Van Quyen et al., 2010). To perform this, each spike, consisting of 32 data points, identified using the steps described in Yen et al., (2007), was replaced with a linear interpolation between the point immediately preceding the spike and the point immediately following the spike (Figure 3.3). The resulting local field potentials, recorded on the electrodes with the receptive fields highlighted in Figure

3.1, are shown in Figure 3.4.

The filter was applied both in the forward and backward directions, to correct for the phase distortion that results from the nonlinear phase response of the filter. However, to prevent the neural response in the time window of interest (i.e. typically the time window from the stimulus onset to the time of the shortest reaction time across trials) from being contaminated by responses outside the time window due to the forward or backward filtering, we cropped the signal at the smallest reaction time before applying the filter, to ensure that changes in the neuronal response due to eye movements were not smeared into the time window preceding the reaction time as a result of backward filtering. Similarly, we also separated the baseline spontaneous activity period from the evoked response period before performing any analysis using the baseline to minimize contamination from the evoked response due to filtering.

We included both the transient and sustained responses into the analyses. This was necessary, because in our experiment the reaction times were very short (153.23 ± 28.39), and if there were any differences between the responses leading up to the reaction time of the animal, they presumably happened very early and close to the stimulus onset. These were the differences we were particularly interested in.

We only analyzed the trials with reaction times of at least 100 ms, because this gave us an acceptable amount of data for processing, and also because the trials with very small reaction times were most likely the trials in which the monkeys planned a saccade before inspecting the visual stimuli. The trials with large eye movements (defined as eye positions that exceeded a threshold of 0.25˚ from the fixation point for two subjects, and 0.5˚ from the fixation for the third subject) in the time window of interest, were also discarded because in these trials, the eye movements may have

caused the stimulus to drift out of the receptive fields of the recorded neurons, and thus cause changes in the neural response that were not due to the stimulus condition.

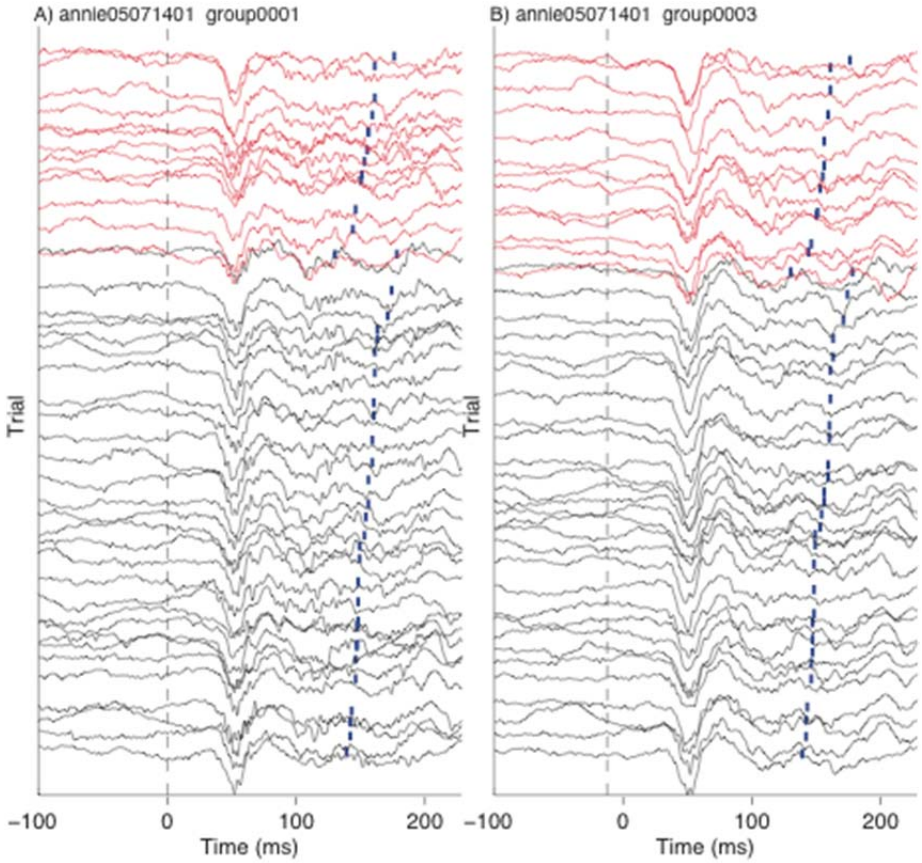

Figure 3.3. Local field potentials (band-passed filtered between 10 and 600 Hz) recorded simultaneously on two electrodes for the high-salience figure condition, aligned to stimulus onset (t = 0 ms). The responses are sorted with respect to reaction times (blue vertical lines), and separated into correct (black) and incorrect trials (red).

Finally, we discarded the sites in which one of the stimulus conditions contained fewer than 20 trials after the preprocessing steps. For the remaining data, if we were left with different numbers of trials in different stimulus conditions, we subsampled the trials across conditions to equalize the number of trials to avoid spurious differences that could be introduced due to differences in the number of trials.

3.2.2. Single-units and multi-units

For extraction and sorting of the single-units, any local minima that exceeded 6 times the standard deviation of the noise level were identified, and then 32 data points around each minima were stored to extract the spikes. The single units were isolated using the spike sorting method described in Yen et al. (2007).

To obtain the multi-unit activity at each site, we re-extracted the spike waveforms from the raw signals using three times the standard deviation of the noise level, instead of six times the standard deviation used for extracting the single unit spikes. Then we eliminated the spikes with the same time stamps as those in the sorted single units from the newly extracted spikes.

3.3. Single channel analysis

3.3.1. Fourier domain analysis

We applied the Fourier Transform to the filtered waveforms to perform frequency domain analysis of the signals. We used overlapping Hanning windows that were 50 ms in lengths, with steps of 1 ms. We chose window lengths of 50 ms because the reaction times of the animals were quite short, as mentioned above and shown in Figure 3.2, and because were interested in investigating the time course of the evoked response. However, due to the very short window lengths, it was not possible to use the multi-taper method (Jarvis and Mitra, 2001), which otherwise could have provided better energy concentration and lower variance.

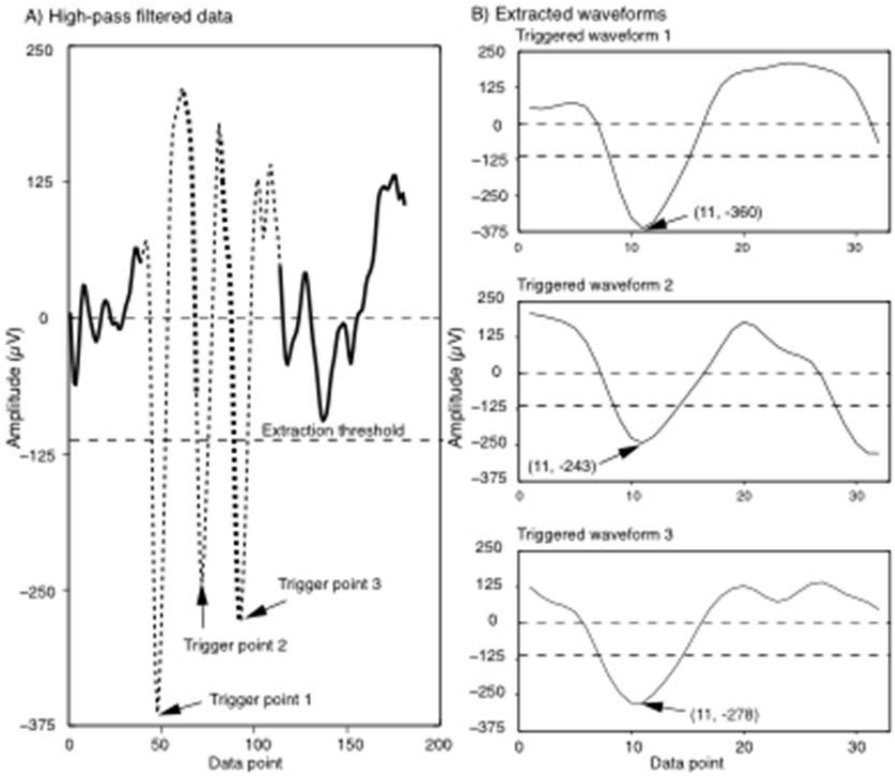

Figure 3.4. Waveform Extraction. A) A short segment of the high-pass filtered data is shown here. Three local minima that exceeded the extraction threshold (dashed line) are highlighted by arrows. The extracted waveforms are indicated by thin broken lines. Regions of overlap between the extracted waveforms are indicated by the thick broken lines. B) The three extracted waveforms corresponding to the three trigger points shown in A. The trigger points appear as data point 11 in each of the extracted waveforms. The first and second numbers in the parentheses indicate the data point number and the voltage respectively.

Response windows

Spontaneous activity: Each trial started with a 500 ms fixation duration. We used a portion of the data in this time window (i.e. 200 ms to 300 ms from the start of the trial) to characterize the spontaneous activity. This allowed us to discard the first 200 ms of each recording to avoid the effects of fixation cross onset (Mathewson, 2009), as well as anticipatory effects before the stimulus onset (Supèr et al., 2003; Lima et al., 2011).

Evoked activity: For each recording session, we found the earliest reaction time across trials and stimulus conditions, and made that the end of the evoked response in each trial. The beginning of the evoked response was defined by the smallest response

onset in the two high-salience conditions, i.e. figure and background. The response onset for each condition was determined by first computing the distribution of power at each frequency in the spontaneous period defined above and then comparing the distribution of power across trials in each window in the evoked response to those found in the spontaneous period using a one sided t-test ($p < 0.001$). Once we found 10 consecutive windows that exhibited significant differences with the spontaneous activity, we considered the beginning of the first window as the response onset.

In a small number of sites, we were not able to compute a response onset for either of the high-salience conditions. These sites were considered nonresponsive and were discarded from the rest of the analyses. We also discarded the sites with response onsets that exceeded the 75th percentile of the response onset distribution for all the sites, i.e. 23 ms after stimulus onset, because for these sites, the time interval between the response onset and the smallest reaction time was very short and resulted in only a few windows to analyze. After this preprocessing step, the total number of sites used for the rest of the analysis was 357 sites (Annie: 172, Clark: 99, and Disco: 86). Figure 3.5 shows the power spectra for all the stimulus conditions for one site. For this site, the power peaked at 40 Hz, and increased as the salience of the figure decreased.

Figure 3.6A shows the power distributions for one site computed across trials for different points in time for the evoked response across all stimulus conditions. The high-salience figure condition is shown in red, while the background condition is shown in black. Finally, for each trial, we normalized the power in each time window and at each frequency by subtracting out the averaged power in the corresponding frequency in the spontaneous period and summed the power computed at each frequency for the evoked response, and considered this the neuronal response for each

trial. We refer to this accumulated power value as the power response, or simply the response throughout the rest of this study.

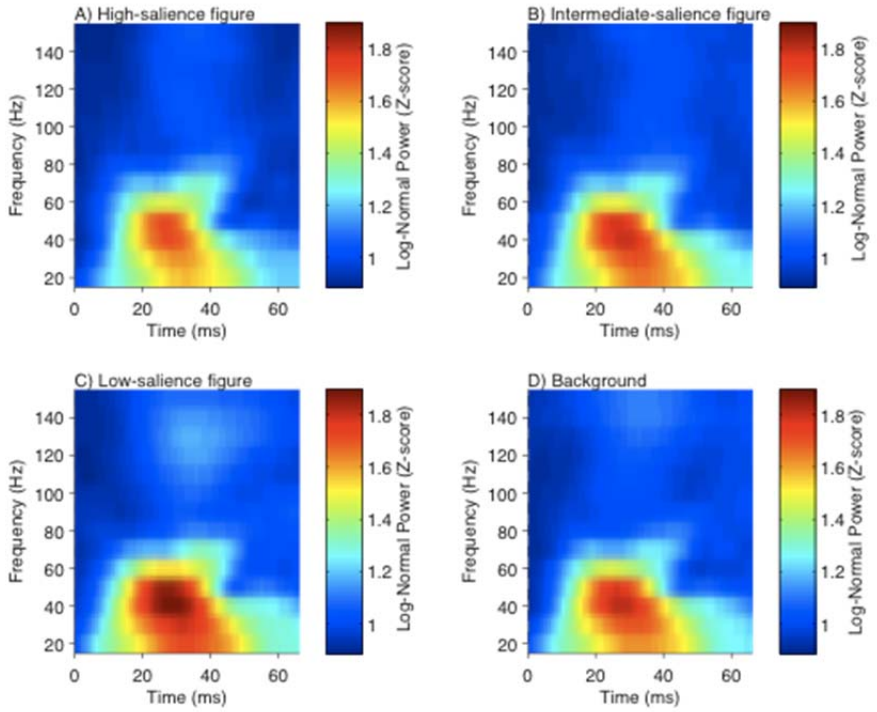

Figure 3.5. The log-normal power spectra for the A) high-, B) intermediate-, C) low-salience figure, and D) background conditions, averaged across trials for one site. The values shown are the logarithm of the Z-scores computed for each frequency by subtracting the mean of the baseline from the power values and dividing the results by the standard deviation of the baseline. Only frequencies below 150 Hz are shown in this figure for clarity although the signals were filtered below 600 Hz.

3.3.2. High-salience figure versus background condition

The first question we were interested in answering was whether we would be able to find differences in the LFP in the high-salience figure and background conditions. To perform this, we generated a receiver operating characteristic (ROC) curve for each site to compare the responses in the high-salience figure condition with the responses for the high-salience background condition. These responses were the power responses, as defined earlier. We then computed the area under the ROC curve (AUC). An AUC value significantly larger than 0.5 indicates that the two

distributions can be discriminated from each other. For instance, for the distributions shown in Figure 3.6A, the AUC value was 0.28. This means that, in this case, the power in the background condition was higher than those in the figure condition. In order to see if we could have gotten this AUC value by chance, we computed the AUC values for 1000 surrogates using a non-parametric permutation test (with $p < 0.05$). This means that we pooled all the trials from the figure and background conditions, and for each surrogate, randomly assigned, with replacement, subsets of these trials to each condition. This allowed us to test the null hypothesis that the responses to the figure and background conditions were not significantly different from each other. The sizes of the subsets were equal to the initial number of trials in each condition. We then computed an AUC value for each surrogate, and repeated this 1000 times, generating a distribution of AUC values. If the AUC value computed for the original data was outside the 95% confidence interval of the surrogate distribution, this suggested that the AUC value was unlikely to have been obtained by chance, and the response difference between the conditions was considered significant. The neuronal responses in the figure condition could be larger than those in the background condition, i.e. larger than 97.5th percentile of the AUC distribution, or they could be smaller, i.e. smaller than 2.5th percentile of the AUC distribution. Figure 3.6C shows the original AUC value computed for the original dataset, along with the distribution of the AUC values obtained by performing the permutation test. In this case, the original AUC value was smaller than the 2.5th percentile of the distribution, so the difference between the power responses for the figure and background conditions (Figures 3.6B and 3.6D) was significant for this site.

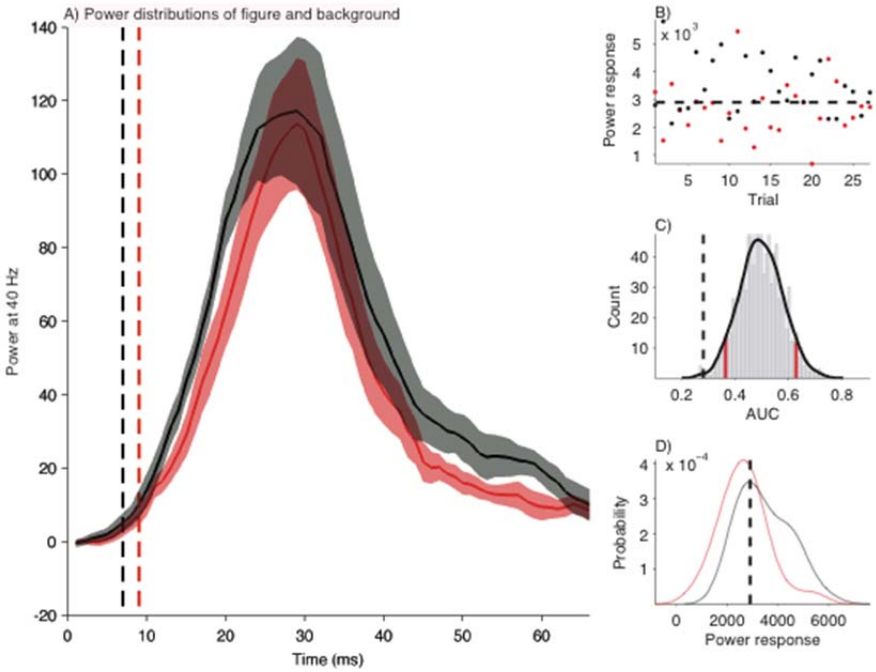

Figure 3.6. A) The medians of the power distributions of the high-salience figure (red) and background (black) conditions at 40 Hz for one site. The shaded regions represent the 95% confidence intervals of the medians computed using the equation described in McGill et al. (1978). The dashed vertical lines indicate the response onsets of the figure (red) and background (black) conditions. B) The power responses in the figure (red) and background conditions (black). C) The AUC value computed for the original data (dashed vertical black line) along with the distribution of the AUC values computed for the permutation test, as described in section 3.3.2. The 5th and 95th percentiles of the distribution are highlighted by red vertical lines. D) The distributions of the power responses of figure (red) and background conditions (black). The dashed horizontal line in (B) and the dashed vertical line in (D) indicate a sample threshold setting that returns a 70% hit rate for the figure responses.

3.3.3. Modulation as a function of saliency

The second question we wanted to investigate was whether we would be able to observe differences in the LFP as the salience of the stimulus changed. As the performance of the monkeys dropped systematically with decreases in saliency (Figure 3.2), we expected that, if the LFP was influencing behavior in any way, the response differences in the LFP should also change as a function of visual saliency. So, for the sites in which the responses for the figure condition were significantly different from the responses for the background condition, we checked to see if the neuronal responses changed as a function of saliency, and if this modulation was correlated with behavior. To perform this, we computed an AUC value for each

possible pair of figure saliency conditions, i.e. high-salience versus intermediate-salience, high-salience versus low-salience, and intermediate-salience versus low-salience figure conditions. If the AUC value was significantly above the chance level (using the same non-parametric permutation test as above, with $p < 0.05$) for one pair, it showed that the distribution of the responses for one saliency condition could be distinguished from the distribution of the responses of another figure saliency condition. Figure 3.7 shows the power distribution for different pairs of figure saliency conditions (Figures 3.7A to 3.7C) and the AUC values computed for individual pairs, along with the 2.5th and 97.5th percentile of the distributions obtained by performing the permutation test for each pair (Figures 3.7D to 3.7F).

In this particular example, the differences between the power for all figure saliency pairs were significantly different from each other, as the original AUC values for these pairs were all larger than the 97.5th percentile of their surrogate distributions. For this particular site, the AUC value that represented the discrimination between high- and low-salience figure conditions (Figures 3.7A and 3.7D) was clearly larger than that for high- and intermediate-salience figures (Figures 3.7B and 3.7E).

Subsequently, for the sites that showed modulation as a function of saliency, we studied the correlation between the neuronal responses and the behavior of the monkeys. For each figure salience condition, we computed the AUC value that represented the discrimination between the responses of that figure condition and the background condition and used this AUC value as the neurometric measure. These three AUC values formed the neurometric curve, while the performance of the monkey at each of the three salience conditions composed the psychometric curve. Then, we computed the correlation coefficient between the neurometric and psychometric curves.

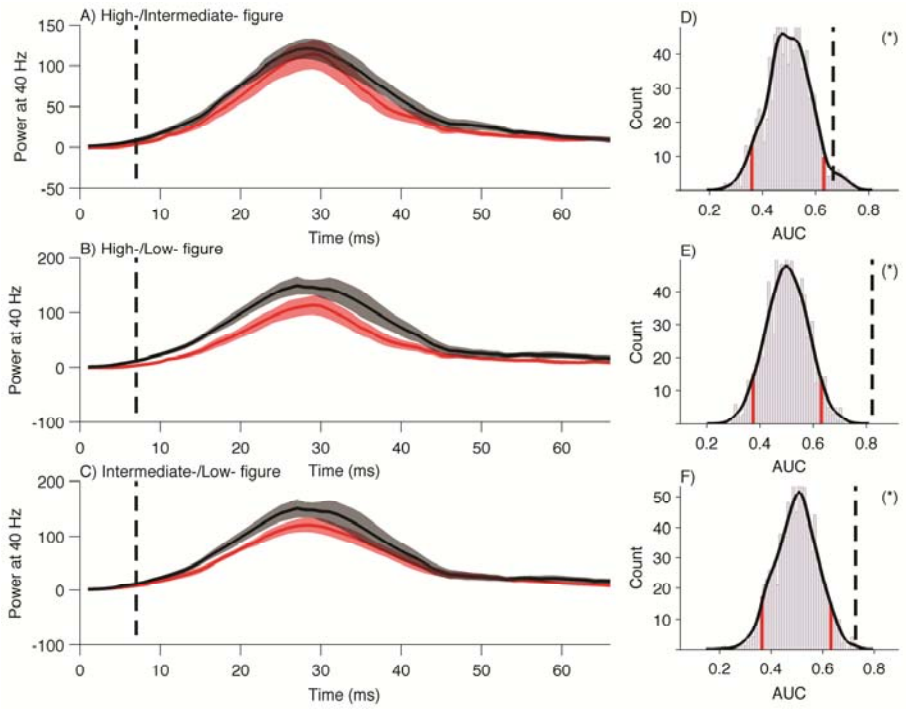

Figure 3.7. A - C) Power distributions for all pairs of figure saliency conditions at 40 Hz for one site. D - F) The AUC value of the original data along with the distribution of the AUC values computed using the permutation test. A, D) high- versus intermediate-salience. B, E) high- versus low-salience. C, F) intermediate- versus low-salience conditions. The conventions are as in Figure 3.6. The vertical lines in A - C represent the smallest response onset of the high-salience figure and the background conditions. The asterisks in D – F indicate that the differences between salience conditions were statistically significant.

Figure 3.8 shows the distributions of the power at 40 Hz for various salience conditions, and the psychometric and neurometric curves for one site. For this site, the neuronal responses and the behavior of the monkey were highly correlated (r = -0.90). We found 106 (29.69%) sites out of 357 recordings exhibited significant differences in the gamma power for high-salience figure and background conditions. Among these sites, 48 (45.28%) sites exhibited higher power for the figure condition compared to the background condition, while more sites 58 (54.71%) exhibited lower power for the figure condition compared to the background condition. The numbers of these sites at individual frequencies are shown in Figure 3.9 for individual subjects and frequencies.

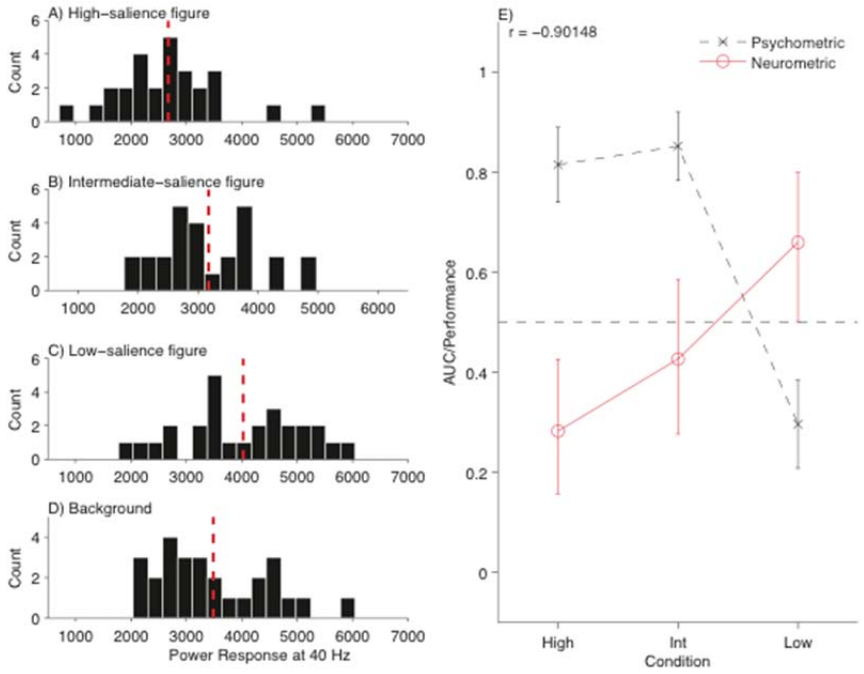

Figure 3.8. A – D) The distributions of the power responses for all figure salience conditions and the background condition at 40 Hz for one site. The vertical red line indicates the mean of the distribution. E) The neurometric (cross) and psychometric (circle) curves. The neurometric measure was the AUC value that represented the difference in the distributions between each salience condition and the background condition. The error bars for the neurometric curve indicate the 95% confidence intervals of the AUC distributions computed by bootstrapping (1000 samples), while the error bars for the psychometric curve indicate the standard errors computed using the assumption that the correct and incorrect responses were from a Bernoulli distribution. (High: high-, Int: intermediate-, and Low: low-salience figure; r: the correlation coefficient between the curves)

Figure 3.10 shows a comparison between the mean power of the figure and background conditions for different frequencies in the gamma band at sites that showed significant differences across all subjects.

For the sites with significant differences between the figure and background conditions, we examined the variation of the responses with saliency. We found 52 (49.05%) sites out of the 106 significant sites exhibited significant variation as a function of visual saliency. 26 of these sites were among the sites in which the power in the figure condition was higher than that for the background condition (54.16%), and 26 of these sites belonged to the reverse case (44.82%). These measures are shown in Table 3.1 for individual subjects.

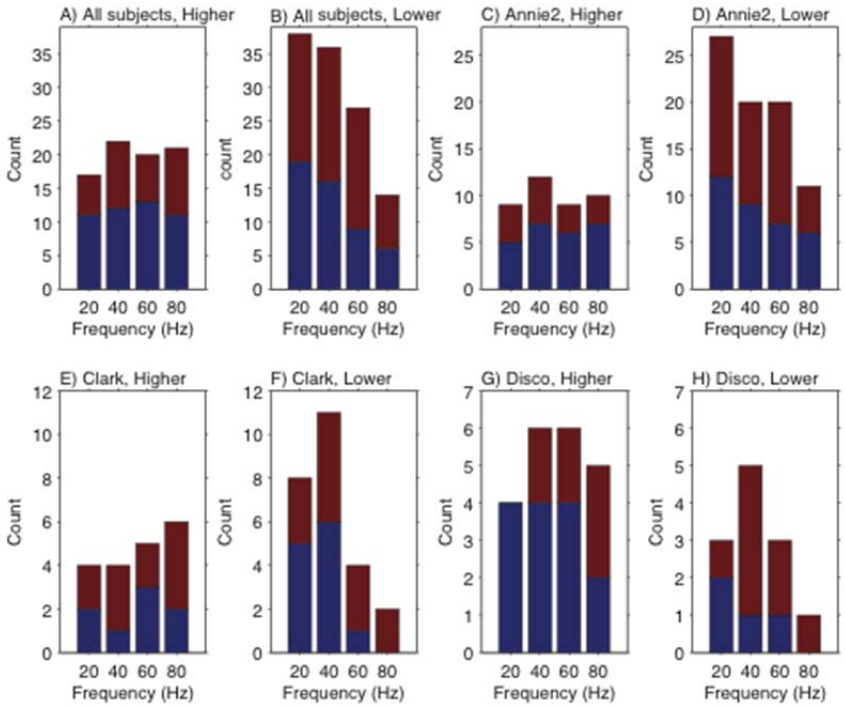

Figure 3.9. The number of sites that showed significant differences between the figure and background conditions for different frequencies. The blue sections of the bars represent the number of the sites that also showed modulation as a function of figure saliency. "Higher" indicates that the power of the figure condition was higher than the power of the background condition, and "Lower" indicates the reverse. A, B) For all three monkeys. C – H) For individual subjects.

For the sites that exhibited modulation with figure saliency, we computed an AUC value for each salience condition, which represented the discrimination between the responses in the figure condition and the responses in the background condition. These AUC values constituted the neurometric curve. Then, we computed the correlation coefficient between the neurometric and the psychometric curves. Figure 3.11 shows the distributions of these correlation coefficients for all subjects and individual subjects. We found that the neurometric measure was inversely correlated with performance when the power in the figure condition was smaller than that in the background condition, while it was directly correlated with performance for the reverse case. This was consistent with the hypothesis that with the decrease in saliency, the responses in the figure condition became more similar to the responses in the background condition.

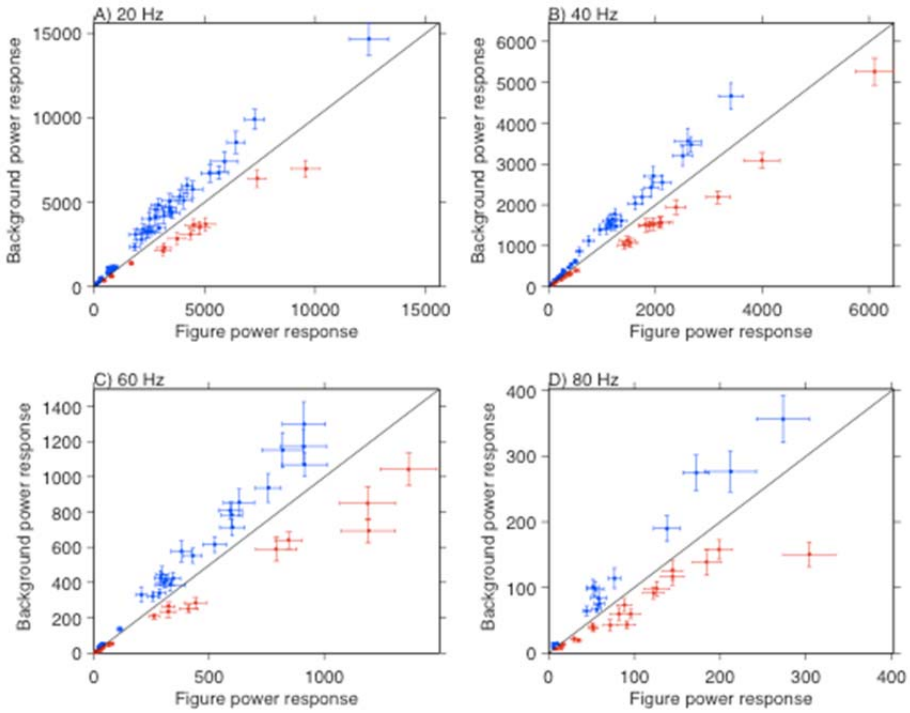

Figure 3.10. Comparison of the power in the figure condition with the power in the background condition at A) 20 Hz, B) 40 Hz, C) 60 Hz, and D) 80 Hz. Each axis represents the power response, i.e. sum of the power in the evoked response, averaged across trials. The error bars are the standard errors of the means

Table 3.1. The number of sites that showed significant differences in power between the figure and background conditions. "Higher" indicates that the power in the figure condition was higher than the background condition, and "Lower" indicates the reverse. The sites that also exhibited modulation in power as a function of contour saliency are shown in parentheses.

	Annie (172)	Clark (99)	Disco (86)
Higher	22 (14)	12 (4)	14 (8)
Lower	34 (17)	16 (7)	8 (2)

3.3.4. Time course

For the recordings sites that exhibited significant differences in the responses to the figure and background conditions, we observed that for some sites, the deviation between the responses started earlier, whereas for others it started later (e.g. the sites shown in Figure 3.12).

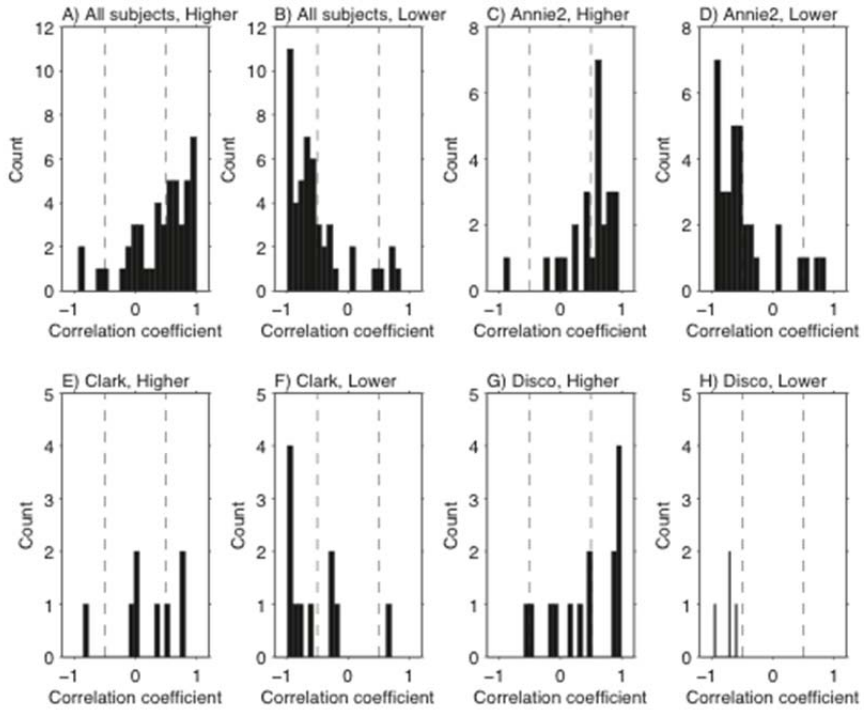

Figure 3.11. The distributions of the correlation coefficients computed between the neurometric and psychometric curves for the sites that showed significant modulation with figure saliency. A, B) For all three monkeys. C – H) For individual subjects. "Higher" indicates that the power in the figure condition was higher than the power in the background condition, and "Lower" indicates the reverse.

We were interested to see if there was a clear distinction between these early and late responses, as early responses could be indicative of feed-forward activity while late responses could be indicative of feedback from extra-striate areas. We examined the time course of the response differences, using the Kolmogorov-Smirnov test ($p < 0.05$), to compare the distributions of power in the figure and background conditions in individual 50 ms windows. Once we found 10 consecutive windows that showed significant differences between the two conditions, we marked the start of the first window as the point at which the responses in the figure and background conditions started to deviate from one another. In Figure 3.12, two sites with two different time courses can be seen. For one site (Figure 3.12A), the responses deviated from each other very early (10 ms after stimulus onset), while for the other site (Figure 3.12B), the deviations emerged later (28 ms after stimulus onset).

We first computed the distributions of all the bins that exhibited significant differences between the two conditions in the different frequency bands under study, because if we could observe bimodality in these distributions, this could suggest separation between the early (feed-forward) response and the late response (feedback). Unfortunately, we did not observe any bimodality in the distributions for any of the frequencies under study (Figure 3.13).

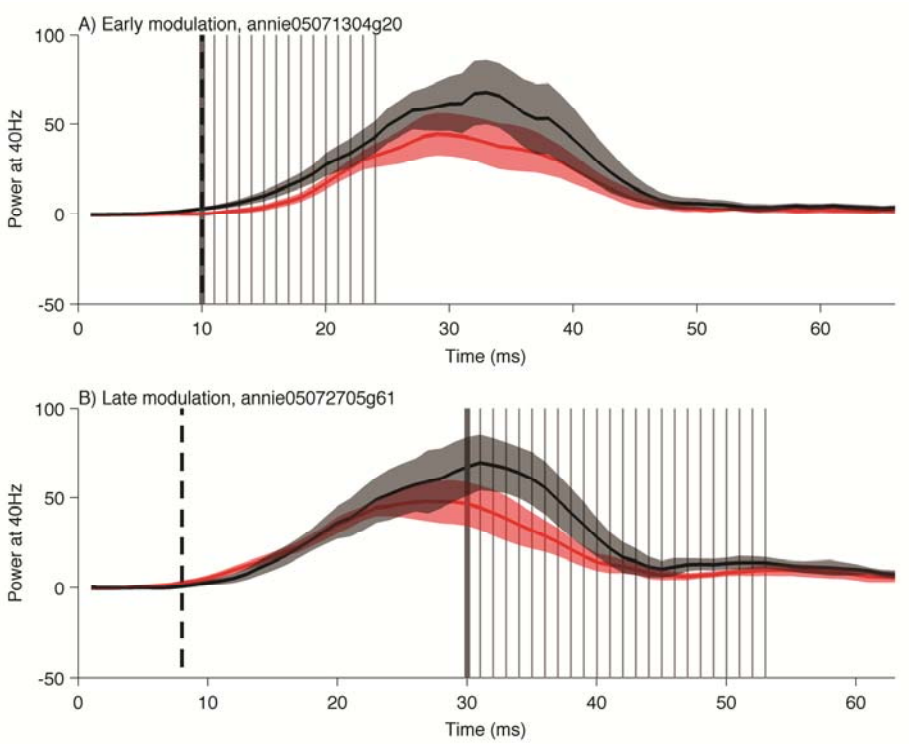

Figure 3.12. Different time courses of the deviation of the responses of the figure condition form the responses of the background condition. A) Early modulation. B) Late modulation. The vertical solid lines are the windows that exhibited significant differences between figure and background conditions. The bold line indicates the first window after the response onset that exhibited significant differences between the two conditions. The vertical dotted line represents the smallest response onset of the high-salience figure and the background conditions.

We also assessed the distribution of the first significant bin, mentioned above (Figure 3.14). It can be seen that these distributions also appeared unimodal.

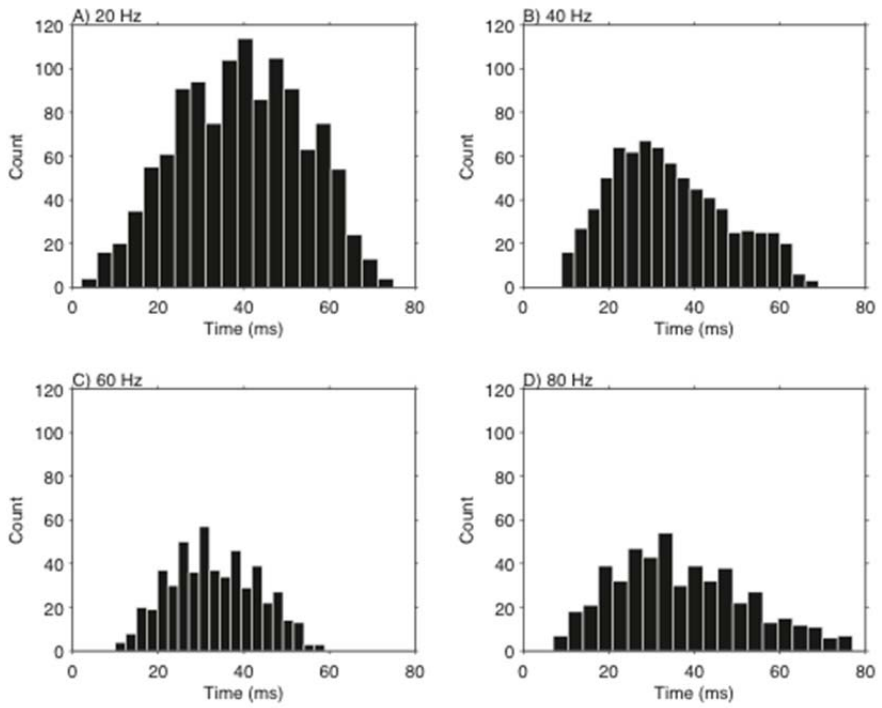

Figure 3.13. The distributions of significant windows for all significant sites at A) 20 Hz, B) 40 HZ, C) 60 Hz, and D) 80 Hz.

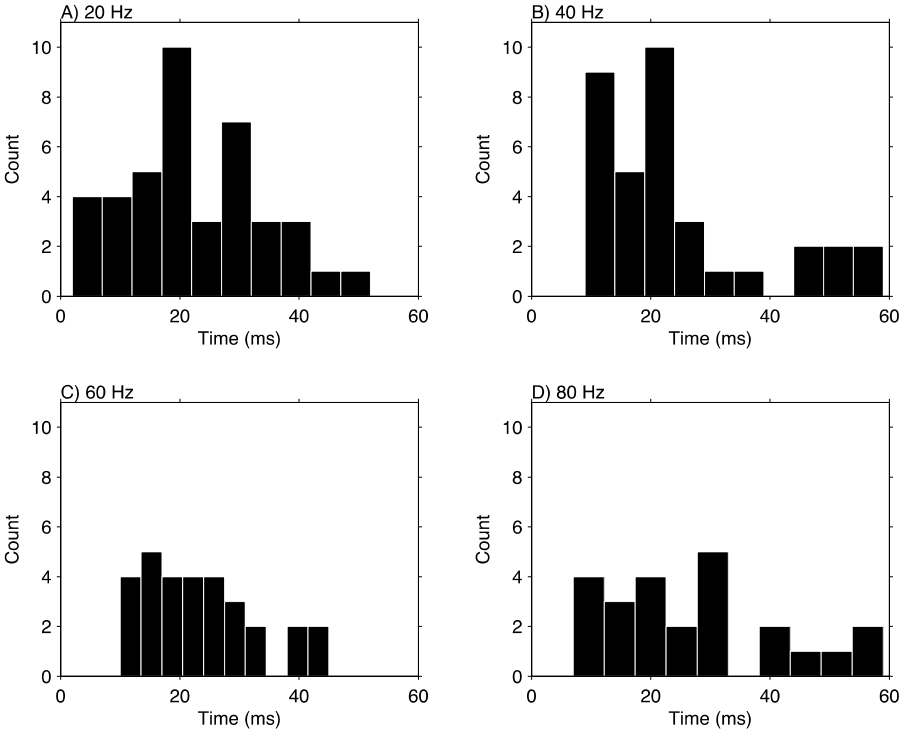

Figure 3.14. The distributions of the first significant window (of at least 10 consecutive significant windows) for all significant sites at A) 20 Hz, B) 40 HZ, C) 60 Hz, and D) 80 Hz.

However, the fact that some of the deviations started earlier than others, and ended earlier (Figure 3.12A), suggested that the responses in the figure and background conditions, i.e. figure-ground segregation, started to deviate in the feed-forward sweep for some sites. These results need to be interpreted cautiously, because the power at each bin was computed over an interval of 50 ms, so it is difficult to determine the exact timing of each event. However, for example, for the site shown in Figure 3.12A, the fact that the differences vanished 25 ms after stimulus onset could indicate that the differences observed from 10 ms to 25 ms after stimulus onset were not due to the contamination of the differences from the late response to the early response.

3.3.5. Dependence on experimental variables

As we found a fairly heterogeneous set of results, we checked to see if we could identify a relationship between the type of response difference, the depths of the recordings, and the tuning preferences of the neurons.

In order to investigate why the response in the figure condition was larger at some of the sites, smaller at other sites, and not significantly different at yet other sites, we grouped the sites that exhibited the different effects together to see if there were any differences in the depth (i.e. cortical layer) of the recording. The depth of each recording was obtained by computing the difference between the depth at which we performed the recording and the depth at which the last activity was recorded when the electrode was retracted (refer to section 3.1.3 for further details).

The recording depths for the different groups for all subjects are shown in Figure 3.15. We did not find any significant differences between the depth of the recording for the sites that exhibited significant differences between figure and

background conditions, and for the sites that did not (Table 3.2), as shown in Figures 3.15A to 3.15C. We found this using the two-sample Kolmogorov-Smirnov test (Annie2: $p > 0.68$, Clark: $p > 0.59$ and Disco: $p > 0.53$).

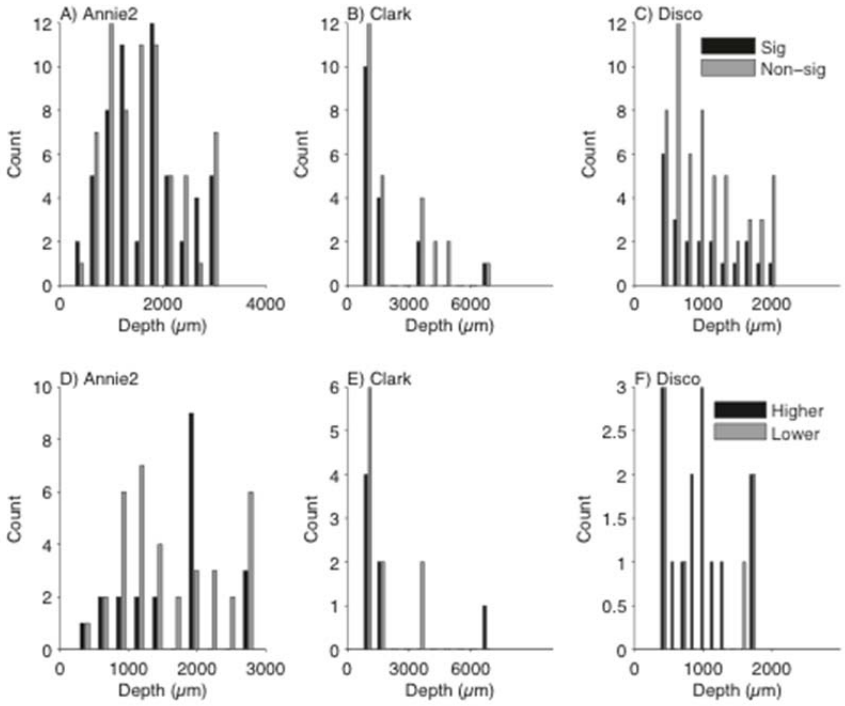

Figure 3.15. Comparison between the depth of the recording for A) "Significant" and "Non-significant" and B) "Lower" and "Higher" sites. "Significant" indicates that at least in one frequency, the power in the figure condition was significantly different from the power in the background condition. "Non-significant" indicates that the power in the figure condition was not significantly different from the power in the background condition in any of the frequencies. (Sig: Significant, Non-Sig: Non-significant). "Higher" indicates that the power in the figure condition was higher than the power in the background condition, and "Lower" indicates the reverse.

This was also the case when we compared the depth of the recording for the sites that showed higher power, and the ones that showed lower power in the figure condition compared to the background condition (Table 3.3), as shown in Figures 3.15D to 3.15F. Again we found this using the two-sample Kolmogorov-Smirnov test (Annie2: $p > 0.49$, Clark: $p > 0.99$ and Disco: $p > 0.76$). We also assessed the relationship between the depth of the recordings and the latency to the emergence of significant differences between the responses in the figure and background conditions (Figure 3.16, Annie2: 16, Clark: 5, Disco: 13 sites). Although there seemed to be a

positive correlation between these measures (Pearson correlation), the correlation was not significant (correlation coefficients and their corresponding p-values are reported in the figure captions).

Table 3-2. The depth of the recording for the sites that exhibited significant differences between figure and background conditions ("Significant") and for the sites that did not ("Non-Significant").

		Annie	Clark	Disco
Site	Significant	57	17	21
Mean ± std		1619.39 ± 757.30	1755.41 ± 631.15	965.52 ± 537.64
Site	Non-Significant	69	26	57
Mean ± std		1636.63 ± 798.68	2295.30 ± 1781.99	1035.10 ± 555.83

Table 3-3. The depth of the recording for the sites that showed higher power ("Higher"), and the ones that showed lower power ("Lower") in the figure condition compared to the background condition.

		Annie	Clark	Disco
Site	Higher	22	7	14
Mean ± std		1634.52 ± 727.29	1986.14 ± 2283.36	929.78 ± 444.95
Site	Lower	36	10	7
Mean ± std		1603.72 ± 774.80	1593.9 ± 1088.04	1037 ± 725

Next, we examined the orientation tuning of the local field potentials. In this analysis, we considered all the recordings, including the recordings that were discarded for our other analyses because of the response onset constraint or the number of trials based on the criteria described in Section 3.2.1. As mentioned in the "Visual stimuli" section, Section 3.1.4, we varied the orientations of the Gabor patches in the receptive fields of the neurons to obtain the orientation tuning of the cells. To compute the tuning curves for the local field potentials, we summed the power responses from 20 to 80 Hz, and then used the averaged value across trials to generate the tuning curve. For single units and multi units, we used the spike count to generate the orientation

tuning curves. Examples of these tuning curves for three example sites are shown in Figure 3.17. We applied a balanced one-way ANOVA test ($p < 0.01$) to identify recording sites that exhibited orientation tuning, and then fitted the responses with a circular Gaussian. We also used the Gaussian fit to quantify the differences between the preferred orientations computed using the local field potentials and those computed from the activity of single units. For the sake of simplicity, we refer to this deviation of the preferred orientation from the stimulus orientation as preferred orientation deviation in the rest of this study. The Gaussian provided us with the tuning width (2 times the standard deviation) and the strength of the orientation tuning (described below).

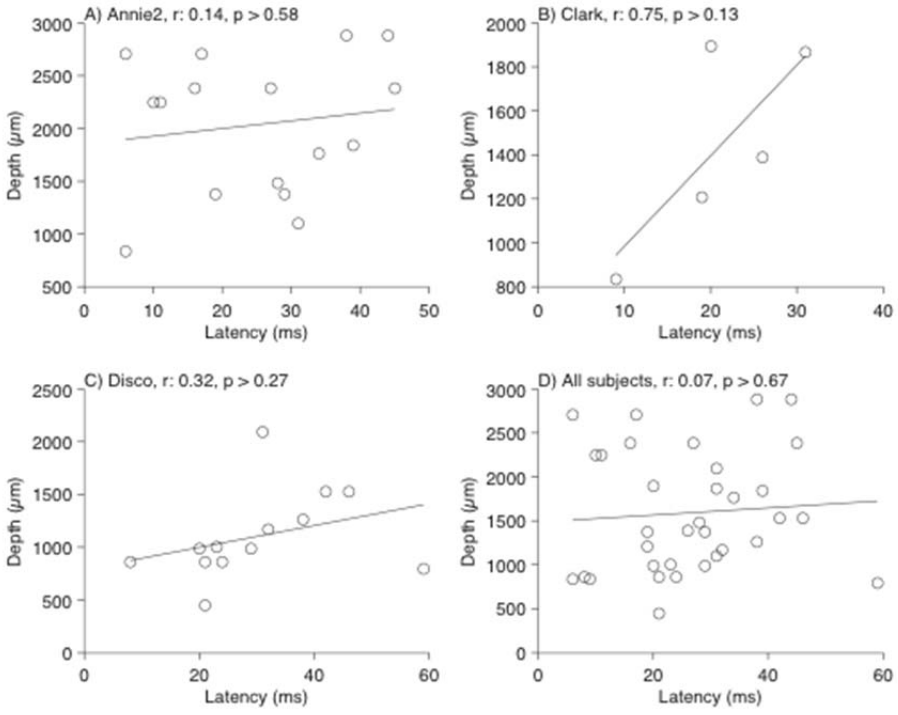

Figure 3.16. Correlation between the depth of the recording and the latency of the response modulation for individual subjects A – C, and all subjects D. (r: correlation coefficient).

To compute the tuning strength we found the data point on the tuning curve that was the closest to the baseline of the fitted Gaussian, and divided the peak value of the Gaussian fit by the standard deviation of the tuning curve at this point. This

method takes into account the fact that the variability in local field potentials is much larger than single unit and multi unit activity, which can be observed in Figure 3.17. This was necessary because otherwise the tuning strength of local field potentials may spuriously seem higher than single unit and multi unit activities as stated by Berens et al. (2008). We also examined other measures such as peak to baseline ratio and the p-value returned by ANOVA test, but the results were very similar, so we only reported the results obtained using the first method.

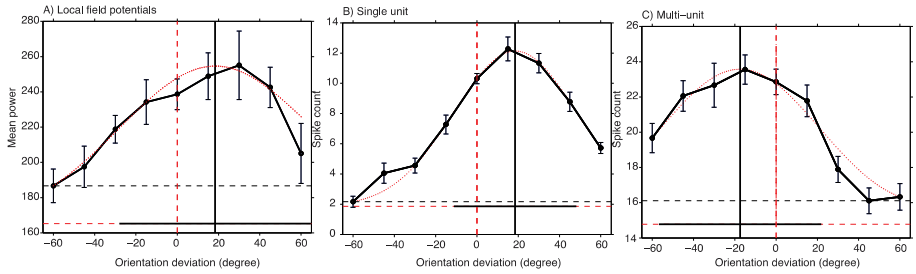

Figure 3.17. Example tuning curves for three different sites. A) LFP (preferred orientation deviation = 18.31, width = 97.73, strength = 7.24), B) SU (preferred orientation deviation = 18.51, width = 59.34, strength = 19.09) and C) MU (preferred orientation deviation = 17.41, width = 78.58, strength = 10.35). The dashed vertical line indicates the orientation of the hand-mapped receptive fields, while the dashed horizontal line indicates the baseline activity.

The strength and width of the orientation tuning of the local field potentials and the preferred orientation deviation of the LFPs are shown in Figure 3.18. We found 56 sites in which the local field potentials exhibited clear orientation tuning preferences.

This was consistent with other studies that reported the tuning of local field potentials with orientation (Eckhorn et al., 1988; Frien et al., 2000; Kayser et al., 2004), although this constituted a small percentage (11.55%) of all the recordings (485 sites). This was probably because the LFP represents the activity of a large population of neurons with different orientation tuning preferences. This may have caused some of the responses to cancel each other out, and lead to a much weaker overall response.

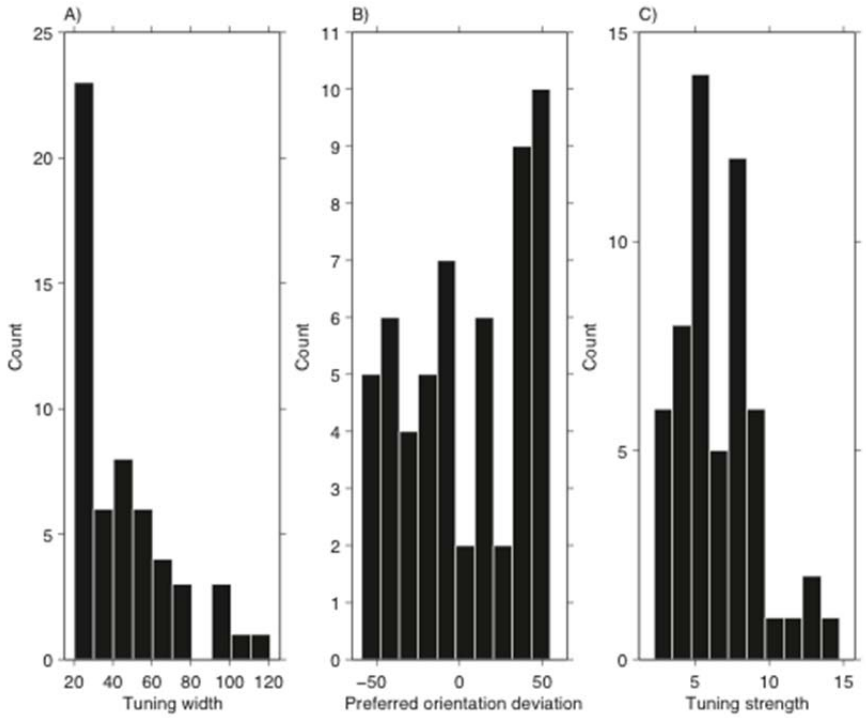

Figure 3.18. Characteristics of the orientation tuning found in the local field potentials. A) Tuning width. B) Preferred orientation deviation. This orientation is the preferred orientation of the LFP relative to the stimulus orientation. C) Tuning strength.

In comparison, we generated tuning curves using the multi-unit and single-unit activity (MUA and SUA, respectively) for sites in which they were available. The percentage of tuned multi-units and single-units was 56.13% (270 out of 481), and 49.10% (164 out of 334), respectively. In investigating the relationship between unit and LFP tuning, we found 15 occurrences in which both the LFPs and SUAs were tuned, and 39 occurrences in which both LFPS and the MUAs were tuned. Figure 3.19 shows the comparison between the width and the strength of the orientation tuning, and the preferred orientation deviations in the SUA and MUA versus the LFPs. The same data is shown for 115 MUAs versus SUAs as a reference. The strength of the tuning in the SUAs and MUAs were significantly larger compared to the LFPs, the strength of tuning in SUAs were significantly larger compared to MUAs, and the width of the tuning in the MUAs were significantly larger compared to the SUAs (sign

test, $p < 0.05$). However, there were no significant differences between the other tuning characteristics (sign test, for tuning width, LFP vs. SUA: $p > 0.3$, LFP vs. MUA: $p > 0.25$, for preferred orientation deviation, LFP vs. SUA: $p = 1$, LFP vs. MUA: $p > 0.19$, MUA vs. SUA: $p > 0.35$). We were especially surprised to find that the tuning widths for the LFPs were not significantly wider than the MUAs, given previous reports that higher orientation sensitivity was reported for MUAs compared to LFPs (Frien et al, 2000; Berens et al, 2008). This discrepancy may potentially be due to the fact that in our data, the number of sites with both tuned LFP and tuned SUA was relatively small.

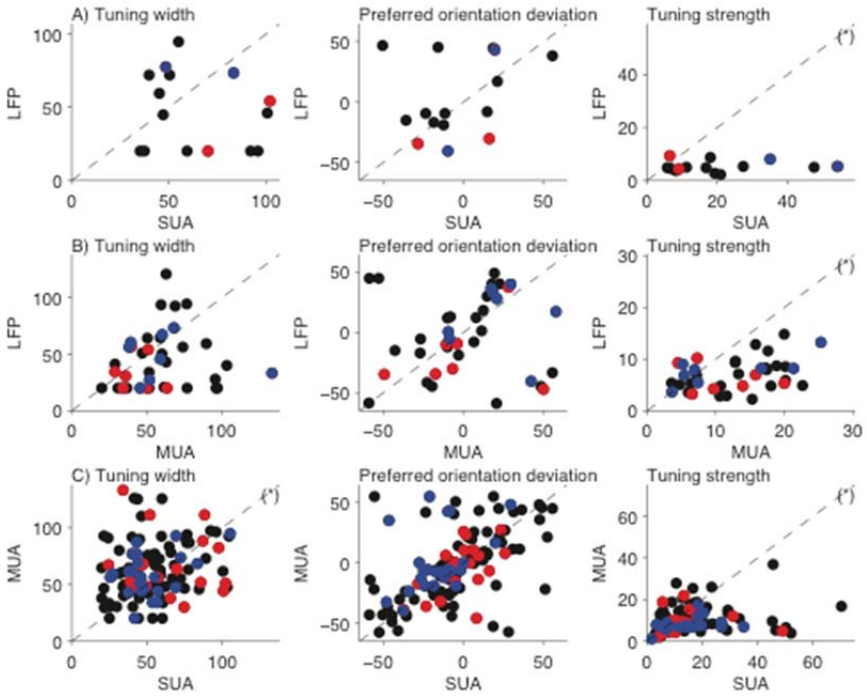

Figure 3.19. Comparison of the orientation tuning characteristics of A) LFPs and SUAs, B) LFPs and MUAs, and C) SUAs and MUAs. The sites that showed significant differences between figure and background conditions are shown in red (higher power in figure compared to background conditions) and blue (lower power in figure compared to background conditions). The black dots represent non-significant sites.

For the sites that showed both orientation tuning and a significant difference between the figure and background conditions ($n = 18$), we compared the strength and

width of the tuning, as well as the preferred orientation deviation, with sites that did not show significant differences (n = 35). We did not find any significant differences between the tuning characteristics of these groups. We examined this using the two-sample Kolmogorov-Smirnov test for tuning width ($p > 0.88$) and tuning strength ($p > 0.44$) and the Kuiper's test for preferred orientation deviation ($p > 0.1$). This was also the case when we performed the same comparison in sites in which the figure response was larger (n = 8 tuned sites) and sites in which it was smaller (n = 11 tuned sites). This was also examined using the two-sample Kolmogorov-Smirnov test for tuning width ($p > 0.85$), tuning strength ($p > 0.23$), and the Kuiper's test for preferred orientation deviation ($p > 0.1$). The means and standard deviations for tuning width, tuning strength, and preferred orientation deviation of all these cases are shown in Tables 3.4 and 3.5.

Table 3-4. The means and standard deviations of the orientation tuning characteristics in the LFPs for sites that exhibited significant differences between figure and background conditions ("Significant") and the ones that did not ("Non-significant").

	Width	Preferred orientation deviation	Strength
Significant	43.95 ± 23.91	-3.73 ± 34.44	6.91 ± 2.50
Non-significant	42.25 ± 27.06	3.37 ± 34.43	6.28 ± 2.97

Table 3-5. The means and standard deviations of the orientation tuning characteristics of local field potentials for sites in which the power response in the figure condition was higher than the power response in the background condition ("Higher"), and the sites in which the response in the figure condition was lower ("Lower").

	Width	Preferred orientation deviation	Strength
Higher	39.17 ± 21.38	-12.06± 31.01	6.12 ± 2.45
Lower	50.47 ± 26.45	7.49 ± 35.89	7.40 ± 2.46

For two of the monkeys, we also found significant differences between the figure and background conditions, as well as across saliency conditions using single

unit and multi unit activities (Bong et al., 2012). We were interested to see if there was a correlation between those sites and the ones that showed significant differences using LFPs. Out of 21 significant single units in one subject, 10 sites also showed significant differences between LFPs. In the other subject, 1 out of 3 single units showed significant differences in the LFPs. 60 local field potentials for one subject and 26 for the other subject showed significant differences even though the single units were not significant. We also performed the same analysis using the multiunit activity. Out of 15 significant multi units in one monkey, 3 sites also showed significant differences using LFPs, and in the other monkey, this was 2 out of 3. 67 LFPs for one subject and 25 for the other subject showed significant differences, while the multi unit activities were not significantly different from each other. This implies that LFPs and spikes may carry different information about the stimulus in accordance with Pesaran et al. (2002), Mehring et al. (2003), and Belitski et al. (2008).

Chapter 4

Multi-Channel Analysis

In the previous chapter, we described changes in the oscillatory power of the LFPs at individual recording sites that reflected figure-ground segmentation, as well as changes that reflected stimulus saliency. In this chapter, we investigated the relationship between the stimulus conditions described previously and the LFPs at paired recording sites.

4.1. Synchrony analysis using phase-locking value

As described in Chapter 3, we typically recorded simultaneously from two or more electrodes in each experiment. The receptive fields of the neurons recorded on these electrodes were either all part of the figure, or all part of the background. To investigate the relationship between these populations of neurons, we measured the phase-locking (i.e. synchronous oscillations) between pairs of simultaneously recorded LFPs, and compared the degree of synchrony across conditions. We also recorded simultaneously from more than two electrodes in a few cases. In those cases, we computed the phase-locking between all possible pairs of LFPs. For simplicity, throughout the rest of this chapter, we refer to each of these pairs of simultaneously recorded activities as “a pair”, and to each of the members of a pair as an “electrode”.

The LFPs were obtained using the method explained in Chapter 3. One example of a LFP recording is shown in Figure 4.1A. All the preprocessing steps were the same as those described in Section 3.2.1. The only exception was that we did not equalize the number of trials, but instead used other methods to compensate for the differences in the number of trials of the conditions. These methods will be explained in each section correspondingly.

To measure synchrony, we applied the Hilbert transform to the filtered waveforms in order to compute the analytical form of the waveforms, and to obtain both the instantaneous phase and instantaneous amplitude. The analytical form of a waveform can be defined as follows.

$$S_a(t) = S(t) + i\tilde{S}(t) = A(t)e^{i\varphi(t)} \tag{4.1}$$

in which $\tilde{S}(t)$ is the Hilbert transform of the signal, *A(t)* is the amplitude envelope, and *φ(t)* is the instantaneous phase. The Hilbert transform can be defined as the convolution of a signal with 1/πt as follows.

$$\tilde{s}(t) = \frac{1}{\pi} P.V. \int_{-\infty}^{+\infty} \frac{s(t)}{t-\tau} d\tau \tag{4.2}$$

In this integral, *s(t)* is the signal and $\tilde{s}(t)$ is the Hilbert transform of the signal, while P.V. is the Cauchy principal value of the ill-defined integral. The instantaneous phase of this analytical form, i.e. *φ(t)*, is physiologically meaningful only if the bandwidth of the waveform, i.e. *S(t)*, is narrow (Le Van Quyen et al., 2001). Thus, we filtered the LFPs in relatively narrow frequency bands using a

Chebyshev Type II filter. When assessing the Fourier power spectra, we found that most of the trials were oscillating in the frequency range of 20 Hz to 80 Hz (Figure 3.4). This was important because although phase-locking can be defined for two non-oscillating signals as well, in the context of a biological explanation, it may not be very easy to justify. So we plotted the histogram of the z-scores computed for the power spectra for both electrodes for the figure condition, and ensured that the histogram was bimodal, showing that there was a clear modulation in gamma band power. We band-passed filtered the LFPs in consecutive frequency bands centered at frequencies from 20 to 80 Hz (gamma band) in steps of 10 Hz, and in the range of [-5 5] Hz around each central frequency (e.g. 15 – 25 Hz, 25 – 35 Hz, 35 – 45 Hz, etc.).

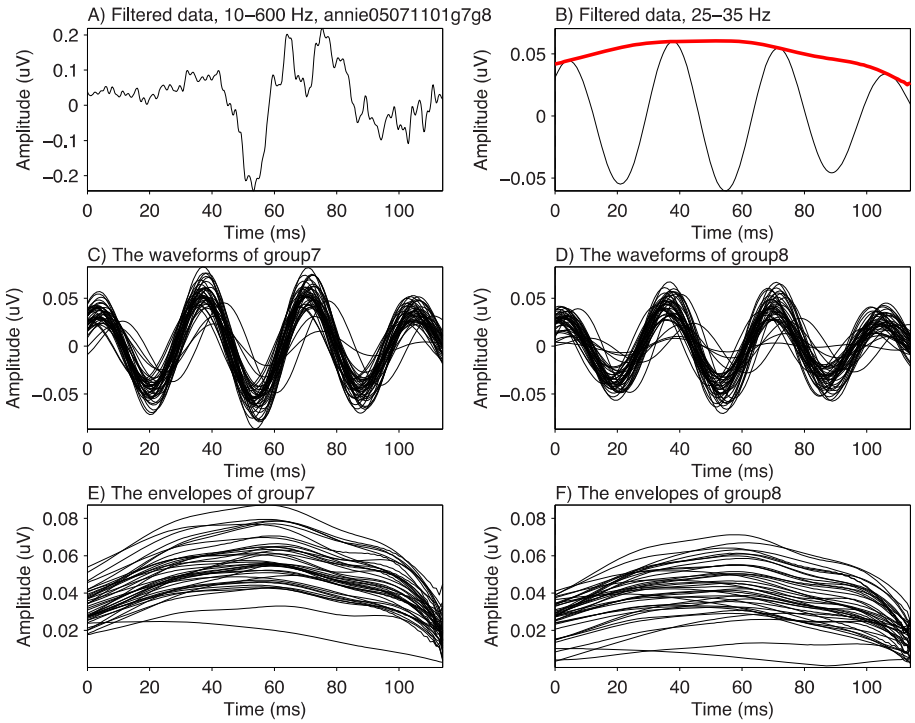

Figure 4.1. A) A sample LFP. B) The waveform in (A) after it was band-passed filtered in the 25 – 35 Hz frequency band. The amplitude envelope of the waveform is shown in red. C, D) Band-passed filtered waveforms in the 25 – 35 Hz frequency band for a pair of simultaneously recorded LFPs (groups 7 and 8). E, F) The amplitude envelopes of the waveforms in C and D, respectively.

Figure 4.1B shows the waveform in Figure 4.1A after it was band-passed filtered in the 25 – 35 Hz frequency band along with its amplitude envelope. All the waveforms that were recorded simultaneously on the two electrodes of one pair, are shown in Figures 4.1C and 4.1D after they had been band-passed filtered in the 25 – 35 Hz frequency band, while their amplitude envelopes are shown in Figures 4.1E and 4.1F.

This method does not impose any constraints regarding the stationarity of the signal (Le Van Quyen et al., 2001). It should be noted that, in contrast to the short-time Fourier Transform analysis, this method does not explicitly require processing data in short windows, which restricts the frequency resolution of the method. However, the time-frequency uncertainty principle (Gabor, 1946) applies to this method, and due to the filtering of the signal into narrow frequency bands, the time resolution of the analysis is limited.

After computing the analytical form of the waveforms, we quantified the phase-locking between the waveforms recorded simultaneously on two different electrodes using the phase-locking value (PLV) measure (Lachaux et al., 1999):

$$PLV(f,t) = \left| \frac{1}{N_{trial}} . \sum_{trial=1}^{N_{trial}} \exp(j(\phi_{y,trial}(f,t) - \phi_{x,trial}(f,t))) \right| \tag{4.3}$$

in which

$$\exp(j(\phi_y(f,\tau) - \phi_x(f,\tau))) = \frac{s_{ax}(\tau,f)s_{ay}^{*}(\tau,f)}{|s_{ax}(\tau,f)||s_{ay}(\tau,f)|} \tag{4.4}$$

and $\phi_y(f,\tau)$- $\phi_x(f,\tau)$ is the difference between the instantaneous phases of the recorded waveforms on electrodes *x* and *y* at time τ, after they were band-passed filtered in frequency band *f*, while S_{ax} and S_{ay} are the analytical forms of the waveforms. The PLV represents the circular variance of the phase differences (Young and Eggermont, 2009), and varies between 0 and 1, with 1 indicating perfect phase-locking between the waveforms, and 0 indicating no phase-locking.

To compute this measure, averaging across trials is essential, as the PLV measures the consistency of the phase difference across repetitions assuming the stationarity of phase shifts across trials. It should be noted that while a large PLV indicates a consistency of phase-shifts across trials, it does not necessarily imply synchrony (0 phase shift). In order to look at synchrony, we would need to verify that the PLV was also associated with a small phase shift. Figure 4.2 shows the PLVs computed for different stimulus conditions during spontaneous (as defined in Chapter 3, -300 ms to -200 ms from the start of the trial) and evoked activity for the pair shown in Figure 4.1. It can be seen that the PLVs during the evoked response (from the stimulus onset to the smallest reaction time, across all stimulus conditions) were typically very high, probably due to the large transient response. The PLV is not sensitive to the amplitude of the signals, and measures phase-locking independent of the amplitude correlation (Lachaux et al., 1999), but stimulating the neurons simultaneously apparently introduces a very large stimulus locked component that is reflected in the PLVs. However, we assumed that this component was present in all the trials across all conditions, and were interested in identifying differences between stimulus conditions that may be present in spite of this large underlying similarity. We will discuss how we achieved this in a later section.

We studied these differences in intervals in which at least one of the PLVs exceeded the mean of the PLVs in the baseline period by 3 times the standard deviation of the PLVs in the baseline (Figure 4.2). If some pairs exhibited a decrease in synchrony compared to the baseline, imposing this constraint would have eliminated those pairs from our analysis. However, as we did not observe any pairs with a significant decrease in synchrony, we considered this constraint valid.

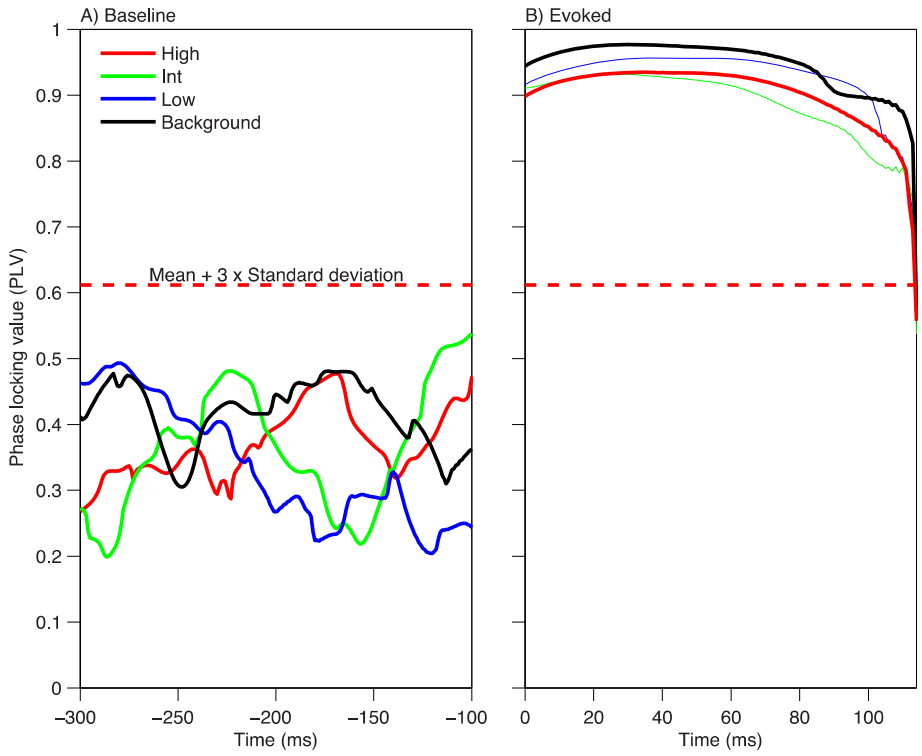

Figure 4.2. Phase-locking values (PLV) for the high-salience (red), intermediate-salience (green), and low-salience (blue) figure, and background (black) conditions. A) The window in the spontaneous activity used to compute the threshold. B) Evoked response period. The horizontal dashed line represents the mean plus 3 times the standard deviation in the baseline period. High: high-salience figure; Int: intermediate-salience figure; Low: low-salience figure.

4.2. Figure versus background condition

First, we were interested in detecting the differences between the responses in the high-salience figure and background conditions. We assessed these differences in

the different frequency bands described earlier. We computed the PLVs in each frequency band for the figure and background conditions, and then found the time intervals in which the PLVs in the figure condition were significantly different from the PLVs in the background condition. To test the significance of the differences between the PLVs in these two conditions, we bootstrapped the trials in each condition to assess the variability around each of the two PLVs. In each bootstrap sample, we computed the PLVs for the figure and background condition, and performed a point-wise subtraction of the resulting PLVs. By repeating this for 1000 times, we obtained a distribution of the differences between the PLVs in these two conditions at each time point. Due to the elimination of some trials because of excessive eye movements, and the reaction time constraints described in Section 3.2.1, we often ended up with different numbers of trials in the two conditions. To account for the variations that could have occurred because of this difference, we used the smaller number in the two conditions to perform the bootstrap. We used the criterion that 95% of the bootstrapped differences had to lie outside 0 in order for the difference in PLV for a particular pair to be significant. If the PLVs of background and figure conditions were significantly different from each other for at least 20 ms in the evoked response, we considered the differences in synchrony between the figure and background conditions significant in that frequency band. Figure 4.3 shows the PLVs for the figure and background conditions for the same pair as Figure 4.1, i.e. for the waveforms filtered in the 25 – 35 Hz frequency band. It also shows the differences between the PLVs of these conditions. The bins that exhibited significant differences are highlighted in red. As the differences were observed for more than 20 ms for this pair, i.e. from 13 ms to 72 ms after stimulus onset, this pair was considered a

significant pair in this frequency band. This pair did not exhibit significant differences between the two conditions in other frequency bands.

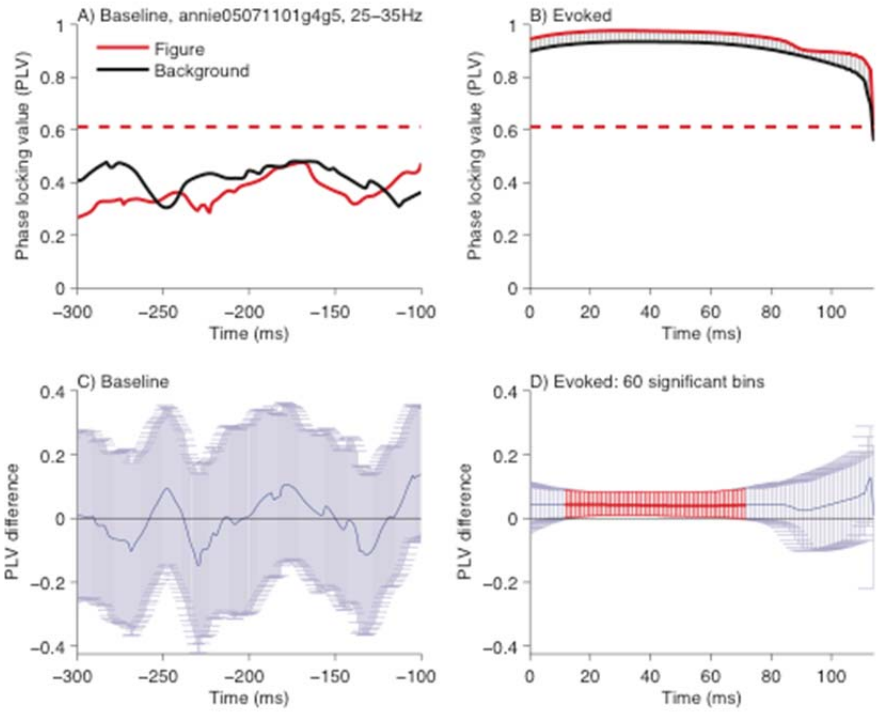

Figure 4.3. A, B) The phase-locking values for the figure and background conditions in the 25 – 35 Hz frequency band during the baseline (A) and evoked periods (B). The horizontal dashed line indicates the same threshold explained in Figure 4.2. C, D) The mean of the differences between the PLVs of the figure and background conditions obtained from 1000 bootstrapped samples. The error bars are the 95% confidence intervals of the differences. The red bars indicate the time points in which 95% of the bootstrapped distribution laid outside 0. Zero time represents stimulus onset.

To illustrate significant differences in the PLV in an alternative manner, Figure 4.4 plots the troughs of the LFPs for the pair shown in Figure 4.3. The troughs of the filtered waveforms on one electrode were first aligned independently at two time points. This is shown as the two black lines. The phase shift between the two filtered waveforms is then used to plot the trough on the other electrode in red. From the figure, we can see that in the figure condition, the troughs of the filtered LFPs were much closer to each other (and sometimes even coincident) for many of the trials compared to the background stimulus condition.

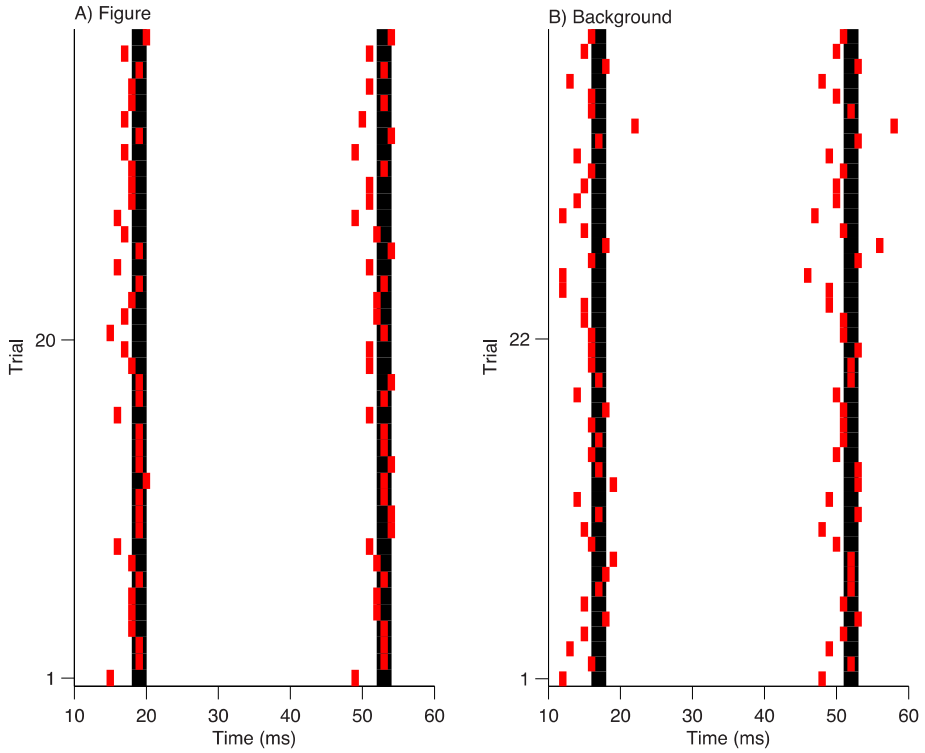

Figure 4.4. The troughs of two simultaneously recorded LFPs (filtered in 25 – 35 Hz frequency band) that exhibited PLVs that were significantly different for figure (A) and background (B) stimulus conditions. The first local minimum on electrode 1 (found around 20 ms) was first aligned across trials to form the first vertical black line. The phase shift between the two filtered waveforms at the point of the local minimum on electrode 1 was then used to plot the trough on the other electrode in red. This was repeated for the second local minimum on electrode 1 (found around 50 ms). This means that the two local minima in electrode 1 were aligned independently for illustration purposes, and were not as precise and regular in reality.

As mentioned earlier, phase-locking does not necessarily mean synchrony, so after we found significant differences in the phase-locking across trials in the two stimulus conditions, we examined the phase shift values between the trials to ensure that the phase shifts were small. Figure 4.5 shows the phase shift values between the simultaneously recorded waveforms for all the trials in the pair shown in Figure 4.3 for the figure and background conditions. The distributions of these phase-shifts for all the trials in the time windows in which the difference between the PLVs was significant (60 bins) are also shown (Figure 4.5C and 4.5D).

Next, we computed the circular mean of these phase shifts, using the Circular Statistics Toolbox Berens (2009). Circular mean can be computed using the following formula, in which α_j is a phase shift value:

$$\bar{\alpha} = \arg\left(\frac{1}{n} \cdot \sum_{j=1}^{n} \exp(i \cdot \alpha_j)\right) \tag{4.5}$$

In Figure 4.5 (C and D), these values were 9.91 ± 13.58 for the figure and 10.91 ± 24.44 for the background conditions. The distributions of these mean values for all pairs in the figure and background conditions are also shown in Figure 4.5E and 4.5F. It can be seen that although the mean phase-shifts of the pairs were not zero, they were relatively small.

4.3. Modulation as a function of saliency

After we found pairs that exhibited significant differences in LFP synchrony in the figure and background conditions, we examined if the LFP synchrony was also modulated as a function of visual saliency, and if this modulation was correlated with behavior. So, for pairs that showed significant differences between the figure and background conditions, we also compared the PLVs for all pairs of figure saliency conditions: high-salience versus intermediate-salience, high-salience versus low-salience, intermediate-salience versus low-salience. Pairs in which the PLV for at least one figure saliency condition was significantly different from the PLVs of another figure saliency condition were then considered to exhibit modulation as a function of visual saliency. We adopted the same technique used earlier to assess the

significance of the differences between the figure and the background stimulus conditions to examine the significance of the differences in the PLVs between pairs of figure saliency conditions.

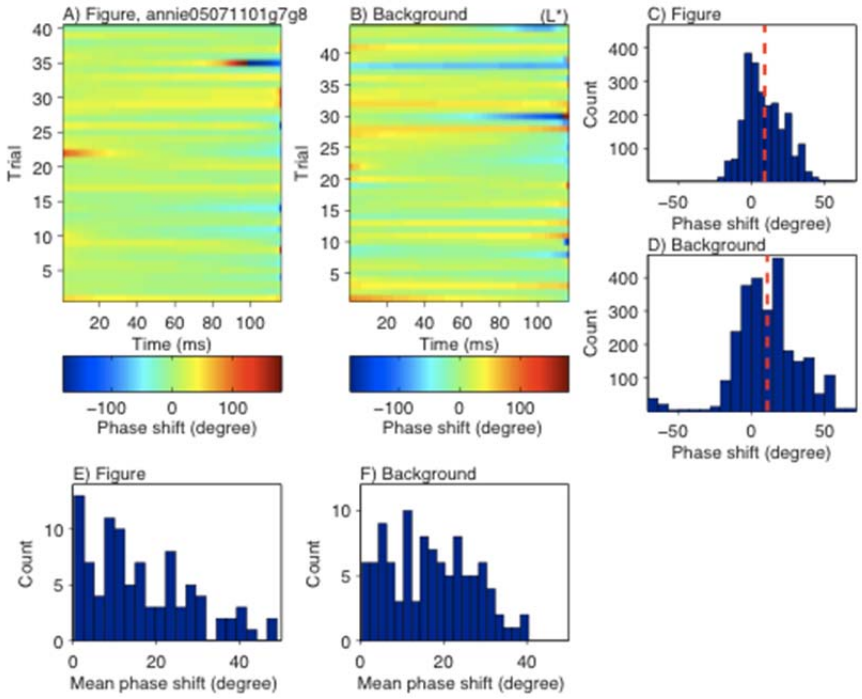

Figure 4.5. The magnitude of the phase-shifts. A, B) The phase shifts between simultaneously recorded LFPs for individual trials, in degrees. Time zero indicates stimulus onset. C, D) The distributions of phase shifts in a window (13 ms to 72 ms after stimulus onset) that exhibited significant differences between the PLVs in the figure and background conditions across trials. The red vertical line indicates the circular mean of the phase shifts. E, F) The distribution of the mean phase shifts for all the pairs. A, C, E) The figure condition. B, D, F) The background condition.

Figure 4.6 shows the PLVs for different pairs of figure saliency conditions, in the 25 – 35 Hz frequency band, for the same pair of LFPs discussed in the previous figures. It can be seen that for this LFP pair, the difference between the PLVs for high-salience and intermediate-salience figures, as well as for high-salience and low-salience figures, was significant, while it was not significant for intermediate-salience and low-salience figures.

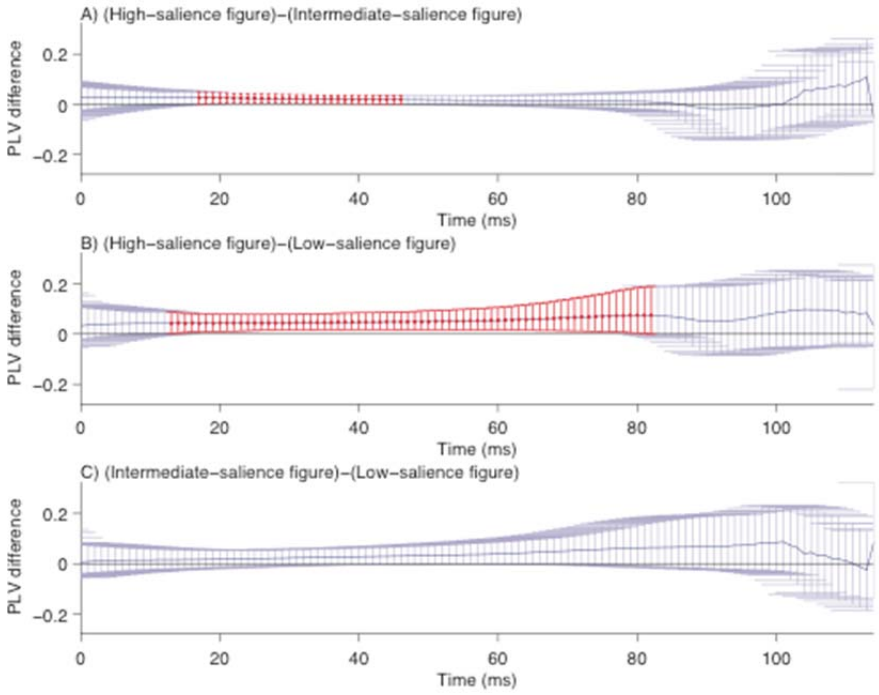

Figure 4.6. The differences in the phase-locking values obtained from 1000 bootstrapped samples for different pairs of figure saliency conditions. A) High-salience minus intermediate-salience. B) High-salience minus low-salience. C) Intermediate-salience minus low-salience. The conventions are as in Figure 4.3C. The difference was significant for (A) from 18 ms to 47 ms, and for (B) from 14 ms to 83 ms after stimulus onset.

Subsequently, for the pairs that showed modulation as a function of saliency, we computed the mean PLVs in a time window encompassing all the bins in which the figure saliency conditions exhibited significant differences with each other, and used this as the neurometric measure for the high-, intermediate-, and low-salience figure conditions. This measure could be interpreted as the level of synchrony for each condition. For example, for the pair in Figure 4.6 we computed the mean PLVs for all the conditions from 14 ms to 83 ms after stimulus onset as shown in Figure 4.7. Figure 4.7 shows the PLV curves for the three figure salience conditions for the same pair discussed earlier, along with the PLV curve for the background condition.

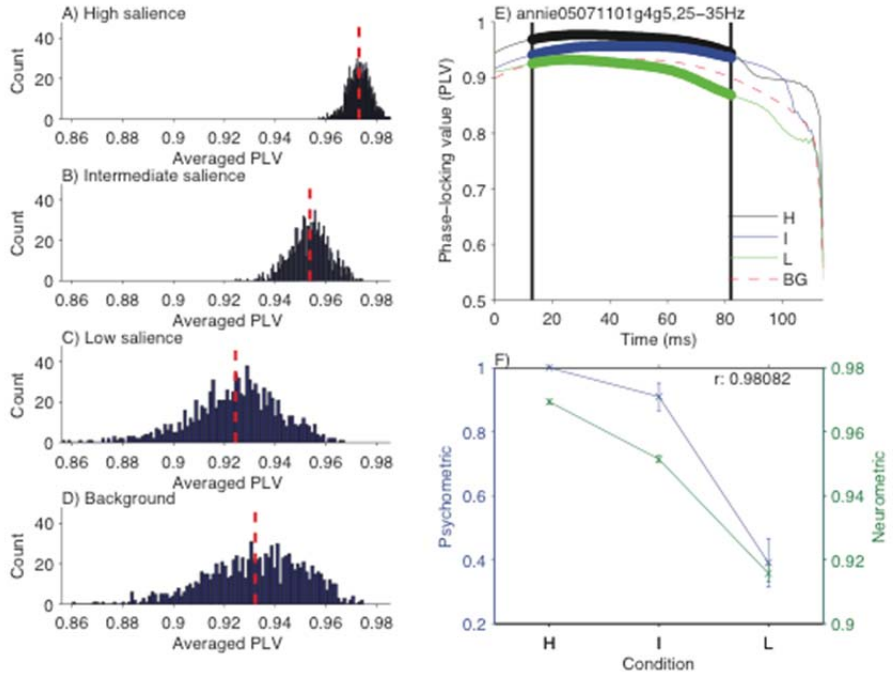

Figure 4.7. Correlation between synchrony and behavior. A, B, C, D) The averaged PLVs for different conditions computed by bootstrapping the trials in each condition for 1000 times. A) High- B) Intermediate- C) Low-salience figure D) Background condition. E) The phase-locking values (PLVs) for the high-, intermediate- and low-salience figure conditions. The PLV curve for the background condition is also shown using a dashed line. F) The neurometric (green) and psychometric (blue) curves. The error bars for the neurometric curve indicate the standard errors of the mean, while the error bars for the psychometric curve indicate the standard errors computed using the assumption that the correct and incorrect responses were from a Bernoulli distribution. (r: correlation coefficient for the neurometric and psychometric curves; H: high-salience figure; I: intermediate-salience figure; L: low-salience figure; BG: background).

The distributions of the PLVs computed at each time point in this interval and their mean values (i.e. the neurometric measure) are shown in Figure 4.7A to 4.7D. The neurometric and psychometric curves (i.e. performance of the monkey for different figure saliency conditions) are also shown (Figure 4.7F). We computed the correlation coefficient between the neurometric and psychometric curves to examine the correlation between the level of synchrony and behavior. For the pair shown in this figure, the neurometric and psychometric curves were highly correlated (r = 0.98).

4.4. Stimulus-locked versus stimulus-induced

After we found significant differences between the figure and background conditions, we were also interested in examining if these differences in synchrony were stimulus-locked or stimulus-induced. In other words we wanted to investigate if the observed differences in synchrony were solely due to common input from the stimulus, or due to processing that happened inside the region (Engel and Singer, 2001; Lachaux et al., 2000). Consequently, for both the figure and background conditions, we shuffled the trials on one electrode while maintaining the order of the trials on the other electrode. We repeated this for 1000 times, computed the PLVs each time, and obtained the distribution of the differences between the PLV traces. If 0 was outside the 95% confidence interval of these differences at a particular time point, we considered the difference between the PLVs significant at that time point. If the significant bins of the shuffled data set intersected with the significant bins that we found earlier for the original data, we considered the differences between figure and background stimulus-locked. Otherwise, we considered them stimulus-induced. This was because we assumed that, if after shuffling, we found the same synchrony as in the original data, the synchrony was probably solely due to the onset of the stimulus (Perkel et al., 1967).

4.5. Dependence on tuning and depth

In order to make sense of any heterogeneity in the results, we looked at the relationship between our results and the tuning properties of the underlying neurons, although it has been shown that the synchrony of LFPs were not dependent on the orientation preferences of the cells when the cells had non-overlapping receptive

fields in cats (Engel et al., 1990). Since our PLV analysis was performed independently in different frequency bands, we also performed our analysis of the orientation tuning in individual frequency bands. This way, we were able to more directly compare the PLV and orientation tuning results. We used the average of the amplitude envelope of the waveforms across time and across trials to compute the tuning curves in that frequency band. If the synchrony in the figure condition was significantly different from the synchrony in the background condition in a particular frequency band, we computed the correlation coefficient between the tuning curves of the two electrodes in that frequency band, to assess the correlation between these differences in synchrony and the similarity of the orientation tuning in the two electrodes of that pair. In other words, we examined if the similarity or dissimilarity between the tuning of the responses might have resulted in higher or lower synchrony for one condition compared to the other condition. We used this method instead of comparing tuning characteristics such as tuning width and preferred orientation because using the measure discussed in section 3.3.5 for determining the tuning of a neuronal response, only 3 pairs showed orientation tuning for both electrodes in the narrow frequency bands we were interested in.

We also assessed the potential effect of differences in the depth of the recordings (i.e. cortical layer) on differences in synchrony of the figure and background conditions, as it has been shown that synchrony in the gamma band could vary as a function of cortical depth (Buffalo et al., 2011). The depth of each recording was obtained by computing the difference between the depth at which we performed the recording, and the depth at which the last activity was recorded when the electrode was retracted (refer to section 3.1.3 for further details).

4.6. Results

When we assessed the differences in synchrony for the figure and background conditions, we observed pairs with higher and lower synchrony in the figure condition compared to the background condition. While an example of a pair with higher synchrony in the figure condition is shown in Figure 4.3, Figure 4.8 shows another example pair with lower synchrony in the figure condition.

.

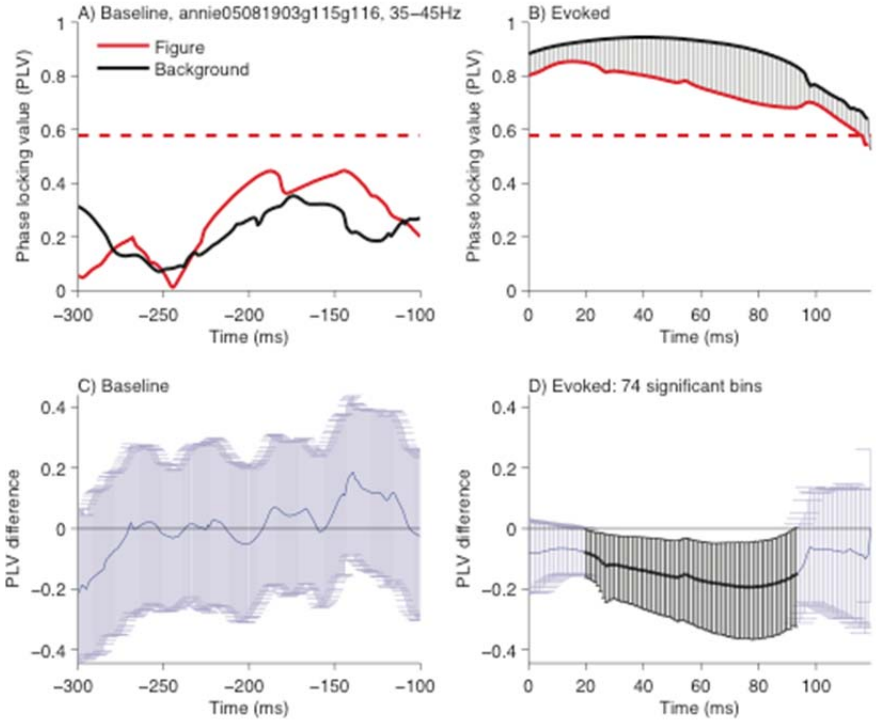

Figure 4.8. A, B) The phase-locking values for the figure and background conditions in the 35 – 45 Hz frequency band during the baseline (A) and evoked periods (B). The horizontal dashed line indicates the same threshold that was used in Figure 4.2. C, D) The mean of the differences between the PLVs in the figure and background conditions obtained from 1000 bootstrapped samples. The error bars are the 95% confidence intervals of the differences. The black bars indicate the time points in which 95% of the bootstrapped distribution laid outside 0. Zero time represents stimulus onset.

For the pair in Figure 4.3, the PLVs in the figure condition in the 25 to 35 Hz frequency band were significantly larger than the PLVs in the background condition

within the interval highlighted in red, while for the pair in Figure 4.8, the PLVs in the figure condition in the 35 to 45 Hz frequency band were significantly smaller than the PLVs in the background condition within the interval highlighted in black.

The pair showed in these two figures exhibited significant differences between the figure and background condition only in one frequency band, while some other pairs exhibited significant differences in several frequency bands

Figure 4.9 shows the distribution of the frequency bands in which the synchrony in the figure condition was significantly different from the synchrony in the background condition for each pair.

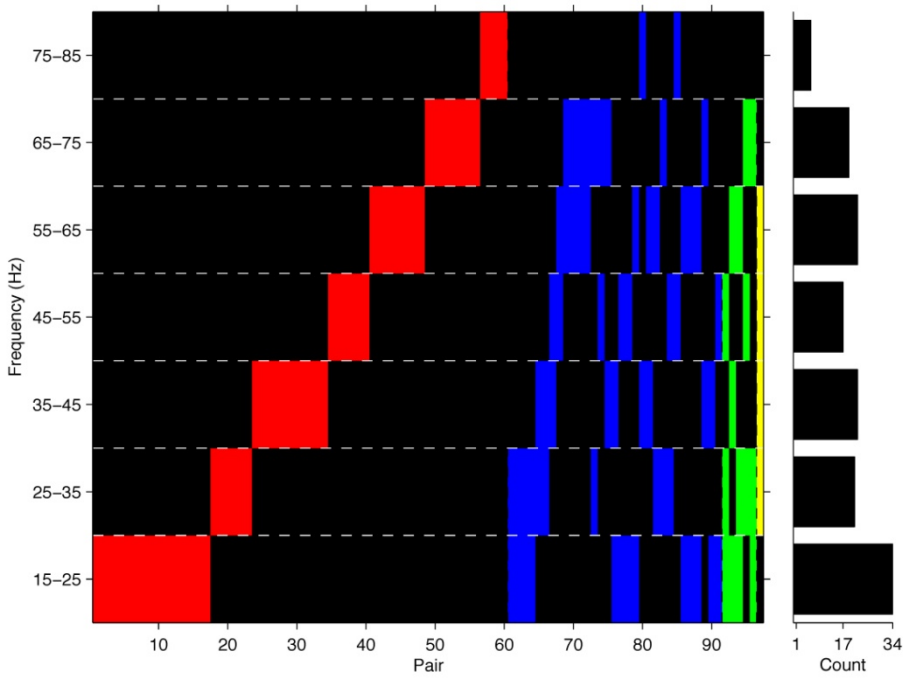

Figure 4.9. Pairs that exhibited significant differences in synchrony in the figure and background conditions across frequency bands for all subjects. From left to right, the pairs that exhibited significant differences in one (red), two (blue), three (green), and four (yellow) frequency bands. The bar plot on the right represents the number of pairs that showed significant differences in each frequency band.

As described in Section 4.3, for pairs that exhibited significant differences in synchrony when comparing the figure and background condition, we also compared

the distributions of PLVs for all possible pairs of saliency conditions to see if the synchrony varied as a function of saliency. While Figure 4.4 shows these distributions for a pair with significantly higher synchrony in the high-salience figure condition compared to the intermediate- and low-salience conditions, Figure 4.10 shows the same distributions for a pair (shown also in Figure 4.8) with significantly lower synchrony in the high-salience figure condition compared to the low-salience condition, and lower synchrony in the intermediate-salience condition compared to the low-salience condition.

Table 4.1 shows the number of pairs that exhibited significant differences between the figure and background conditions, separated into pairs in which the synchrony between the simultaneously recorded electrodes was higher for the figure condition compared to the background condition, and pairs in which it was lower. The pairs that exhibited significant differences across multiple frequency bands were counted only once. The distributions of these significant pairs in the different frequency bands are shown in Figure 4.11, for all subjects (A and B), and for individual subjects (C to H). As shown in this figure, and also in Figure 4.9, there was surprisingly little frequency preference, with pairs showing significant differences over a fairly large range of frequencies. The numbers of pairs that exhibited a significant modulation of synchrony as a function of saliency are also shown in Figure 4.11 and Table 4.1. If the synchrony in the figure condition was significantly different from the background condition in multiple frequency bands, that pair was counted only once in the results shown in Table 4.1. Overall 97 (48.74%) of the pairs showed significant differences between figure and background conditions in at least one frequency band, and 66 out of these 97 pairs (68.04%) also exhibited significant differences as a function of visual saliency.

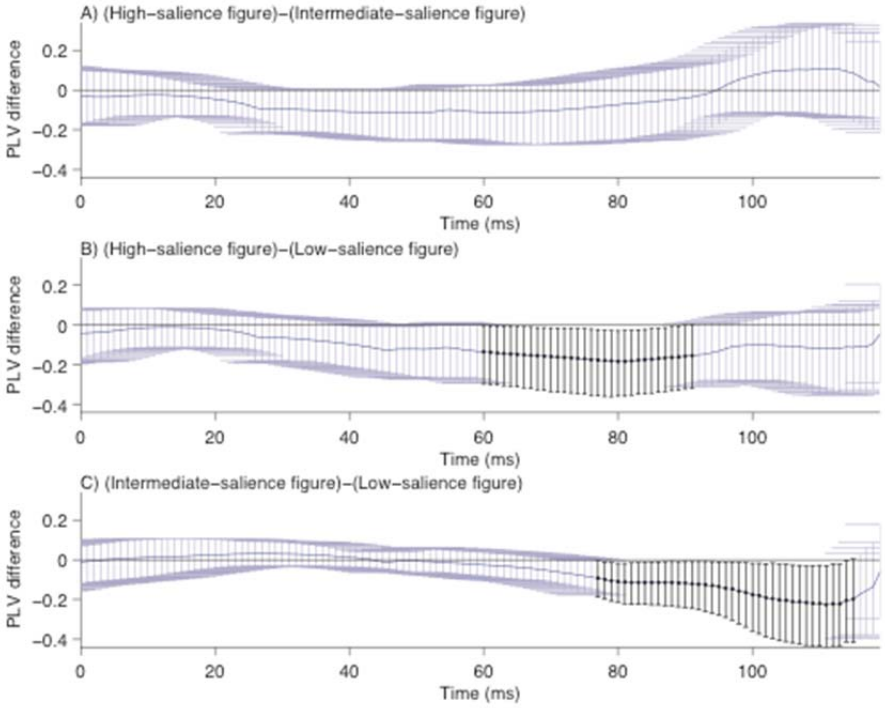

Figure 4.10. The differences in the phase-locking values obtained from 1000 bootstrapped samples for different pairs of figure saliency conditions. A) High-salience minus intermediate-salience. B) High-salience minus low-salience. C) Intermediate-salience minus low-salience. The conventions are as in Figure 4.9C. The difference was significant for (B) from 61 ms to 92 ms, and for (C) from 78 ms to 116 ms after stimulus onset.

As mentioned earlier, we averaged the PLVs in selected windows for the high-, intermediate- and low-salience figure conditions to generate the neurometric curve. We then computed the correlation coefficient between the neurometric and psychometric curves. Figure 4.12 shows the histograms of these correlation coefficients, collapsed across subjects, as well as for individual subjects, for the pairs that exhibited higher synchrony in the figure condition with respect to the background condition, and for the reverse. As we analyzed the different frequency bands separately, there might be multiple correlation coefficients for a pair corresponding to different frequency bands. We found that 29% of the correlation coefficients (23 out of 79) were larger than 0.5 or smaller than -0.5. This suggested that for these pairs, the synchrony may be directly related to the behavior of the subjects. The fact that

other pairs did not exhibit such large correlations may be due to the high heterogeneity present in neuronal populations (Shamir and Sompolinsky, 2006; Yen et al., 2007; Chelaru and Dragoi, 2008).

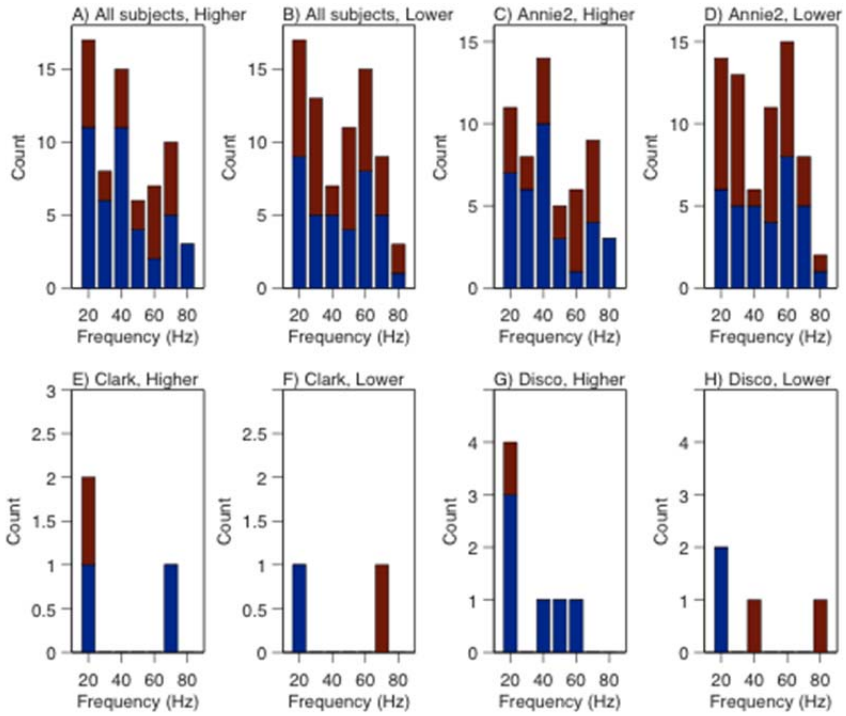

Figure 4.11. The number of pairs that showed significant differences between the figure and the background conditions for different frequency bands under study. The blue sections of the bars represent the number of pairs that also showed modulation as a function of figure saliency. "Higher" indicates that the synchrony in the figure condition was higher than the synchrony in the background condition, and "Lower" indicates the reverse. A, B) Results from all three subjects. C – H) Results from individual subjects. Each number on the x-axis represents the center frequency for the frequency band used in the analysis. For example, 20 Hz represents the frequency band of 25 to 35 Hz.

Table 4.1. The number of pairs that showed significant differences in synchrony between the figure and background conditions. "Higher" indicates that the synchrony in the figure condition was higher than the synchrony in the background condition, and "Lower" indicates the reverse. The pairs that also exhibited modulations in synchrony as a function of contour saliency are shown in parentheses.

	Annie (137)	Clark (28)	Disco (34)
Higher	43 (30)	3 (2)	6 (6)
Lower	49 (28)	2 (1)	4 (2)

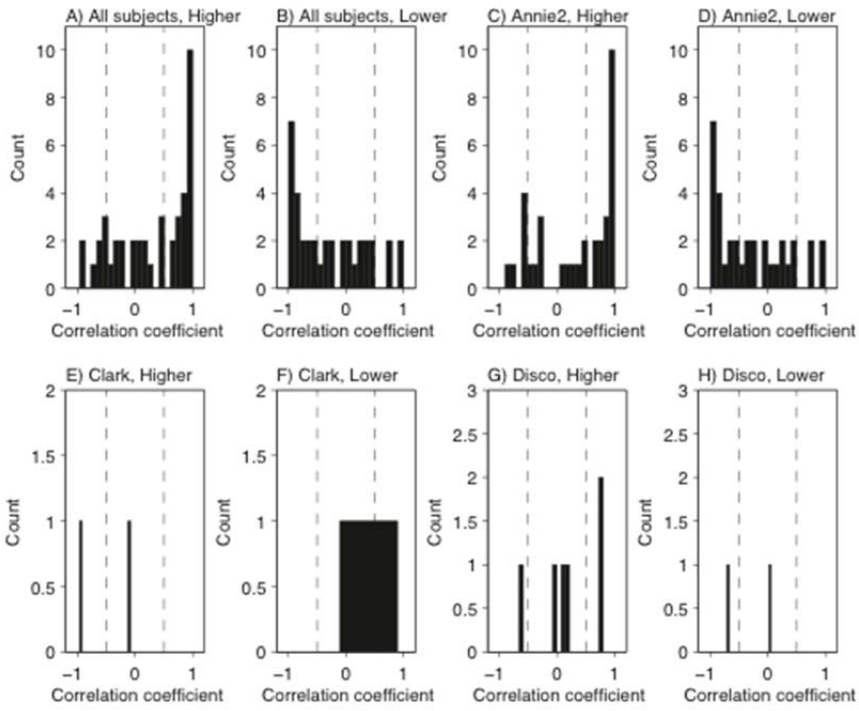

Figure 4.12. The distributions of the correlation coefficients computed between the neurometric and the psychometric curves for pairs that showed significant modulation with contour saliency. A, B) Results for all three subjects. C –H) Results for individual subjects. "Higher" indicates that the synchrony for the figure condition was higher than the synchrony for the background condition, and "Lower" indicates the reverse. The vertical dashed lines are -0.5 and 0.5.

Interestingly, we observed that for many of the pairs (64%, 27 out of 42 correlation coefficients) that exhibited higher synchrony in the figure condition compared to the background condition, the correlation coefficients were positive, i.e. direct correlation between performance and level of synchrony, while for the pairs that exhibited lower synchrony in the figure condition compared to the background condition most of the correlation coefficients were negative (65%, 24 out of 37 correlation coefficients), i.e. inverse correlation between performance and level of synchrony. Examples of both these trends can be seen in Figure 4.7 and Figure 4.13 respectively. Figure 4.7 shows the correlation between performance and level of synchrony for a pair with higher synchrony in the figure condition (also shown in Figure 4.3) with a positive correlation between the neurometric and psychometric curves. On the other hand, Figure 4.13 shows this correlation for a pair with lower

synchrony in the figure condition (also shown in Figure 4.10), with a negative correlation between the neurometric and psychometric curves. We observed the same trend for the correlation coefficients in our single channel analysis (Chapter 3) as well. As mentioned in that Chapter, this was consistent with the hypothesis that the responses in the figure condition converge to the responses in the background condition as the visual saliency decreases.

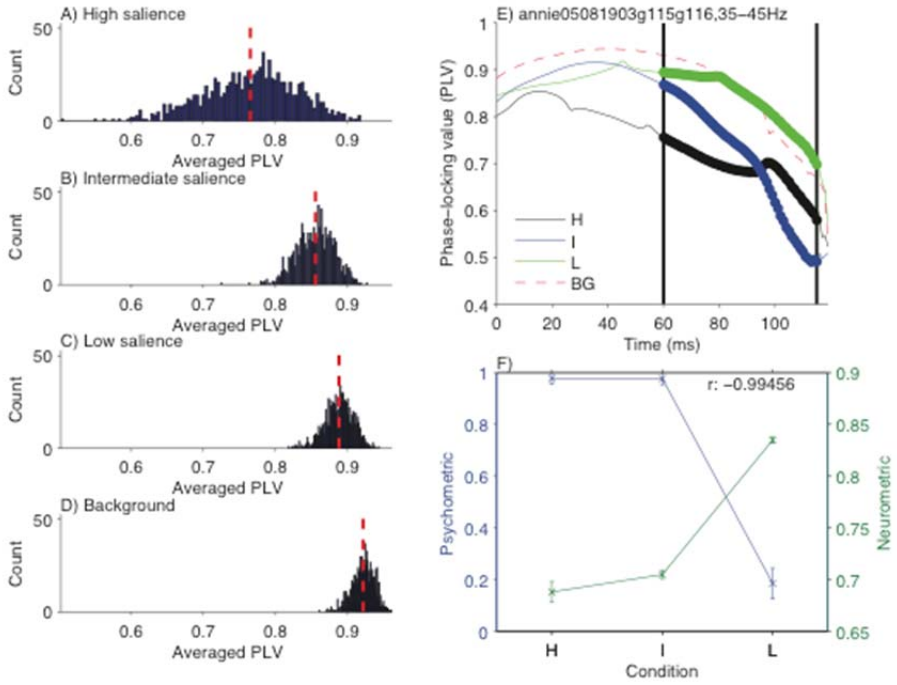

Figure 4.13. Inverse correlation between synchrony and behavior for a pair with lower synchrony in the figure condition compared to the background condition. A, B, C, D) The averaged PLVs for different conditions computed by bootstrapping the trials in each condition 1000 times. A) High-, B) Intermediate-, C) Low-salience figure, D) Background condition. E) The phase-locking values (PLVs) for the high-, intermediate- and low-salience figure conditions. The PLV curve for the background condition is also shown using a dashed line. F) The neurometric (green) and psychometric (blue) curves. The error bars for the neurometric curve indicate the standard errors of the mean, while the error bars for the psychometric curve indicate the standard errors computed using the assumption that the correct and incorrect responses were from a Bernoulli distribution. (r: correlation coefficient for the neurometric and psychometric curves; H: high-salience figure; I: intermediate-salience figure; L: low-salience figure; BG: background).

As described in Section 4.4, we also used trial shuffling to identify pairs in which significant differences between figure and background were stimulus-induced

and not stimulus-locked (i.e. due to common input from the stimulus). Table 4.2 shows the numbers for these pairs.

The numbers in the parentheses indicate the number of these pairs that also exhibited significant variations with visual saliency. It can be seen that for a substantial number of pairs, the differences were stimulus-induced, which means for these pairs, the differences in synchrony in the figure and background conditions vanished when we shuffled the trials. Thus, in these pairs, the differences cannot be attributed to common input originating from the stimulus.

Table 4.2. The number of pairs that showed significant differences in synchrony between the figure and background conditions that were likely stimulus-induced and not stimulus-locked. The conventions are as in Table 4.1.

	Annie (137)	Clark (28)	Disco (34)
Higher	26 (18)	3 (2)	5 (5)
Lower	28 (14)	1 (0)	3 (1)

In order to investigate why some pairs exhibited higher synchrony in the figure condition, while others exhibited lower synchrony in the background condition, and yet others did not exhibit significantly different results, we investigated how orientation tuning and recording depth (Section 4.5) affected the results. Figure 4.14 shows examples of the tuning curves computed using the LFP power in the 25 – 35 Hz frequency band. Figure 4.14A shows the tuning curve for the same pair discussed in Figures 4.3, 4.6, and 4.7. As this pair exhibited significant differences in the 25-35 Hz frequency band, we assessed the tuning curve of the LFPs in this frequency band.

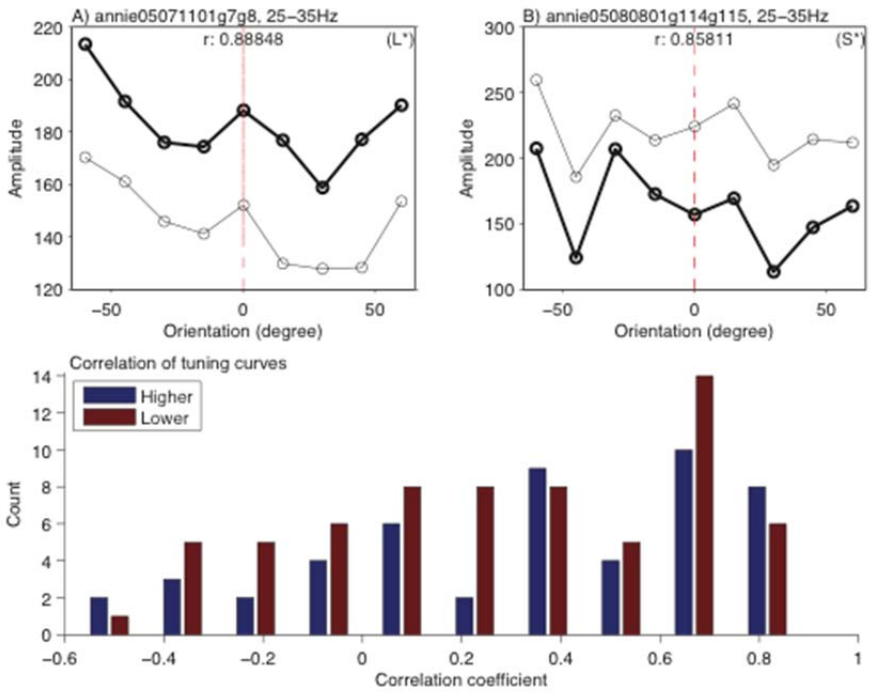

Figure 4.14. The effect of orientation tuning on differences in synchrony in the figure and background conditions. A, B) Examples of the orientation tuning curves obtained from each of the two electrodes in: A) a pair that exhibited higher synchrony in the figure condition with respect to the background condition in the 25-35 Hz frequency band; B) a pair that exhibited the reverse in the 25-35 Hz frequency band. (Thick line: the orientation tuning curve of electrode 1; Thin line: the orientation tuning curve of electrode 2). Zero represents the stimulus orientation, which was determined using hand mapping during the experiment. C) The distribution of correlation coefficients between the orientation tuning curves of the two electrodes for all the frequency bands under study, and across all subjects. “Higher” indicates that the synchrony for the figure condition was higher than the synchrony for the background condition, and “Lower” indicates the reverse.

Figure 4.14B shows the tuning curves for another pair that exhibited lower synchrony for the figure condition with respect to the background condition in the frequency band 25-35 Hz. It can be seen that for both pairs, the correlation between the tuning curves was high, indicating that the orientation tuning was fairly similar in both cases.

Thus, this suggested that similarities or differences in orientation tuning may not be able to predict whether one pair will exhibit higher or lower synchrony in the

figure condition. A comparison between the correlation coefficients that were computed for pairs that exhibited higher synchrony in the figure condition, and pairs that exhibited lower synchrony seemed to agree with this conclusion, as these two distributions (Figure 4.14C) were not significantly different from each other (Kolmogorov-Smirnov test, $p > 0.42$).

The distributions shown in Figure 4.14C were the correlation coefficients computed between the tuning curves of all significant pairs across all the frequency bands under study. As mentioned earlier in Section 4.5, if a pair exhibited significant differences in a certain frequency band, the tuning curve for that pair was computed in that particular frequency band for our analysis.

The other factor that could likely affect the difference in the synchrony in the figure and background conditions was the difference between the depths of the recordings of the two electrodes .This was because the larger the distance, the more likely that the responses were recorded from different layers of the cortex. Figure 4.15 shows a comparison between the depth of the recordings of the two electrodes for the pairs that exhibited higher synchrony in the figure condition and for the reverse (Figure 4.15A), as well as the differences between these depths (Figure 4.15A) for all subjects. Again, there was no clear grouping for pairs with higher or lower synchrony in the depth of the electrodes (Figure 4.15A), (the 95% confidence interval of the slopes of the linear fits are reported in the figure caption) or in the differences in depth between the electrodes (Kolmogorov-Smirnov test, $p > 0.18$) as shown in Figure 4.15B.

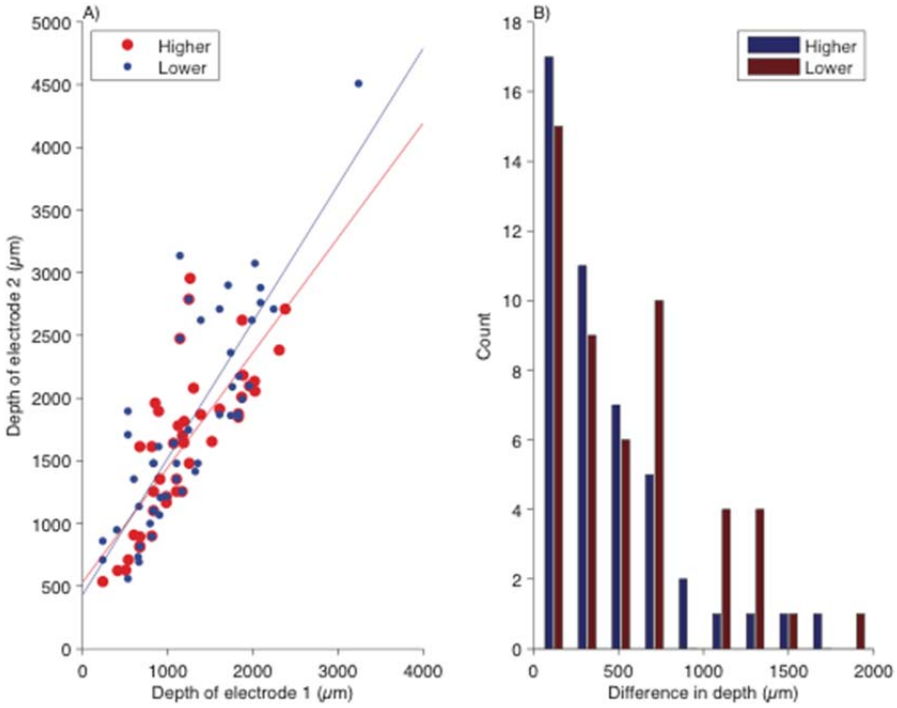

Figure 4.15. The effect of recording depths on synchrony. A) The depth of the recording for electrode 1 versus electrode 2 in each pair, and B) the distribution of the depth differences between the two electrodes, separated into pairs in which the LFPs were more synchronous in the figure condition, and pairs in which they were more synchronous in the background condition. In (A) electrode 1 was the electrode with the shallower recording depth. The depth measurement for the outlying point was probably inaccurate, which led to its very large deviation from the rest of the data. The solid red line represents the linear fit to the data points in the "Higher" condition (slope, lower bound and upper bound of the 95% confidence interval of the slope were 0.91, 0.74 and 1.08). The solid blue line represents the same fit for the "Lower" condition (slope, lower bound and upper bound of the 95% confidence interval of the slope were 1.08, 0.87 and 1.30). "Higher" indicates that the synchrony for the figure condition was higher than the synchrony for the background condition, and "Lower" indicates the reverse.

For two of the monkeys, we also found significant differences between the figure and background conditions, as well as across saliency conditions using single unit and multi unit activities (Bong et al., 2012). Although these differences were observed in the firing rates of the neurons and not their synchrony, we were interested to see if the pairs that contained single units that exhibited significant differences in their firing rates were more likely to also exhibit significant differences in the synchrony using LFP. Out of 92 pairs in which we found significant differences between the synchrony in the figure and background conditions, we found 1 pair in

which the single units recorded on the two electrodes also showed significant differences in their firing rates, and 13 pairs where only one of the single units showed significant differences. For 13 pairs (3 of these pairs were common with the pairs mentioned for single unit activity) out of 92 pairs, one of the multi-unit recording sites exhibited significant differences in their firing rates between the figure and background conditions. This suggested that for the majority of the pairs in our recordings, the variation in synchrony observed in the LFPs were not related to significant changes in the firing rate in the single-unit or multi-unit activity.

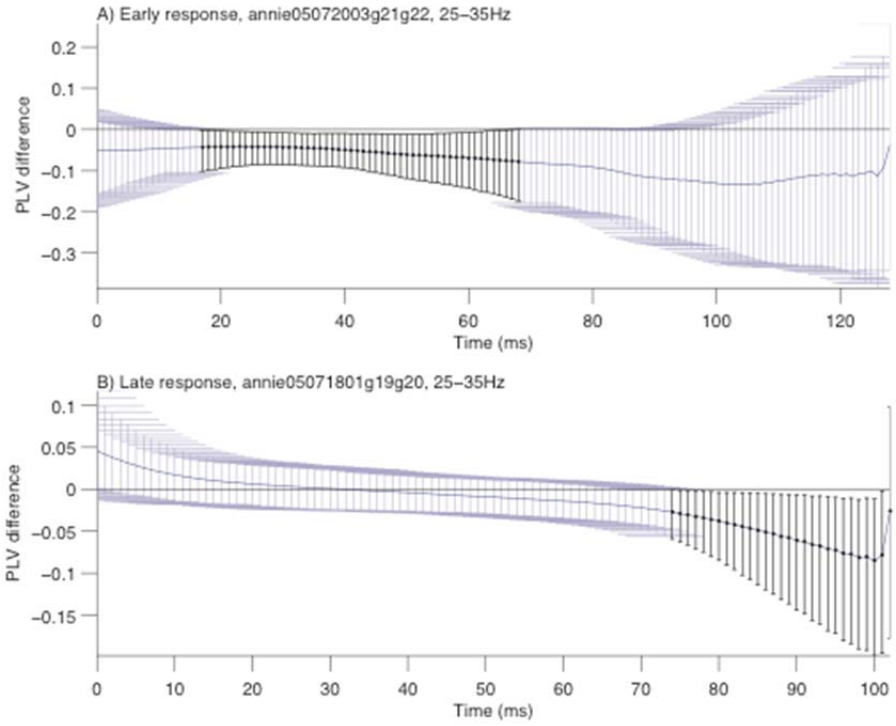

Figure 4.16. Different time courses of the deviation of the responses in the figure condition from the responses in the background condition. A and B) Early modulation. C and D) Late modulation. The interval in which the PLVs in the figure condition were significantly different (lower) from the background condition (lower) are highlighted in black.

Finally, one question that we were particularly interested in was whether the primary visual cortex was able to detect a contour, or figure, in the feedforward sweep without the contribution of feedback from extrastriate areas. The feedforward

influence would have been reflected in the differences between the neuronal responses shortly after stimulus onset, while the later would have been reflected in the late response. We found pairs in which the difference in synchrony in the figure and backgrounds condition appeared very early, and pairs in which these differences appeared late. Figure 4.16A shows one pair in which the significant differences in the figure and background conditions occurred relatively early, 18 to 69 ms after stimulus onset. In contrast, the pair in Figure 4.17B exhibited differences that occurred much later, 75 to 103 ms after stimulus onset.

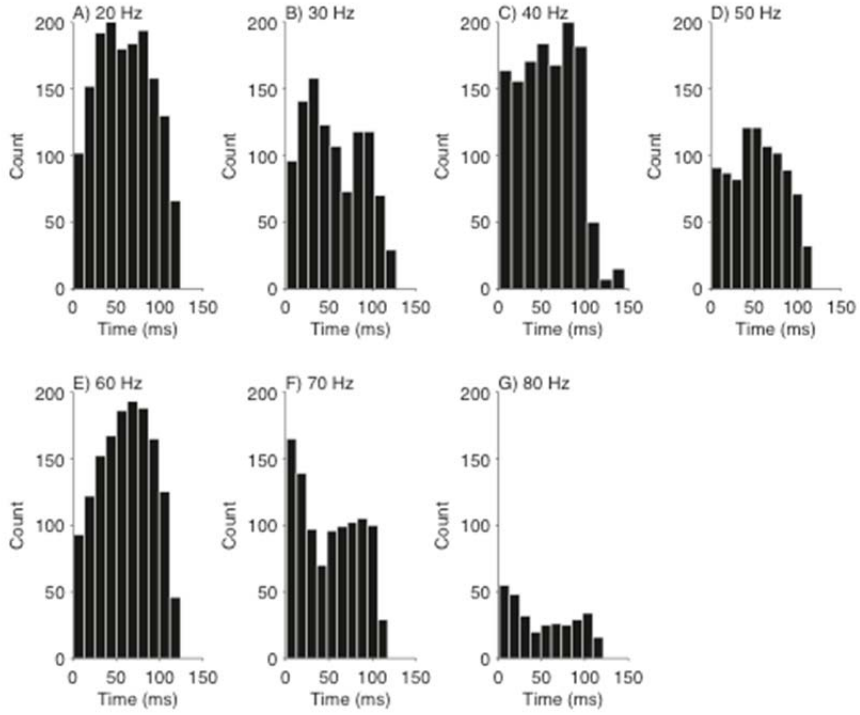

Figure 4.17. The distributions of significant windows for all significant pairs at 20 to 80 Hz (A – G). Each value on the horizontal axis represents the center frequency for the frequency band used in the analysis. For example, 20 Hz represents the frequency band of 25 to 35 Hz.

However, when we plotted the histograms of the time points in which significant differences were observed (Figure 4.17), we did not observe any bimodality in these distributions. However, if we, instead, used only the first window

in which the PLVs were significantly different from each other for each pair, some of the histograms appeared bimodal (Figure 4.18). This could suggest a distinction between the pairs that contributed to contour detection in the feed-forward sweep and the ones that were sensitive to feedback from extra-striate areas.

Unfortunately, these results may not be very conclusive, because the time resolution of the method we used to assess synchrony was poor and the application of filters to separate the signal into narrow frequency bands led to smearing of differences into neighboring time windows. This could be seen in the histograms shown in Figures 4.17 and 4.18, because some of the differences were detected right after stimulus onset. This is highly suspicious, given the fact the initial responses to a visual stimulus can be recorded in striate cortex only nearly 40 ms after stimulus onset.

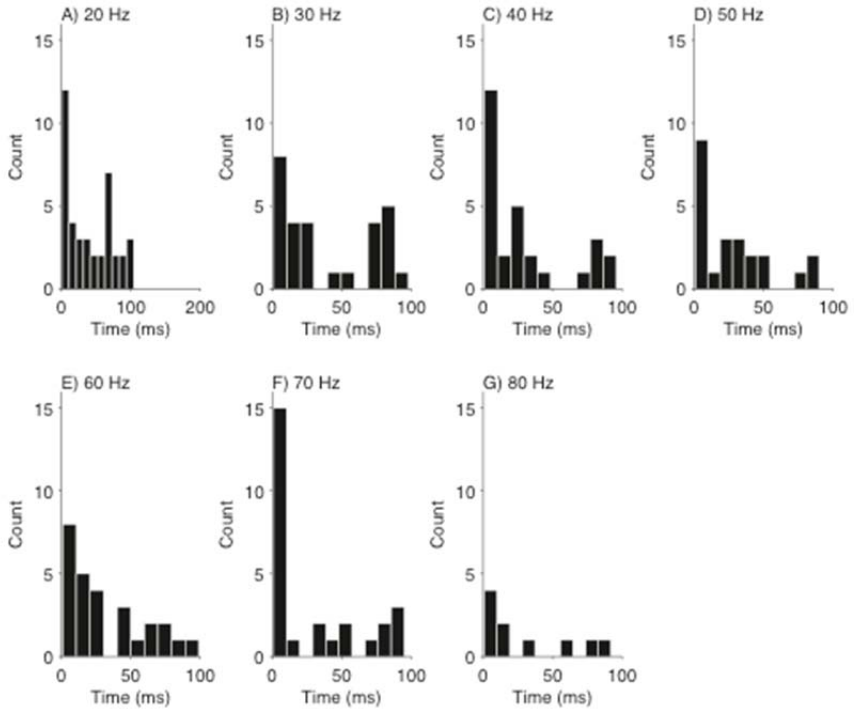

Figure 4.18. The distributions of the first significant window (of at least 20 consecutive significant windows) for all the significant pairs at 20 to 80 Hz (A - G). Each value on the x-axis represents the center frequency for the frequency band used for the analysis. For example, 20 Hz represents the frequency band of 25 to 35 Hz.

Chapter 5

Discussions and future work

5.1. Discussions

The aim of this study was to investigate the role of oscillations and synchrony in visual grouping.

To perform this, we used the stimuli and the experimental paradigm that met some of the criteria that seemed essential for investigating the binding-by-synchrony hypothesis (Gray, 1999), but were absent in most previous experiments. The stimuli inside the receptive fields of the recorded neurons were kept constant, while the saliency of the figure was changed only by contextual variation. Also, the animals were awake and were involved in a figure-ground segregation task that demanded a fast reaction time. This increased the likelihood that the grouping occurred bottom-up. The difficulty of the task could be changed by changing the saliency of the figure providing the opportunity to investigate correlation between neuronal responses that were probably associated with visual grouping and the performance of the subjects in the task.

After analyzing the power of gamma oscillations in local field potentials on single electrodes, and synchrony between local field potentials in the gamma frequency band in pairs of electrodes, we found that at the level of single electrodes, the gamma power responses in some sites were significantly different in the figure

condition when compared to the background condition. High gamma power might imply that a large population of neurons at the recording site was oscillating in the gamma band, as local field potentials are considered to be the synaptic aggregate of a large population of neurons surrounding the tip of the electrode. Also we found that the gamma power response was modulated as a function of figure saliency. This variation in the power across conditions probably showed that these oscillations could be correlated with visual grouping.

At the level of pairs of electrodes, when we directly measured the synchrony between the neuronal responses recorded simultaneously, we observed differences in the level of synchrony between these responses when both groups responded to the figure compared to when they responded to the background. Similar to the power in the gamma band, we observed that the level of synchrony between these groups changed when we varied the saliency of the figure. This again could imply a correlation between synchrony and visual grouping.

According to the binding-by-synchrony hypothesis, we expected to observe higher synchrony in response to the figure condition compared to the background condition. In addition, we expected that the synchrony would decline as we decreased the saliency of the figure. However, in addition to pairs of responses that exhibited responses that were consistent with our expectation, we also found some pairs with lower synchrony in the figure condition compared to the background condition.

We could not find any correlation between this effect and the similarity in the orientation tuning of the individual LFPs or the difference between their recording depths. This could be because the cells are also selective for other stimulus properties like spatial frequency, disparity, etc., and our characterization of the recoded neurons

using only a limited range of orientations was insufficient to identify cells that were optimally stimulated (and thus presumably exhibited increased synchrony in the figure condition), and those that were not (and thus exhibited decreased synchrony in the figure condition). We speculate that the cells that were more optimally stimulated would increase their synchrony, and inhibit or suppress the synchrony in the cells that were less optimally stimulated, thus leading to an amplification of the output signal to extra-striate cortex. In addition, our measurements of the depths of the recordings were not very accurate, as there was typically some dimpling of the brain when the electrode first started to penetrate the brain tissue. This dimpling continued until the electrode finally penetrated into the tissue. However, by this time, it would not be clear how deep the electrode was. Perhaps with more accurate information regarding the cortical layers of the neurons we recorded from, it might be possible to observe some differences in the pairs that exhibited increased synchrony and pairs that exhibited decreased synchrony in the figure condition.

More experiments will be required to investigate these speculations. However, our current data suggests that changes in synchrony were highly correlated with changes in the saliency of the figure, and as a result, potentially responsible for the performance of the subjects. In our view, the significant finding in our study was that visual grouping affected the synchrony of the responses.

The other question we tried to answer was the time course of the modulation of the responses of the V1 neurons with visual grouping, as this could contribute to the understanding the role of V1 in grouping. In this regard, we assessed the time course of the emergence of the differences between the responses to figure and background and observed some early modulations in the responses. We concluded that the responses in V1 could potentially be modulated shortly after stimulus onset

due to visual grouping. This could support the hypothesis that V1 may be the first region in visual cortex that represents pre-attentive grouping based on Gestalt cues, independent of the feedback from higher visual areas. Although this conclusion seems at odds with the other studies that failed to find early representations of visual grouping in primary visual cortex (Lamme, 1995; Zipser et al., 1996; Gail et al., 2000), we suggest that some of the techniques used in the current study might have contributed to revealing this early modulation. The timing of the experiment could be the main factor, as in contrast to other studies (Gail et al., 2000; Limma et al., 2010), our subjects were required to respond rapidly to the stimulus. Also, in this study we used LFPs that were probably more sensitive in reflecting synchrony. We also applied a technique to measure synchrony that could quantify phase-locking independent of the correlation in the amplitude of the responses, which probably helped in revealing subtle modulations of synchrony in the presence of large amplitude correlation in the transient responses. It should be noted that because of the low time resolution, primarily due to the large time windows needed to perform frequency analysis and the short reaction times in our subjects, it was not possible to determine the exact time of the emergence of this modulation. This finding will have to be confirmed using single-unit and multi-unit recordings.

Finally, it is worth mentioning that although the main focus of this study was to investigate the potential role of synchrony in binding, several other neural codes could be assumed to mediate binding, such as rate codes (Roelfsema, 2006), latency codes (Fries et al., 2001a, Meirovithz et al., 2010), and, phase-of-firing coding (Montemurro et al., 2008; Kayser et al., 2009). Experimental evidence may support these hypotheses as well, but these may not contradict each other, and it is possible that all these are in fact different manifestations of the same phenomena. As an

example, a proposed communication mechanism based on gamma band oscillations and phase-of-firing coding (Fries et al., 2007) suggests that spikes that fired in certain phases of the gamma cycle, i.e. the troughs, could be more effective when they reach the target neuronal populations, consistent with binding by synchrony hypothesis. They propose that this is because the gamma oscillations in the source and target populations could be phase-locked, and as a result these spikes reach their targets when the post-synaptic neurons are also in their most depolarized state. They also later extended their model by providing experimental evidence that neurons with higher firing rates tended to fire earlier in the gamma cycle (Vinck et al., 2010). Assuming such a mechanism was involved in binding, it can be seen that depending on the methods used in a particular study, different neuronal correlates may be identified to be responsible for binding, as the cells that are grouped together may exhibit higher firing rates, higher synchrony, and shorter latencies compared to the ones that are not grouped together. This may not be compatible with the view that synchrony should exist in conjunction with rate codes to distinguish between neuronal responses to different features, as cells may respond to different features with similar spike rates (Singer 1995; but see Roelfsema 2007). It is also possible that each one of these schemas comes into play based on the task, and for instance, the level of difficulty of the task. For example, Stopfer et al. (1997) showed that in the olfactory bulb of the honeybee, disruption in synchrony impaired the odorant discrimination only when the odorants were very similar. Although, behavioral assessments and electrophysiological recordings were not simultaneously done in this study, later Beshel et al. (2007) performed electrophysiological recordings in intact behaving rats and provided more evidence supporting this.

In conclusion, we found evidence supporting the binding-by-synchrony hypothesis, and the role of primary visual cortex in visual grouping in the feedforward sweep of the scene segmentation process.

5.2. Future work

As mentioned earlier we found pairs in which the synchrony in the figure condition was lower compared to the synchrony in the background condition, which is not consistent with the binding-by-synchrony hypothesis. We speculated that this could be because the neurons were not optimally stimulated by the Gabor patches in their receptive fields. So, in future experiments, either the stimulus should be more carefully customized to the preferences of the neurons, or more information should be collected about the tuning characteristics of the neurons to contribute towards explaining the results.

We assessed the transient response, which has been often overlooked in previous studies in favor of the sustained response (Palanca et al., 2005, Lima et al., 2010). Some detailed analytical work may help to ensure that the observed differences are real and not due to the large stimulus-locked response.

Simultaneous recording from more than two neuronal groups can be useful. For example, by simultaneously recording from the figure and background one may perform the synchrony analysis at the level of single trials, which was not possible in our recordings.

Although we found differences in synchrony in the figure and background conditions, supporting the binding-by-synchrony hypothesis, in the current visual

stimulus, only one object, the figure, is present in the scene. To investigate the ability of this hypothesis to address the binding problem, the hypothesis needs to be tested when multiple objects are present, and when multiple features define which components belong to which object.

We postulated that primary visual cortex may play a role in a feedforward manner in visual binding independent of the feedback from extra-striate regions. The short reaction times of our subjects, and the requirement of relatively large time windows necessary to perform frequency analysis limits our ability to determine the exact time course of the modulation due to the time-frequency uncertainty principle (Gabor, 1946). A more reliable method in testing this idea could be to use a method like transcranial magnetic stimulation (TMS) to diminish the responses of extra-striate regions shortly after stimulus onset in order to assess their effects on grouping.

While TMS may be used to investigate the role of primary visual cortex in visual grouping, some further investigations may be performed to shed light on the causal role of synchrony in binding. This type of assessment of the binding-by-synchrony hypothesis would be the most convincing. Almost all the experimental evidence provided so far in support of this hypothesis were correlative, so it is possible that all the observed oscillation and synchrony were just epiphenomena of some other type of cognitive processing. Some studies have provided support for a causal role for synchrony in odor discrimination in the olfactory bulb of insects (Stopfer, 1997) and the role of interneurons in generating gamma oscillations in barrel cortex of mice using optogenetic techniques (Cardin et al., 2009). However, to the best of our knowledge, in visual cortex, only Kiper and Gegenfurtner (1996) attempted to directly assess the causal effect of synchrony on visual grouping. In a psychophysical experiment, they tried to manipulate the synchrony of neurons using

flickering bars, and argued that as neurons have been shown to oscillate at the frequency of the flickering bars, and phase-lock to the bars, they can use these bars to disrupt the synchrony between cells. They showed that this disruption of synchrony did not affect the perception of the subjects. Although these results seem solid, other studies have shown that brain may ignore temporal features in the presence of dominant spatial features (Fahle and Koch, 1995; Leonards et al., 1996; Usher and Donnelly, 1998). So, a plausible explanation for the observed results could be that in this experiment the grouping actually was performed based on common orientation, i.e. the dominant spatial feature, and not based on temporal frequency, which was disrupted. In fact it seems that this study demonstrated the ability of the brain in ignoring non-relevant features in scene segmentation, rather than presenting evidence for rejecting the causal role of synchrony. As a result it seems that rigorous studies still need to be carried out to investigate the causal role of synchrony in visual grouping, and novel methods such as optogenetics (Deisseroth et al., 2006) seem very appealing in performing this type of analysis.

References

Alais, D., Blake, R. and Lee, S. (1998) Visual features that vary together over time group together over space. Nat Neurosci. 1, 160-164.

Alonso, J., Usrey, W. and Reid, R. (1996) Precisely correlated firing in cells of the lateral geniculate nucleus. Nature 383, 815-819.

Andersen, R., Musallam, S. and Pesaran, B. (2004) Selecting the signals for a brain-machine interface. Current opinion in neurobiology 14, 720-726.

Azouz, R. and Gray, C. M. (2003) Adaptive coincidence detection and dynamic gain control in visual cortical neurons in vivo. Neuron 37, 513-523.

Bartos, M., Vida, I. and Jonas, P. (2007) Synaptic mechanisms of synchronized gamma oscillations in inhibitory interneuron networks. Nat Rev Neurosci 8, 45-56.

Bédard, C. and Destexhe, A. (2009) Macroscopic models of local field potentials and the apparent 1/f noise in brain activity. Biophysical journal 96, 2589-2603.

Bédard, C., Kröger, H. and Destexhe, A. (2004) Modeling extracellular field potentials and the frequency-filtering properties of extracellular space. Biophysical journal 86, 1829-1842.

Bédard, C., Kröger, H. and Destexhe, a. (2006) Model of low-pass filtering of local field potentials in brain tissue. Phys. Rev. E 73, 1-15.

Belitski, A., Gretton, A., Magri, C., Murayama, Y., Montemurro, M. a., Logothetis,

N. K. and Panzeri, S. (2008) Low-frequency local field potentials and spikes in primary visual cortex convey independent visual information. J Neurosci 28, 5696-5709.

Berens, P. (2009) CircStat: a MATLAB toolbox for circular statistics. Journal of Statistical Software 31,

Berens, P., Keliris, G. A., Ecker, A. S., Logothetis, N. K. and Tolias, A. S. (2008) Comparing the feature selectivity of the gamma-band of the local field potential and the underlying spiking activity in primate visual cortex. Frontiers in Systems Neuroscience 2,

Bergen, J. R. and Adelson, E. H. (1988) Early vision and texture perception. Nature 333, 363-364.

Beshel, J., Kopell, N. and Kay, L. M. (2007) Olfactory bulb gamma oscillations are enhanced with task demands. J Neurosci 27, 8358-8365.

Bong, J., Salazar, R., Gray, C. and Yen, S. (2012) Neuronal correlates of perceptual salience in the primary visual cortex. (submitted)

Bosking, W. H., Zhang, Y., Schofield, B. and Fitzpatrick, D. (1997) Orientation selectivity and the arrangement of horizontal connections in tree shrew striate cortex. J Neurosci 17, 2112-2127.

Bour, L. J., Gisbergen, J. A. v., Bruijns, J. and Ottes, F. P. (1984) The double magnetic induction method for measuring eye movement-results in monkey and man. IEEE Trans Biomed Eng 31, 419-427.

Bradley, D. and Petry, H. (1977) Organizational determinants of subjective contour: the subjective Necker cube. Am J Psychol 90, 253-262.

Bragin, A., Jandó, G., Nádasdy, Z., Hetke, J. F., Wise, K. D. and Buzsáki, G. (1995) Gamma (40-100 Hz) oscillation in the hippocampus of the behaving rat. J

Neurosci 15, 47-60.

Brosch, M., Bauer, R. and Eckhorn, R. (1997) Stimulus-dependent modulations of correlated high-frequency oscillations in cat visual cortex. Cereb Cortex 7, 70-76.

Brosch, M., Budinger, E. and Scheich, H. (2002) Stimulus-related gamma oscillations in primate auditory cortex. J Neurophysiol 87, 2715-2725.

Bruno, R. M. and Sakmann, B. (2006) Cortex is driven by weak but synchronously active thalamocortical synapses. Science 312, 1622-1627.

Buffalo, E. A., Fries, P., Landman, R., Buschman, T. J. and Desimone, R. (2011) Laminar differences in gamma and alpha coherence in the ventral stream. Proc. Natl. Acad. Sci. USA 108, 11262–11267.

Buschman, T. J. and Miller, E. K. (2007) Top-down versus bottom-up control of attention in the prefrontal and posterior parietal cortices. Science 315, 1860-1862.

Buzsáki, G. (2002) Theta oscillations in the hippocampus. Neuron 33, 325-340.

Buzsáki, G. (2006) Rhythms of the brain. Oxford: Oxford UP.

Caesar, K., Thomsen, K. and Lauritzen, M. (2003) Dissociation of spikes, synaptic activity, and activity-dependent increments in rat cerebellar blood flow by tonic synaptic inhibition. Proc. Natl. Acad. Sci. USA 100, 16000-16005.

Cardin, J. A., Carlén, M., Meletis, K., Knoblich, U., Zhang, F., Deisseroth, K., Tsai, L. H. and Moore, C. I. (2009) Driving fast-spiking cells induces gamma rhythm and controls sensory responses. Nature 459, 663-667.

Castelo-Branco, M., Goebel, R., Neuenschwander, S. and Singer, W. (2000) Neural synchrony correlates with surface segregation rules. Nature 405, 685-689.

Chelaru, M. I. and Dragoi, V. (2008) Efficient coding in heterogeneous neuronal

populations. Proc. Natl. Acad. Sci. USA 105, 16344-16349.

Csibra, G., Davis, G., Spratling, M. and Johnson, M. (2000) Gamma Oscillations and Object Processing in the Infant Brain. Science 290, 1582-1585.

Csicsvari, J., Jamieson, B., Wise, K. D. and Buzsáki, G. (2003) Mechanisms of gamma oscillations in the hippocampus of the behaving rat. Neuron 37, 311-322.

Deisseroth, K., Feng, G., Majewska, A. K., Miesenböck, G., Ting, A. and Schnitzer, M. J. (2006) Next-generation optical technologies for illuminating genetically targeted brain circuits. J Neurosci 26, 10380-10386.

Denker, M., Roux, S., Lindén, H., Diesmann, M., Riehle, A. and Grün, S. (2011) The local field potential reflects surplus spike synchrony. Cereb. Cortex 21, 2681-2695.

Eckhorn, R., Bauer, R., Jordan, W., Brosch, M., Kruse, W., Munk, M. and Reitboeck, H. (1988) Coherent oscillations: A mechanism of feature linking in the visual cortex? Biol. Cybern. 60, 121-130.

Eckhorn, R., Bruns, A., Saam, M., Gail, A., Gabriel, A. and Brinksmeyer, H. J. (2001) Flexible cortical gamma-band correlations suggest neural principles of visual processing. Visual Cognition 8, 519-530.

Eckhorn, R., Frien, A., Bauer, R., Woelbern, T. and Kehr, H. (1993) High frequency (60-90 Hz) oscillations in primary visual cortex of awake monkey. Neuroreport 4, 243-246.

Engel, A., Fries, P., Goebel, R. and Neuenschwander, S. (1998) Synchronization induced by moving random-dot patterns in cat striate cortex. Society for Neuroscience Abstracts 4, 1257.

Engel, A., König, P., Kreiter, A. and Singer, W. (1991a) Interhemispheric

synchronization of oscillatory neuronal responses in cat visual cortex. Science 252, 1177-1179.

Engel, A. and Singer, W. (2001) Temporal binding and the neural correlates of sensory awareness. Trends Cogn Sci. 5, 16-25.

Engel, A. K., König, P., Gray, C. M. and Singer, W. (1990) Stimulus-dependent neuronal oscillations in cat visual cortex: inter-columnar interaction as determined by cross-correlation analysis. European Journal of Neuroscience 2, 588-606.

Engel, A. K., Kreiter, A. K., König, P. and Singer, W. (1991b) Synchronization of oscillatory neuronal responses between striate and extrastriate visual cortical areas of the cat. Proc. Natl. Acad. Sci. USA 88, 6048-6052.

Fabre-Thorpe, M., Delorme, A., Marlot, C. and Thorpe, S. (2001) A limit to the speed of processing in ultra-rapid visual categorization of novel natural scenes. J Cogn Neurosci 13, 171-180.

Fahle, M. and Koch, C. (1995) Spatial displacement, but not temporal asynchrony, destroys figural binding. Vision Res. 35, 491-494.

Farin, G. (1990) Curves and surfaces for computer aided geometric design: a practical guide (2nd ed.). Boston: Academic Press

Field, D. J., Hayes, A. and Hess, R. F. (1993) Contour Integration by the Human Visual System: Evidence for a Local “Association Field”. Vision Res. 33, 173-193.

Fiser, J., Chiu, C. and Weliky, M. (2004) Small modulation of ongoing cortical dynamics by sensory input during natural vision. Nature 431, 573-578.

Fitzpatrick, D. (2000) Seeing beyond the receptive field in primary visual cortex. Current opinion in neurobiology 10, 438-443.

Freiwald, W. A., Kreiter, A. K. and Singer, W. (1995) Stimulus dependent intercolumnar synchronization of single unit responses in cat area 17. Neuroreport 6,

Frien, A., Eckhorn, R., Bauer, R., Woelbern, T. and Gabriel, A. (2000) Fast oscillations display sharper orientation tuning than slower components of the same recordings in striate cortex of the awake monkey. European Journal of Neuroscience 12, 1453-1465.

Frien, A., Eckhorn, R., Bauer, R., Woelbern, T. and Kehr, H. (1994) Stimulus-specific fast oscillations at zero phase between visual areas V1 and V2 of awake monkey. Neuroreport 5, 2273–2277.

Fries, P., Neuenschwander, S., Engel, A., Goebel, R. and Singer, W. (2001a) Rapid feature selective neuronal synchronization through correlated latency shifting. Nat Neurosci. 4, 194-200.

Fries, P., Reynolds, J. H., Rorie, A. E. and Desimone, R. (2001b) Modulation of Oscillatory Neuronal Synchronization by Selective Visual Attention. Science 291, 1560-1563.

Fries, P., Roelfsema, P. R., Engel, A. K., König, P. and Singer, W. (1997) Synchronization of oscillatory responses in visual cortex correlates with perception in interocular rivalry. Proc. Natl. Acad. Sci. USA 94, 12699-12704.

Fries, P., Nikolić, D. and Singer, W. (2007) The gamma cycle. Trends Neurosci. 30, 309-316.

Fries, P., Womelsdorf, T., Oostenveld, R. and Desimone, R. (2008) The effects of visual stimulation and selective visual attention on rhythmic neuronal synchronization in macaque area V4. J Neurosci 28, 4823-4835.

Gabor, D. (1946) Theory of communication. IEEE Journal of the Institution of

Electrical Engineers 93, 429-457.

Gail, A., Brinksmeyer, H. J. and Eckhorn, R. (2000) Contour decouples gamma activity across texture representation in monkey striate cortex. Cereb Cortex 10, 840-850.

Gail, A., Brinksmeyer, H. J. and Eckhorn, R. (2004) Perception-related modulations of local field potential power and coherence in primary visual cortex of awake monkey during binocular rivalry. Cereb. Cortex 14, 300-313.

Ghose, G. and Freeman, R. (1992) Oscillatory discharge in the visual system: does it have a functional role? J Neurophysiol 68, 1558-1574.

Gilaie-Dotan, S., Perry, A., Bonneh, Y., Malach, R. and Bentin, S. (2009) Seeing with profoundly deactivated mid-level visual areas: non-hierarchical functioning in the human visual cortex. Cereb. Cortex 19, 1687-1703.

Gilbert, C. D. (1992) Horizontal integration and cortical dynamics. Neuron 9, 1-13.

Gilbert, C., Ito, M., Kapadia, M. and Westheimer, G. (2000) Interactions between attention, context and learning in primary visual cortex. Vision Res. 40, 1217-1226.

Gilbert, C. and Wiesel, T. (1983) Clustered intrinsic connections in cat visual cortex. J Neurosci 3, 1116-1133.

Gilbert, C. D. and Wiesel, T. N. (1989) Columnar specificity of intrinsic horizontal and corticocortical connections in cat visual cortex. J Neurosci 9, 2432-2442.

Grammont, F. and Riehle, A. (2003) Spike synchronization and firing rate in a population of motor cortical neurons in relation to movement direction and reaction time. Biol. Cybern. 88, 360-373.

Gray, C. (1999) The Temporal Correlation Hypothesis Review of Visual Feature Integration: Still Alive and Well. Neuron 24, 31-47.

Gray, C., Goodell, B. and Lear, A. (2007) Multichannel micromanipulator and chamber system for recording multineuronal activity in alert, non-human primates. J Neurophysiol 98, 527-536.

Gray, C., König, P., Engel, A. and Singer, W. (1989) Oscillatory responses in cat visual cortex exhibit inter-columnar synchronization which reflects global stimulus properties. Nature 338, 334-337.

Gray, C. and McCormick, D. (1996) Chattering cells: superficial pyramidal neurons contributing to the generation of synchronous oscillations in the visual cortex. Science 274, 109-113.

Gray, C. M., Engel, A. K., König, P. and Singer, W. (1990) Stimulus-Dependent Neuronal Oscillations in Cat Visual Cortex: Receptive Field Properties and Feature Dependence. European Journal of Neuroscience 2, 607-619.

Gray, C. M. and Viana Di Prisco, G. (1997) Stimulus-Dependent Neuronal Oscillations and Local Synchronization in Striate Cortex of the Alert Cat. J Neurosci 17, 3239-3253.

Gray, C. M. and Singer, W. (1989) Stimulus-specific neuronal oscillations in orientation columns of cat visual cortex. Proc. Natl. Acad. Sci. USA 86, 1698-1702.

Grice, S. J., Spratling, M. W., Karmiloff-Smith, A., Halit, H., Csibra, G., Haan, M. d. and Johnson, M. H. (2001) Disordered visual processing and oscillatory brain activity in autism and Williams Syndrome. NeuroReport 12, 2697-2700.

Grosof, D. H., Shapley, R. M. and Hawken, M. J. (1993) Macaque V1 neurons can signal ‘illusory’ contours. Nature 365, 550-552.

Gross, C. G. (2002) Genealogy of the “grandmother cell”. Neuroscientist 8, 512-518.

Grün, S., Diesmann, M. and Aertsen, A. (2002a) Unitary events in multiple single-

neuron spiking activity: I. Detection and significance. Neural Computation 14, 43-80.

Grün, S., Diesmann, M. and Aertsen, A. (2002b) Unitary events in multiple single-neuron spiking activity: II. Nonstationary data. Neural Computation 14, 81-119.

Guttman, S. E., Gilroy, L. A. and Blake, R. (2005) Mixed messengers, unified message: spatial grouping from temporal structure. Vision Res. 45, 1021-1030.

Gysels, E., Renevey, P. and Celka, P. (2005) SVM-based recursive feature elimination to compare phase synchronization computed from broadband and narrowband EEG signals in Brain-Computer Interfaces. Signal Processing 85, 2178-2189.

Hasenstaub, A. R., Shu, Y., Haider, B., Kraushaar, U., Duque, A. and McCormick, D. A. (2005) Inhibitory postsynaptic potentials carry synchronized frequency information in active cortical networks. Neuron 47, 423-435.

Hatsopoulos, N., Ojakangas, C., Paninski, L. and Donoghue, J. (1998) Information about movement direction obtained from synchronous activity of motor cortical neurons. Proc. Natl. Acad. Sci. USA 95, 15706-15711.

Hegdé, J. and Felleman, D. J. (2003) How selective are V1 cells for pop-out stimuli? J Neurosci 23, 9968-9980.

Heinzle J, König P, Salazar RF (2007) Modulation of synchrony without changes in firing rates. Cogn Neurodyn. 1, 225-235.

Henrie, J. A. and Shapley, R. (2005) LFP power spectra in V1 cortex: the graded effect of stimulus contrast. J Neurophysiol 94, 479-490.

Herrmann, C. S., Munk, M. H. and Engel, A. K. (2004) Cognitive functions of gamma-band activity: memory match and utilization. Trends Cogn Sci. 8, 347-

355.

Hoogenboom, N., Schoffelen, J., Oostenveld, R., Parkes, L. M. and Fries, P. (2006) Localizing human visual gamma-band activity in frequency, time and space. NeuroImage 29, 764-773.

Jarvis, M. R. and Mitra, P. P. (2001) Sampling properties of the spectrum and coherency of sequences of action potentials. Neural Computation 13, 717-749.

Jensen, O., Gelfand, J., Kounios, J. and Lisman, J. E. (2002) Oscillations in the alpha band (9-12 Hz) increase with memory load during retention in a short-term memory task. Cereb Cortex 12, 877-882.

Jia, X., Smith, M. A. and Kohn, A. (2011) Stimulus selectivity and spatial coherence of gamma components of the local field potential. J Neurosci 31, 9390-9403.

Joseph, J. S., Chun, M. M. and Nakayama, K. (1997) Attentional requirements in a 'preattentive' feature search task. Nature 387, 805-807.

Judge, S. J., Richmond, B. J. and Chu, F. C. (1980) Implantation of magnetic search coils for measurement of eye position: an improved method. Vision Res. 20, 535-538.

Julesz, B. (1975) Experiments in the visual perception of texture. Sci Am 232, 34-43.

Kandil, F. I. and Fahle, M. (2004) Figure-ground segregation can rely on differences in motion direction. Vision Res. 44, 3177-3182.

Kanisza (1979) The Organization of Vision. New York: Praeger

Kapadia, M., Ito, M., Gilbert, C. and Westheimer, G. (1995) Improvement in visual sensitivity by changes in local context: parallel studies in human observers and in V1 of alert monkeys. Neuron 15, 843-856.

Kapadia, M., Westheimer, G. and Gilbert, C. (2000) Spatial Distribution of Contextual Interactions in Primary Visual Cortex and in Visual Perception. J

Neurophysiol 84, 2048-2062.

Katzner, S., Nauhaus, I., Benucci, A., Bonin, V., Ringach, D. L. and Carandini, M. (2009) Local origin of field potentials in visual cortex. Neuron 61, 35-41.

Kayser, C. and König, P. (2004) Stimulus locking and feature selectivity prevail in complementary frequency ranges of V1 local field potentials. European Journal of Neuroscience 19, 485-489.

Kayser, C., Montemurro, M. a., Logothetis, N. K. and Panzeri, S. (2009) Spike-phase coding boosts and stabilizes information carried by spatial and temporal spike patterns. Neuron 61, 597-608.

Kayser, C., Petkov, C. I. and Logothetis, N. K. (2007) Tuning to sound frequency in auditory field potentials. J Neurophysiol 98, 1806-1809.

Kayser, C., Salazar, R. and König, P. (2003) Responses to natural scenes in cat V1. J Neurophysiol 90, 1910-1920.

Keil, A., Müller, M., Ray, W. J., Gruber, T. and Elbert, T. (1999) Human Gamma Band Activity and Perception of a Gestalt. J Neurosci 19, 7152-7161.

Kiani, R., Esteky, H., Mirpour, K. and Tanaka, K. (2007) Object category structure in response patterns of neuronal population in monkey inferior temporal cortex. J Neurophysiol 97, 4296-4309.

Kiper, D., Gegenfurtner, K. and Movshon, J. (1996) Cortical oscillatory responses do not affect visual segmentation. Vision Res. 36, 539-544.

Koffka, K. (1935) Principles of Gestalt Psychology. New York: Harcourt, Brace and World

Koffka, K. (1969) The task of Gestalt psychology. Princeton: Princeton University Press

Köhler, W. (1930) Gestalt Psychology. London: G. Bell & Sons 312.

König, P., Engel, A. K. and Singer, W. (1996) Integrator or coincidence detector? The role of the cortical neuron revisited. Trends Neurosci. 19, 130-137.

Kreiman, G., Hung, C. P., Kraskov, A., Quiroga, R. Q., Poggio, T. and DiCarlo, J. J. (2006) Object selectivity of local field potentials and spikes in the macaque inferior temporal cortex. Neuron 49, 433-445.

Kreiter, A. and Singer, W. (1996) Stimulus-dependent synchronization of neuronal responses in the visual cortex of the awake macaque monkey. J Neurosci 16, 2381-2396.

Kreiter, A. K. and Singer, W. (1992) Oscillatory Neuronal Responses in the Visual Cortex of the Awake Macaque Monkey. European Journal of Neuroscience 4, 369-375.

Lachaux, J., Lutz, A., Rudrauf, D., Cosmelli, D., Le Van Quyen, M., Martinerie, J. and Varela, F. (2002) Estimating the time-course of coherence between single-trial brain signals: an introduction to wavelet coherence. Neurophysiol Clin 32, 157-174.

Lachaux, J., Rodriguez, E., Martinerie, J., Adam, C., Hasboun, D. and Varela, F. (2000) A quantitative study of gamma-band activity in human intracranial recordings triggered by visual stimuli. European Journal of Neuroscience 12, 2608-2622.

Lachaux, J., Rodriguez, E., Martinerie, J. and Varela, F. (1999) Measuring phase synchrony in brain signals. Human brain mapping 8, 194-208.

Lakatos, P., Shah, A. S., Knuth, K. H., Ulbert, I., Karmos, G. and Schroeder, C. E. (2005) An oscillatory hierarchy controlling neuronal excitability and stimulus processing in the auditory cortex. J Neurophysiol 94, 1904-1911.

Lamme, V., Rodriguez-Rodriguez, V. and Spekreijse, H. (1999) Separate processing

dynamics for texture elements, boundaries and surfaces in primary visual cortex of the macaque monkey. Cereb. Cortex 9, 406-413.

Lamme, V. and Spekreijse, H. (1998) Neuronal synchrony does not represent texture segregation. Nature 396, 362-366.

Lamme, V. a. (1995) The neurophysiology of figure-ground segregation in primary visual cortex. J Neurosci 15, 1605-1615.

Lamme, V. A. F., Zipser, K. and Spekreijse, H. (1998) Figure-ground activity in primary visual cortex is suppressed by anesthesia. Proc. Natl. Acad. Sci. USA 95, 3263-3268.

Le Van Quyen, M., Foucher, J., Lachaux, J., Rodriguez, E., Lutz, A., Martinerie, J. and Varela, F. J. (2001) Comparison of Hilbert transform and wavelet methods for the analysis of neuronal synchrony. Journal of neuroscience methods 111, 83-98.

Le Van Quyen, M., Staba, R., Bragin, A., Dickson, C., Valderrama, M., Fried, I. and Engel, J. (2010) Large-scale microelectrode recordings of high-frequency gamma oscillations in human cortex during sleep. J Neurosci 30, 7770-7782.

Lee, S. and Blake, R. (2001) Neural synergy in visual grouping: when good continuation meets common fate. Vision Res. 41, 2057-2064.

Lee, S. H. and Blake, R. (1999) Visual form created solely from temporal structure. Science 284, 1165-1168.

Lee, T. S., Mumford, D., Romero, R. and Lamme, V. A. (1998) The role of the primary visual cortex in higher level vision. Vision Res. 38, 2429-2454.

Lee, T. S., Yang, C., Romero, R. and Mumford, D. (2002) Neural activity in early visual cortex reflects behavioral experience and higher-order perceptual saliency. Nat Neurosci. 5, 589-597.

Leonards, U., Singer, W. and Fahle, M. (1996) The influence of temporal phase differences on texture segmentation. Vision Res. 36, 2689-2697.

Li, W., Piëch, V. and Gilbert, C. D. (2006) Contour saliency in primary visual cortex. Neuron 50, 951-962.

Li, W., Piëch, V. and Gilbert, C. D. (2008) Learning to link visual contours. Neuron 57, 442-451.

Lima, B., Singer, W., Chen, N. and Neuenschwander, S. (2010) Synchronization Dynamics in Response to Plaid Stimuli in Monkey V1. Cereb. Cortex 20, 1556-1573.

Lima, B., Singer, W. and Neuenschwander, S. (2011) Gamma responses correlate with temporal expectation in monkey primary visual cortex. J Neurosci 31, 15919-15931.

Liu, J. and Newsome, W. T. (2006) Local field potential in cortical area MT: stimulus tuning and behavioral correlations. J Neurosci 26, 7779-7790.

Livingstone, M. (1996) Oscillatory firing and interneuronal correlations in squirrel monkey striate cortex. J Neurophysiol 75, 2467-2485.

Llinás, R. R., Grace, A. A. and Yarom, Y. (1991) In vitro neurons in mammalian cortical layer 4 exhibit intrinsic oscillatory activity in the 10- to 50-Hz frequency range. Proc. Natl. Acad. Sci. USA 88, 897-901.

Logothetis, N. K. (2003) The underpinnings of the BOLD functional magnetic resonance imaging signal. J Neurosci 23, 3963-3971.

Logothetis, N. K., Kayser, C. and Oeltermann, A. (2007) In vivo measurement of cortical impedance spectrum in monkeys: implications for signal propagation. Neuron 55, 809-823.

Logothetis, N. K., Pauls, J., Augath, M., Trinath, T. and Oeltermann, A. (2001)

Neurophysiological investigation of the basis of the fMRI signal. Nature 412, 150-157.

Malach, R., Amir, Y., Harel, M. and Grinvald, A. (1993) Relationship between intrinsic connections and functional architecture revealed by optical imaging and in vivo targeted biocytin injections in primate striate cortex. Proc. Natl. Acad. Sci. USA 90, 10469-10473.

Maldonado, P., Babul, C., Singer, W., Rodriguez, E., Berger, D. and Grün, S. (2008) Synchronization of neuronal responses in primary visual cortex of monkeys viewing natural images. J Neurophysiol 100, 1523-1532.

Maldonado, P., Friedman-Hill, S. and Gray, C. (2000) Dynamics of striate cortical activity in the alert macaque: II. Fast time scale synchronization. Cereb Cortex 10, 1117-1131.

Manning, J. R., Jacobs, J., Fried, I. and Kahana, M. J. (2009) Broadband shifts in local field potential power spectra are correlated with single-neuron spiking in humans. J Neurosci 29, 13613-13620.

Martinovic, J. and Busch, N. a. (2011) High frequency oscillations as a correlate of visual perception. Int. J. Psychophysiol. 79, 32-38.

Mathewson, K. E., Gratton, G., Fabiani, M., Beck, D. M. and Ro, T. (2009) To see or not to see: prestimulus alpha phase predicts visual awareness. J Neurosci 29, 2725-2732.

McGill, R., Tukey, J. W. and Larsen, W. A. (1978) Variations of box plots. The American Statistician 32, 12-16.

McManus, J., Li, W. and Gilbert, C. (2011) Adaptive shape processing in primary visual cortex. Proc. Natl. Acad. Sci. USA 108, 9739-9746.

Mehring, C., Rickert, J., Vaadia, E., Cardosa de Oliveira, S., Aertsen, A. and Rotter,

S. (2003) Inference of hand movements from local field potentials in monkey motor cortex. Nat Neurosci. 6, 1253-1254.

Meirovithz, E., Ayzenshtat, I., Bonneh, Y. S., Itzhack, R., Werner-Reiss, U. and Slovin, H. (2010) Population response to contextual influences in the primary visual cortex. Cereb. Cortex 20, 1293-1304.

Milner, P. M. (1974) A model for visual shape recognition. Psychol. Rev. 816, 521-535.

Mitzdorf, U. (1985) Current source-density method and application in cat cerebral cortex: investigation of evoked potentials and EEG phenomena. Physiol Rev 65, 37-100.

Montemurro, M. A., Rasch, M. J., Murayama, Y., Logothetis, N. K. and Panzeri, S. (2008) Phase-of-firing coding of natural visual stimuli in primary visual cortex. Current biology 18, 375-380.

Morita, K., Kalra, R., Aihara, K. and Robinson, H. P. (2008) Recurrent synaptic input and the timing of gamma-frequency-modulated firing of pyramidal cells during neocortical “UP” states. J Neurosci 28, 1871-1881.

Müller, M., Bosch, J., Elbert, T., Kreiter, A., Sosa, M. V., Sosa, P. V. and Rockstroh, B. (1996) Visually induced gamma-band responses in human electroencephalographic activity- a link to animal studies. Exp Brain Res 112, 96-102.

Müller, M. M., Junghöfer, M., Elbert, T. and Rockstroh, B. (1997) Visually induced gamma-band responses to coherent and incoherent motion : a replication study. NeuroReport 8, 2575-2579.

Nakayama, K. and Silverman, G. H. (1986) Serial and parallel processing of visual feature conjunctions. Nature 320, 264-265.

Nauhaus, I., Busse, L., Carandini, M. and Ringach, D. L. (2009) Stimulus contrast modulates functional connectivity in visual cortex. Nat Neurosci. 12, 70-76.

Nir, Y., Fisch, L., Mukamel, R., Gelbard-Sagiv, H., Arieli, A., Fried, I. and Malach, R. (2007) Coupling between neuronal firing rate, gamma LFP, and BOLD fMRI is related to interneuronal correlations. Current biology 17, 1275-1285.

Oram, M. W. and Perrett, D. I. (1992) Time course of neural responses discriminating different views of the face and head. J Neurophysiol 68, 70-84.

Page, M. (2000) Connectionist modelling in psychology: A localist manifesto. Behavioral and Brain Sciences 23, 443-467.

Palanca, B. and DeAngelis, G. C. (2005) Does neuronal synchrony underlie visual feature grouping? Neuron 46, 333-346.

Perez-Orive, J., Bazhenov, M. and Laurent, G. (2004) Intrinsic and circuit properties favor coincidence detection for decoding oscillatory input. J Neurosci 24, 6037-6047.

Perkel, D., Gerstein, G. and Moore, G. (1967) Neuronal spike trains and stochastic point processes. II. Simultaneous spike trains. Biophysical journal 7, 419-440.

Pesaran, B., Pezaris, J. S., Sahani, M., Mitra, P. P. and Andersen, R. a. (2002) Temporal structure in neuronal activity during working memory in macaque parietal cortex. Nat Neurosci. 5, 805-811.

Pipa, G., Wheeler, D., Singer, W. and Nikolić, D. (2008) NeuroXidence: reliable and efficient analysis of an excess or deficiency of joint-spike events. J Comput Neurosci 25, 64-88.

Pogosyan, A., Gaynor, L. D., Eusebio, A. and Brown, P. (2009) Boosting cortical activity at Beta-band frequencies slows movement in humans. Curr Biol 19, 1637-1641.

Polat, U., Mizobe, K., Pettet, M., Kasamatsu, T. and Norcia, A. M. (1998) Collinear stimuli regulate visual responses depending on cell's contrast threshold. Nature 391, 580-584.

Quiroga, R. Q., Kreiman, G., Koch, C. and Fried, I. (2008) Sparse but not 'grandmother-cell' coding in the medial temporal lobe. Trends Cogn Sci. 12, 87-91.

Rainer, G. (2008) Previews Localizing Cortical Computations during Visual Selection. Neuron 57, 480-481.

Rao, R. and Ballard, D. (1999) Predictive coding in the visual cortex: a functional interpretation of some extra-classical receptive-field effects. Nat Neurosci. 2, 79-87.

Riehle, A., Grammont, F., Diesmann, M. and Grün, S. (2000) Dynamical changes and temporal precision of synchronized spiking activity in monkey motor cortex during movement preparation. J Physiol Paris 94, 569-582.

Riehle, A., Grün, S., Diesmann, M. and Aertsen, A. (1997) Spike synchronization and rate modulation differentially involved in motor cortical function. Science 278, 1950-1953.

Rodriguez, E., George, N., Lachaux, J., Martinerie, J., Renault, B. and Varela, F. J. (1999) Perception's shadow: long- distance synchronization of human brain activity. Nature 397, 430-433.

Roelfsema, P. (2006) Cortical algorithms for perceptual grouping. Annu. Rev. Neurosci. 29, 203-227.

Roelfsema, P., Lamme, V. and Spekreijse, H. (2004) Synchrony and covariation of firing rates in the primary visual cortex during contour grouping. Nat Neurosci. 7, 982-991.

Roelfsema, P. R., Tolboom, M. and Khayat, P. S. (2007) Different processing phases for features, figures, and selective attention in the primary visual cortex. Neuron 56, 785-792.

Roskies, A. L. (1999) The Binding Problem. Neuron 24, 7-9.

Roux, S., Mackay, W. a. and Riehle, A. (2006) The pre-movement component of motor cortical local field potentials reflects the level of expectancy. Behavioural brain research 169, 335-351.

Samonds, J. M., Zhou, Z., Bernard, M. R. and Bonds, A. B. (2006) Synchronous activity in cat visual cortex encodes collinear and cocircular contours. J Neurophysiol 95, 2602-2616.

Schadow, J., Dettler, N., Paramei, G. V., Lenz, D., Fründ, I., Sabel, B. A. and Herrmann, C. S. (2009) Impairments of Gestalt perception in the intact hemifield of hemianopic patients are reflected in gamma-band EEG activity. Neuropsychologia 47, 556-568.

Schoffelen, J., Oostenveld, R. and Fries, P. (2005) Neuronal coherence as a mechanism of effective corticospinal interaction. Science 308, 111-113.

Sekuler, B. A. and Bennett, P. J. (2001) Generalized common fate: grouping by common luminance changes. Psychol Sci 12, 437-444.

Shadlen, M. N. and Movshon, J. A. (1999) Synchrony Unbound A Critical Evaluation of the Temporal Binding Hypothesis. Neuron 24, 67-77.

Shamir, M. and Sompolinsky, H. (2006) Implications of neuronal diversity on population coding. Neural Computation 18, 1951-1986.

Siegel, M., Donner, T., Oostenveld, R., Fries, P. and Engel, A. (2007) High-Frequency Activity in Human Visual Cortex Is Modulated by Visual Motion Strength. Cereb. Cortex 17, 732-741.

Siegel, M., Donner, T. H., Oostenveld, R., Fries, P. and Engel, A. K. (2008) Neuronal synchronization along the dorsal visual pathway reflects the focus of spatial attention. Neuron 60, 709-719.

Singer, W. (1995) Visual feature integration and the temporal correlation hypothesis. Annu. Rev. Neurosci. 18, 555-586.

Smith, M. A., Kelly, R. C. and Lee, T. S. (2007) Dynamics of response to perceptual pop-out stimuli in macaque V1. J Neurophysiol 98, 3436-3449.

Steriade, M., Timofeev, I., Dürmüller, N. and Grenier, F. (1998) Dynamic properties of corticothalamic neurons and local cortical interneurons generating fast rhythmic (30-40 Hz) spike bursts. J Neurophysiol 79, 483-490.

Stopfer, M., Bhagavan, S., Smith, B. H. and Laurent, G. (1997) Impaired odour discrimination on desynchronization of odour-encoding neural assemblies. Nature 390, 70-74.

Sugita, Y. (1999) Grouping of image fragments in primary visual cortex. Nature 401, 269-272.

Supèr, H. and Lamme, V. (2007) Altered figure-ground perception in monkeys with an extra-striate lesion. Neuropsychologia 45, 3329-3334.

Supèr, H., Spekreijse, H. and Lamme, V. (2001) Two distinct modes of sensory processing observed in monkey primary visual cortex (V1). Nat Neurosci. 4, 304-310.

Supèr, H., van der Togt, C., Spekreijse, H. and Lamme, V. (2003) Internal state of monkey primary visual cortex (V1) predicts figure-ground perception. J Neurosci 23, 3407-3414.

Suzuki, S. and Grabowecky, M. (2002) Overlapping features can be parsed on the basis of rapid temporal cues that produce stable emergent percepts. Vision Res.

42, 2669-2692.

Tallon-Baudry, C., Bertrand, O., Delpuech, C. and Pernier, J. (1996) Stimulus Specificity of Phase-Locked and Non-Phase-Locked 40 Hz Visual Responses in Human. J Neurosci 16, 4240-4249.

Theeuwes, J., Kramer, A. and Atchley, P. (1999) Attentional effects on preattentive vision: spatial precues affect the detection of simple features. Journal of Experimental Psychology Human Perception and Performance 25, 341-347.

Thiele, A. and Stoner, G. (2003) Neuronal synchrony does not correlate with motion coherence in cortical area MT. Nature 421, 366-370.

Thorpe, S., Fize, D. and Marlot, C. (1996) Speed of processing in the human visual system. Nature 381, 520-522.

Tong, F. (2003) Primary visual cortex and visual awareness. Nat Rev Neurosci 4, 219-229.

Tovee, M. and Rolls, E. (1992) Oscillatory activity is not evident in the primate temporal visual cortex with static stimuli. Neuroreport 3, 369-372.

Treisman, A. M. and Gelade, G. (1980) A feature-integration theory of attention. Cogn Psychol 12, 97-136.

Ts'o, D. Y., Gilbert, C. D. and Wiesel, T. N. (1986) Relationships between horizontal interactions and functional architecture in cat striate cortex as revealed by cross-correlation analysis. J Neurosci 6, 1160-1170.

Uhlhaas, P. J., Pipa, G., Lima, B., Melloni, L., Neuenschwander, S., Nikolić, D. and Singer, W. (2009) Neural synchrony in cortical networks: history, concept and current status. Frontiers in Integrative Neuroscience 3,

Usher, M. and Donnelly, N. (1998) Visual synchrony affects binding and segmentation in perception. Nature 394, 179-182.

Usrey, W., Reppas, J. and Reid, R. (1998) Paired-spike interactions and synaptic efficacy of retinal inputs to the thalamus. Nature 395, 384-387.

Vaadia, E., Haalman, I., Abeles, M., Bergman, H., Prut, Y., Slovin, H. and Aertsen, A. (1995) Dynamics of neuronal interactions in monkey cortex in relation to behavioural events. Nature 373, 515-518.

van der Togt, C., Lamme, V. and Spekreijse, H. (1998) Functional connectivity within the visual cortex of the rat shows state changes. European Journal of Neuroscience 10, 1490-1507.

Vida, I., Bartos, M. and Jonas, P. (2006) Shunting inhibition improves robustness of gamma oscillations in hippocampal interneuron networks by homogenizing firing rates. Neuron 49, 107-117.

Vinck, M., Lima, B., Womelsdorf, T., Oostenveld, R., Singer, W., Neuenschwander, S. and Fries, P. (2010) Gamma-phase shifting in awake monkey visual cortex. J Neurosci 30, 1250-1257.

von der Malsburg, C. (1981) The correlation theory of brain function. Internal report. Max-Planck-Insitute for Biological Chemistry, Gottingen, Germany

von der Malsburg, C. (1985) Nervous structures with dynamical links. Ber. Bunsenges. Phys. Chem 89, 703-710.

Wertheimer, M. (1955) Laws of organization in perceptual forms. In A Source Book of Gestalt Psychology, W.D. Ellis, ed. (London: Routledge and Kegan Paul).

Wilke, M., Logothetis, N. K. and Leopold, D. A. (2006) Local field potential reflects perceptual suppression in monkey visual cortex. Proc. Natl. Acad. Sci. USA 103, 17507-17512.

Womelsdorf, T., Fries, P., Mitra, P. P. and Desimone, R. (2006) Gamma-band synchronization in visual cortex predicts speed of change detection. Nature

439, 733-736.

Womelsdorf, T., Schoffelen, J., Oostenveld, R., Singer, W., Desimone, R., Engel, A. K. and Fries, P. (2007) Modulation of neuronal interactions through neuronal synchronization. Science 316, 1609-1612.

Yen, S-C, Baker, J. and Gray, C. M. (2007) Heterogeneity in the responses of adjacent neurons to natural stimuli in cat striate cortex. J Neurophysiol 97, 1326-1341.

Young, C. K. and Eggermont, J. J. (2009) Coupling of mesoscopic brain oscillations: recent advances in analytical and theoretical perspectives. Progress in neurobiology 89, 61-78.

Young, M. P., Tanaka, K. and Yamane, S. (1992) On oscillating neuronal responses in the visual cortex of the monkey. J Neurophysiol 67, 1464-1474.

Yuval-Greenberg, S., Tomer, O., Keren, A. S., Nelken, I. and Deouell, L. Y. (2008) Transient induced gamma-band response in EEG as a manifestation of miniature saccades. Neuron 58, 429-441.

Zanos, S., Zanos, T., Marmarellis, V., Ojemann, G. and Fetz, E. (2011) Relationships between spike-free local field potentials and spike timing in human temporal cortex. J Neurophysiol [Epub ahead of print].

Zhou, Z., Bernard, M. and Bonds, A. B. (2008) Deconstruction of spatial integrity in visual stimulus detected by modulation of synchronized activity in cat visual cortex. J Neurosci 28, 3759-3768.

Zipser, K., Lamme, V. and Schiller, P. H. (1996) Contextual Modulation in Primary Visual Cortex. J Neurosci 16, 7376-7389.

Appendix A

List of publications

A.1 Peer-reviewed journal publications

Mokri Y, Salazar RF, Goodell B, Baker J, Gray CM, Yen SC. Partially-automated sorting of overlapping spike waveforms (submitted).

Mokri Y, Salazar RF, Gray CM, Yen SC. Modulation of gamma band local field potentials by visual saliency in the macaque primary visual cortex (in preparation).

Mokri Y, Salazar RF, Gray CM, Yen SC. Modulation of synchrony of gamma band local field potentials by visual saliency in the macaque primary visual cortex (in preparation).

A.2 Conference publication

Mokri Y, Yen SC. Spike overlap resolution of electrode and tetrode data from primary visual cortex. *BMC Neuroscience, 9 (Suppl 1):P94, 11 July 2008. CNS, Portland,USA, July 2008.*